Durability and Recoverability of Al-doped ZnO Transparent Electrodes Exposed to a Harsh Environment

Fahmi Machda

Abstract

Transparent electrode (TE) plays essential roles in optoelectronic devices such as light-emitting diode (LED) and photovoltaics (PV). The stability of TEs is contributing significantly to the long-term efficiency of any optoelectronic devices utilizing the TEs. As a kind of TE materials, aluminum-doped zinc oxide (AZO) is an alternative to Indium Tin Oxide (ITO) with a superiority of AZO materials from the viewpoint of cost and environment, although ITO is currently the most widely used transparent electrode material. As the long-term usage of any optoelectronic devices is essential, this study investigated the durability of AZO transparent electrode coated on glass and polyimide (PI) tape substrate evaluated by its conductivity degradation as exposed to a harsh environment, represented as a damp-heat condition.

For AZO films on the glass, a decrease of carrier concentration exhibited the main reason for the damp-heat degradation of the films due to the chemical aspect such as removal of oxygen vacancies and diffusion of hydroxyl groups as the films were exposed to the harsh environment. AZO films with crystal orientation (002) showed better durability as compared to AZO films with other crystal orientations. Furthermore, AZO films with less varied crystal orientations show better durability than AZO films with more varied ones. A higher argon gas flow ratio against oxygen gas in the reactive sputtering could strengthen this crystal orientation of (002). AZO with higher annealing temperature also showed better stability due to the spontaneously formed an ultra-thin oxide layer on top of the AZO films. As found that chemical aspects are playing a vital role in the degradation of the AZO films by decreasing the carrier concentrations, reannealing was purposed to recover the degraded conductivity of the films by removing the diffused hydroxyl groups. As investigated, the degraded thin films due to the harsh environment exposure are recoverable by reannealing the films in the hydrogen atmosphere. In order to produce the initial conductivity of the films, reannealing was conducted at the same temperature as the initial annealing configuration before the damp heat test.

Furthermore, as the sputtering with a very low oxygen-to-argon gas ratio conducted to strengthen the orientation (002), AZO films exhibited high conductivity without post-heat treatment, opening the applicability of polymer-based substrates such as PIs for AZO film deposition by sputtering. To support the film deposition, the PI-tape was attached to the Polycarbonate (PC) materials, labeled as PI-tape/PC substrates. The AZO films were deposited on both glass and PI-tape/PC under the same low ratio of oxygen-to-argon gas and without post-annealing. As compared for the damp-heat durability, the AZO films coated on PI-tape exhibited a different kind of degradation as compared to the AZO films on glass substrates, where the decrease in Hall mobility exhibited as the main reason for the degradation. While AZO coated on glass was very durable with high conductivity and mobility, the physical deformation due to the hydrolysis of PI-tape and polycarbonate caused several cracks to the AZO films on PI-tape/PC substrates. These cracks showed the physical brittleness of conventional flat thin films of AZO transparent electrode materials, causing the significant decrease of Hall mobility as exposed to the damp-heat condition.

To conclude, the degradation of AZO films is very sensitive to the substrate and the crystal orientations. For the AZO film on the glass substrate, chemical aspect is more involved in the degradation, where the durability improvement is achievable by protecting the carrier concentration through providing a top protective layer, conducting a low ratio of oxygen-to-argon gas for reactive sputtering deposition, and strengthening the crystal orientation (002). AZO films on the glass with a strong (002) orientation can provide high conductivity and excellent damp-heat durability of the films, even the films were prepared at a low temperature. On the other hand, the degradation of AZO films coated on PI-tape/PC substrates involves more physical aspect than the chemical aspect, where the cracks or physical damages due to the deformation of PI-tape and polycarbonate decreased the Hall mobility significantly. A strong crystal orientation (002) is crucial for the durability of AZO films on the glass, which could maintain high Hall mobility and conductivity even in the damp heat condition. Furthermore, reannealing the degraded AZO films on the glass could recover the AZO films coated on glass substrates with an approximate of more than 80% of the recovery rate.

Contents

List of Tables

List of Figures

1. Introduction

1.1. Transparent electrodes

As humanity is continuously modernized, the world is moving towards the age of information technology and a more environment-friendly lifestyle. The use of high-performing devices that consume less energy and provide better services is becoming more and more attractive to replace conventional devices whenever fitted and required. For advancing these devices, the utilization of reliable electronic materials is in high demand. Such as in optoelectronic devices in the modern lifestyle, transparent yet conductive materials called as transparent electrodes (TEs) are diversely applied, including general lighting devices, photovoltaic (PV), touchscreens of smart-phones, light-emitting diodes (LED), organic LED (OLED), smart windows, and liquid crystal displays (LCD)[1,2].

For example, the utilization of TEs has made it achievable to develop LED lamps for general lighting devices. These days, the replacement of fluorescent-based lighting and incandescent lamp by LED lamps has already been started all over the world[3], due to the feature of LED lamps as relatively more efficient light sources with longer lifetime. For the LED lighting devices, the TE film is acting as an ohmic contact mounted at the top or bottom active layer, providing high injection current to the active layer as well as a transparent window for the emitted light to go out effectively from the active layer where the energy to light conversion occurs (Fig. 1-1). When the active layer receives high injection currents, and the emitted light is effectively passing the transparent contacts, the LED device will exhibit a high extraction efficiency[4].

For the development of solar cell technologies, the utilization of TEs contributed to the development of thin-film solar cells and other newly emerging photovoltaic technologies, which are lowering the cost by saving both materials and energy in the production of the cells and modules in

comparison with the earlier photovoltaics (PV) technologies such as bulk-Si cells[4]. For the utilization of TEs in the PV technologies, superstrate configuration where the light enters the active layers from the glass substrate is applied in several solar cell technologies such as in the a-Si:H/μc-Si:H solar cells[4] and CdTe solar cells [5] (Fig. 1-2). TEs are layered first with the glass acting as a window for light to pass through to the active junctions. In this configuration, these TCEs are the first deposited layers and must face all later deposition steps and any post-deposition processing[4,5]. As TEs are transparent, sunlight passes through it, and when a photon of the light hits the active material, the light to energy conversion occurs in the form of electron-hole pair or as an exciton. This exciton can recombine, migrate, or separate into charges. At the donor-acceptor interface, charge separation tends to occur, then free electron and hole go to opposite electrodes such as TEs as anode and metal layer as cathode then electric current generates. Thus besides acting as a transparent front contact layer, the TEs are also facilitating the current collection.

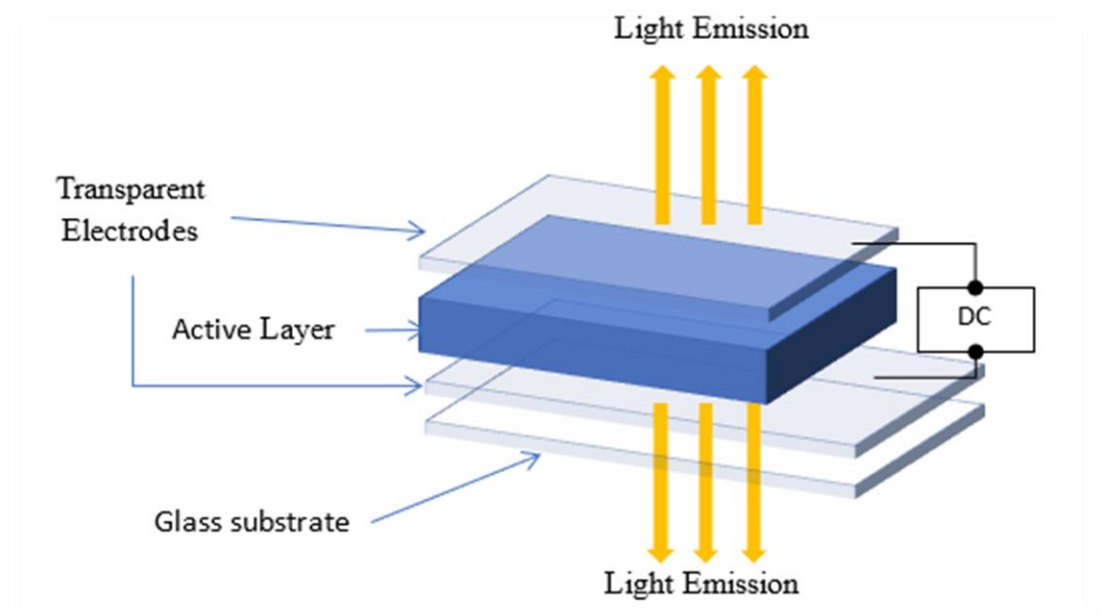

Fig. 1-1. Simplified structures of LED lighting devices including TCE layers

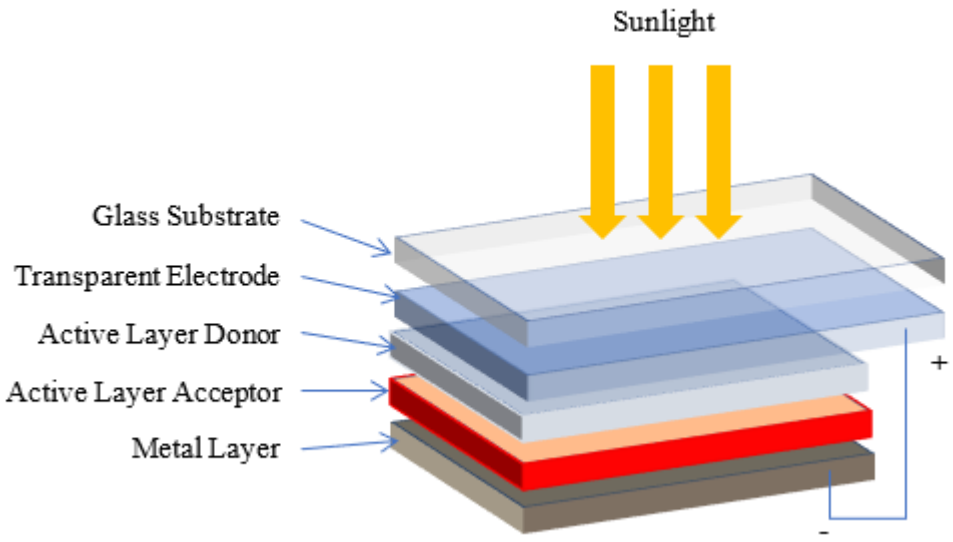

Fig. 1-2. Basic function of a transparent electrode in solar cell applications with superstrate configuration

The quality of TEs is often defined by the total light transmittance and film surface electric conductivity. As defined by Hackee in 1976[6], the figure of merit (Φ_H) of TEs is quantified as:

$$\Phi_H = \frac{T^q}{R_s} = T^q \sigma d \tag{1.1}$$

where T is the transmittance, q is an exponent that determines which transmittance is required for a specific purpose, d is the thickness, σ is the conductivity, and R_s is the sheet resistance of the film. Exponents of q = 10, 20, or 100 lead to transmittance of 0.9, 0.95, or 0.99, respectively. However, q = 10 is usually chosen because a transmittance of 0.9 or 90% is sufficient for most of the device requirements. High transparency or light transmittance of TEs would let the LED lamps emit bright light and also contribute to PV devices to achieve high light-energy conversion efficiency. Lower sheet resistance is better for TEs since it would better conduct the electrical currents, ensure high injection currents, and lower the power consumption of the devices.

a

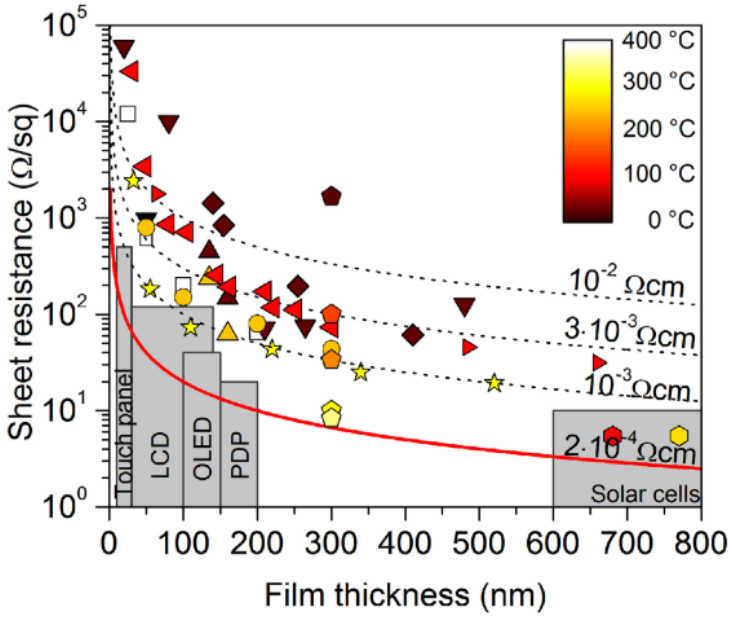

b

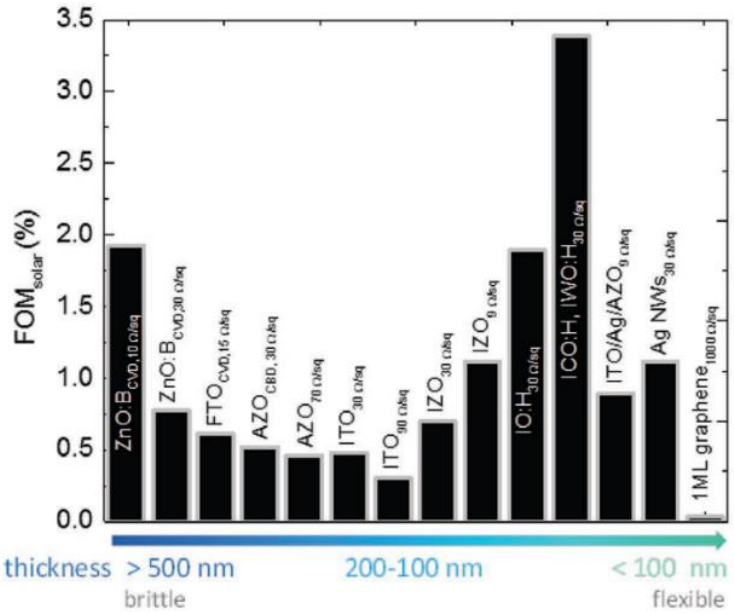

Fig. 1-3. Applications of TEs require specific film thicknesses (a) (After Novák [2]) Role of the thicknesses to brittleness and flexibility of the TE films (b) (After Morales-Masis et al.[1])

Besides the transmittance and conductivity, the film thickness of TEs also limits the application of TEs for specific optoelectronic devices[2]. Such as touchscreen devices that require film thickness less than 50 nm at 500 Ω/□, while solar cell devices require film thickness at 600 – 800 nm at 10 Ω/□ (Fig. 1-3). The temperature development during the thin film deposition and the post-treatment of the film will limit the substrates for the TEs. For flat panel display application, the required resistivity must be lower, which is 10^{-4} Ω.cm prepared at a high deposition rate with 50 nm of thickness and treated with a temperature below 200 °C[7]. While for solar cell applications, lower material cost is preferred[4]. For flexible devices, such as wearable optoelectronic devices, much thinner films and much lower temperature processes are preferred to ensure its applicability to the flexible substrates.

For these reasons, choosing and developing the right materials for TEs are both very important. The first type of TEs was a thin metal film prepared by evaporation and sputtering, introduced by the end of the nineteenth century [6]. In 1907, Bädeker produced TEs from oxide compounds that coined the term of transparent conductive oxides (TCOs) in the first place, including CdO, Cu_2O, and PbO[6]. For CdO, Bädeker obtained its resistivity as low as 1.2×10^{-3} Ω.cm, which is near to the functional resistivity requirement of TEs in the modern applications[6]. However, the main material of CdO is the cadmium (Cd) and is chemically toxic[7]. Thus, CdO-based TEs are difficult to use in practice. Since then, several attempts have been conducted to synthesize TEs, not only with new material with enhanced conductivity and transparency but also considering safety and sustainability. As the current advancement, tin-doped indium oxides (In_2O_3:Sn or ITO) is the most reliable TE, since it can be produced with practical thickness and lower temperature (200 °C) to be able to obtain good transparency and conductivity[7]. Since then, ITO has been heavily consumed with the boom of the flat-panel display industry.

However, it is expected that there will be a shortage of indium resources[3]. For that reason, it has increased the ITO price up to a factor of approximately ten[6,7]. A stable supply of ITO may be hard to secure for the continuously-expanding market for the flat panel display used in large screens and smart phones[3]. Therefore, the appropriate alternative of tin-doped indium oxides (ITO) is getting more and more urgent as the indium is considered to be highly-priced and expected to be scarce shortly. Moreover, the toxicity concerns of ITO[8] have been pushing, even more,

the research works in the field to find ITO alternatives with no toxicity and also made of more abundant materials. Minami[7] categorized TEs made of Cd-compounds or Indium-compounds are toxic. Therefore, ZnO-based TEs, along with appropriate metal dopants such as Al-doped ZnO (AZO) and Ga-doped ZnO (GZO), are heavily encouraged, as TEs made of abundant and non-toxic materials[4,7].

The research efforts to find the ITO alternatives are running not only through the material selections but also the nano-engineering of thin-film structures. The TE materials can be put as it is as a layer of a transparent conductive thin film or shaped with a nano-structured layer as well as combined or layered with other materials to form a transparent electrode layer. Ellmer[6] proposed four groups of TE structures, including a single-layered thin film, sandwiched or multilayer structures, periodic grids, and nanowire network (Fig. 1-4).

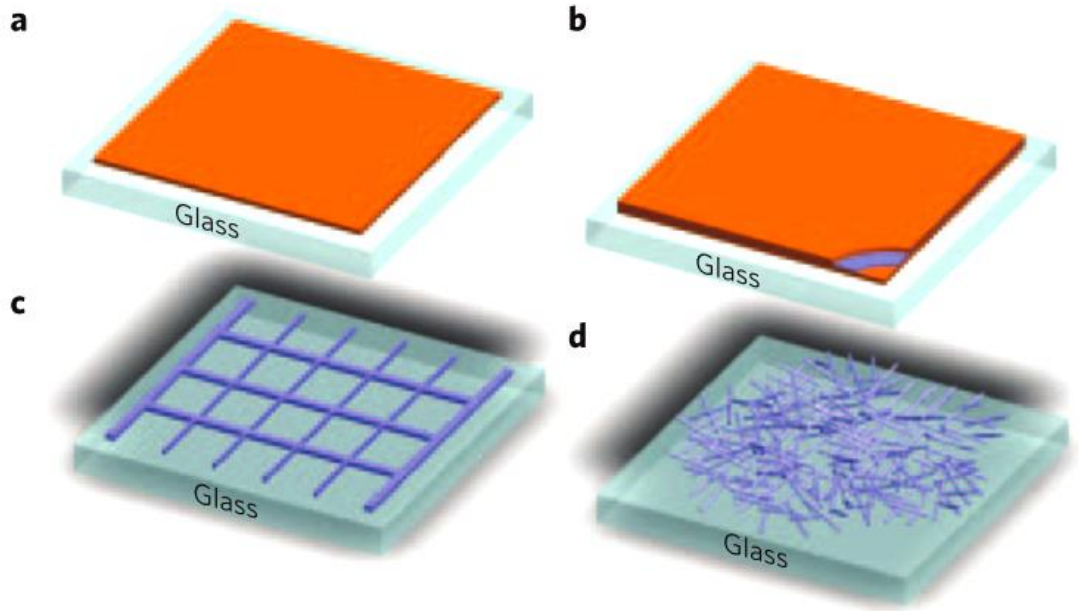

Fig. 1-4. Schematic thin film structures of different TEs including a single layer thin film (a), a sandwiched structure of several thin-film layers (b), periodic grid (c), or nanowire network (d)(After Ellmer [6])

Table 1-1. Reported properties of Several TEs

Structure	TE	Sheet resistance (Ω/□)	Visual transparency (%)	Flexibility	Material Cost	Ref
Single Layer	ITO	12	85	Poor	High	[6,9]
	AZO	10	80	Poor	Low	[23]
	Ag	11	75	Flexible	High	[24]
Nanowire (NW) network	Carbon Nanotube	500	83	Flexible	Low	[16]
	Ag NW	18	82	Flexible	High	[14]
Periodic Grid	Al Grid	18	75	Flexible	Low	[25]
	Ag NW Grid	10	85	Flexible	High	[17]
Multi-layer	ZnO/ Al/ ZnO	7.25	85	Flexible	Low	[20,26]
	AZO/ Al/ AZO	9	84	Flexible	Low	[20,21]
	AZO/ Al	5	65	Flexible	Low	[20,21]
	ZnO/ Ag/ ZnO	4	90	Flexible	High	[20,27]
	AZO/ Ag	6	87	Flexible	High	[9,20]
	Ag NW/ Graphene	33	94	Flexible	High	[28]
	AZO/ Ag NW/ AZO	309	83	Flexible	High	[29]
	Ag Grid/ PEDOT-PSS	9.1	79	Flexible	High	[1,30]

1) Single Layer TEs

Single-layer TEs include a single thin TCO layer (≤1000 nm)[4] or ultra-thin metal layer (≤10 nm)[9] (Fig. 1-4 a). As the dominant material of TEs, ITO employs this single-layer structure of an ITO thin film. TCOs other than ITO, such as F-doped SnO_2[6], AZO[10], and GZO[11], are using the same single-layer structure. Therefore, the applicability of these TCOs to replace ITO is very promising when acceptable transparency and conductivity are ensured while using the same single-layer structure and its similarly-associated widely-used preparation techniques. For a single-layered ultra-thin metal layer, the thickness parameter is more sensitive in comparison with the metal-doped oxides. By the thickness less then 1 μm, the metal-doped oxides are considered as transparent, while for the metal layer, it requires the thickness to be as thin as 10 nm or less. However, flexibility and long term electrical stability are still questionable for these single-layer TEs[12,13].

2) Nanowires

The TE layer with nanowire structure could be made of metal nanowire,[14] oxide nanowire,[15] or carbon nanotube[16]. These nanowire layers could achieve comparable electrical and optical properties of ITO with practical flexibility. However, these nanowire networks tend to degrade because of the junction resistance between the nanowires or nanotube[6]. Moreover, instability against oxidation, poor TE-substrate adhesion, and high surface-roughness are some of the key problems for nanowire transparent electrodes[14].

3) Periodic Grid

TEs with a periodic grid structure is reproducible and uniform due to its highly programmable, predictable, and stable fabrication methods such as chemical etching of thin films, metal transfer printing, lithography, and metal lift-off[6,13,17]. This periodic grid structure could be applied to a layer of any TE films, including ultrathin metal films,[6] TCOs,[18] and nanowire[17]. This advantage of this structure is to improve the usability of the TE layer for flexible substrates, increasing its stability in facing bending deformation by stopping the propagation of cracks, especially for TCO layers such as ITO[13].

4) Sandwiched or Multilayer Structures

For sandwiched or multilayer structures, two or more layers of transparent electrodes are sandwiched together to form a new structure of a transparent electrode. Each layer could be one of any TE material with any thin-film structures, including a single layer, periodic grid, or nanowire[6,19]. The combination of dielectric and metal layers, such as TCO/metal/TCO is usually implemented for this multilayer structure[20]. The key advantage of this structure is that the films could reach good conductivity with thinner overall film thickness [21] in comparison with the single layer of a TCO film. Furthermore, processes without annealing or post heat treatment can give an acceptable conductivity at a low temperature, which is suitable for polymer-based flexible substrates.

Table 1-1 summarized several reports on electrical properties and stability as well as the physical characteristics of several TE materials, based on the four TE structures proposed by Ellmer[6]. Out of many types of TEs, AZO has been showing fascinating characteristics, which are very near to ITO properties. Furthermore, several new AZO-based TCEs are being developed, such as in multilayer structures[21] and nanorods[22]. Moreover, Liu et al.[4] emphasized AZO as the best candidate for ITO alternatives from the viewpoint of cost, material availability, and environments. For those reasons, this research is focused on deepening and advancing the insights of AZO TEs.

1.2. Al-doped ZnO (AZO) thin-film as a TE material

ZnO-based TEs are made of abundant materials,[4] relatively lower in material cost,[2] and chemically non-toxic[7] comparatively to ITO [4,7,8]. Out of many ZnO-based TEs, Liu et al. [4] proposed AZO as the most promising one. The more abundant material, lower material cost, and non-toxicity of Al (Fig. 1-5) as the metal dopant are some of the reasons in comparison with other dopants, such as B, Ga, In, and V, for ZnO-based TE counterparts.

AZO and ITO are both included in the TCO group of TEs, applied as a single layer thin film TEs. The similarity in the application and preparation of both, AZO and ITO, could guarantee a smooth transition from ITO to AZO, whenever the stability, thickness, optoelectrical properties of AZO are met as an ITO alternative. For the visual transmittance, AZO material is around 85%, very comparable to ITO [6].

In an un-doped state (Fig. 1-6 a), ZnO is practically an insulator at room temperature with carrier concentrations as low as 10^{-15} cm^{-3}[32]. The creation of defects within the crystal structure, particularly oxygen vacancies (V_o) of ZnO, would provide intrinsic donors and increase the free carrier density. Another intrinsic donor is the Zn interstitial, which should be maintained by avoiding the creation of Zn vacancies (V_{Zn}). With less V_{Zn}, the ZnO-thin film exhibits eventually higher carrier concentration. With this optimization of intrinsic donors, the donor level will rise up, near the conduction band (Fig. 1-6 b).

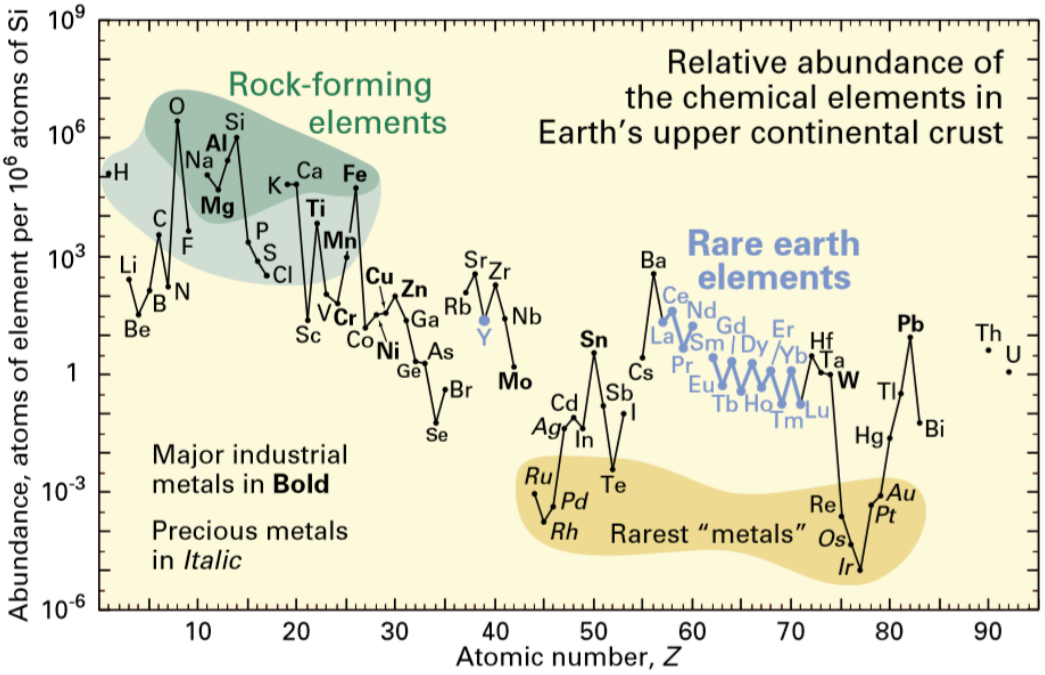

Fig. 1-5. The abundance of Al as a dopant for ZnO-based TEs in comparison with the abundance of other metal dopants, including In, V, Ga, and B (After Haxel et al.[31])

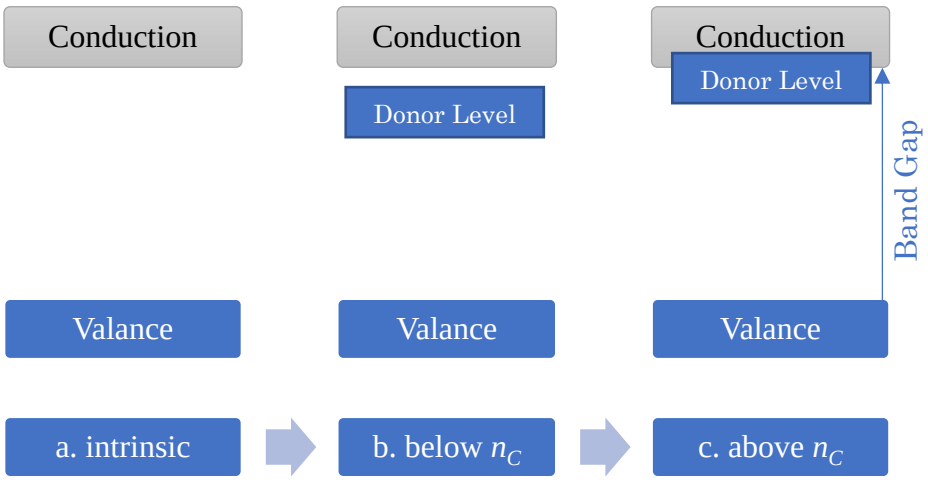

Fig. 1-6. Schematic diagram development from electrical insulating ZnO to electrically conductive AZO (n_c = critical carrier concentrations)

.

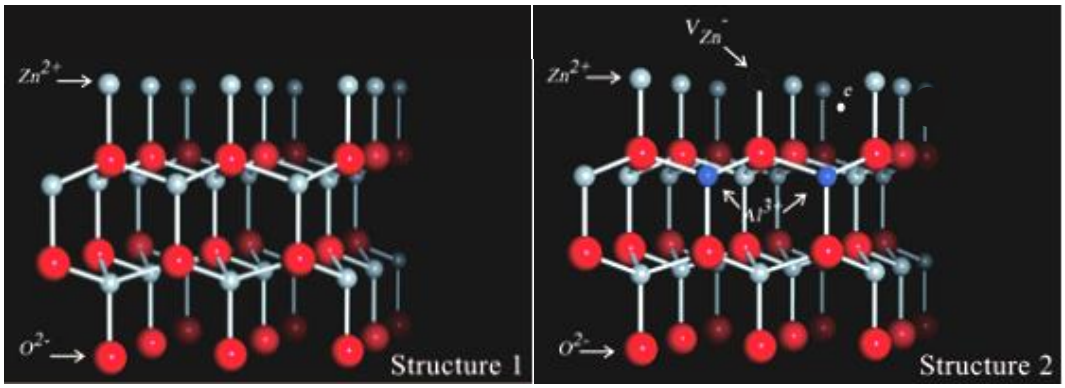

Fig. 1-7. ZnO crystal (structure 1) and AZO crystal (structure 2) where Al substitute Zn at hexagonal lattice at ZnO crystal [22].

However, within the optimization of the intrinsic donors, the critical carrier concentrations n_c are usually not achieved. Therefore, extrinsic doping is realized by putting foreign atoms to the crystal structure of ZnO, wherein the case of AZO, Al^{3+} atom, is introduced to replace Zn^{2+} in the hexagonal lattice (Fig. 1-7).

The introduced Al^{3+} atom is called as dopant or donor, increasing the carrier concentration to reach the critical concentration n_c. At this point, the donor level will overlap the conduction band, and the electrons act the free charge carriers as in the conventional conductive materials (Fig. 1-6 c).

Besides intrinsic and extrinsic donors, crystal growth orientation plays an important role in the conductivity of AZO films[33]. As Al replace the Zn in the hexagonal lattice, the crystal orientation of AZO films naturally follows the orientation of ZnO crystals, including (002), (110), (100), etc. Each crystal orientation will influence the microstructure of the films (Fig. 1-8).

One of the great interests of ZnO-based transparent electrodes, including AZO thin films, is the doping of hydrogen. As reported by Van de Walle and Neugebauer[34], ZnO exhibits different phenomena, where hydrogen is always acting as a donor (Fig. 1-9). On the other hand, the hydrogen could act as both, acceptor and donor in the other semiconductor such as GaN [34,35].

This hydrogen-doping could be conducted by incorporating hydrogen during the deposition of the ZnO-based thin films. Such as in the sputtering method, hydrogen gas could be incorporated with the mixture of Ar and O_2 as a reactive atmosphere in the reactive sputtering. As reported by Ondok and Musil[36], the resistivity of reactive-sputtered TCO is significantly reduced by sputtering that incorporated hydrogen gas.

However, it is not clear if the same improvement would work on ZnO-based TCOs. Through simulation and computational approach, Bustanafruz et al.[37] proposed that doping the ZnO with hydrogen would create O-H bond, located at bond-center in parallel or perpendicular to the *c*-axis (Fig. 1-10).

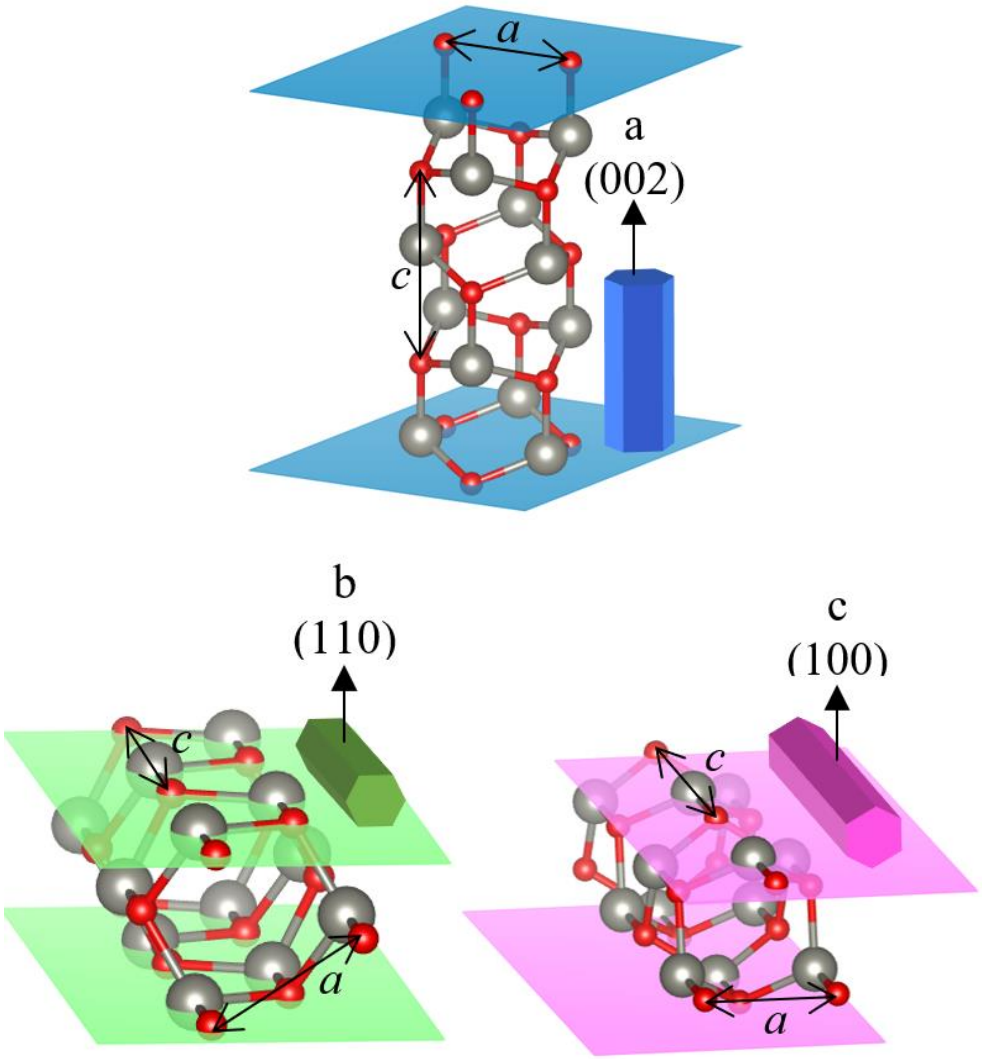

Fig. 1-8. Schematic illustrations about the influence of crystal growth orientation on the microstructure of ZnO films. Growth orientation (002) corresponds to a columned structure where the *c*-axis is perpendicular to the substrate (a); (110) corresponds to a polygon structure where c-axis is parallel to the substrate; (100) corresponds to a pyramid-like structure where c-axis is parallel to the substrate. (Computed and visualized using Vesta, c = 0.530682 nm and a = 0.328910 nm, with data from materialsprojects.org)

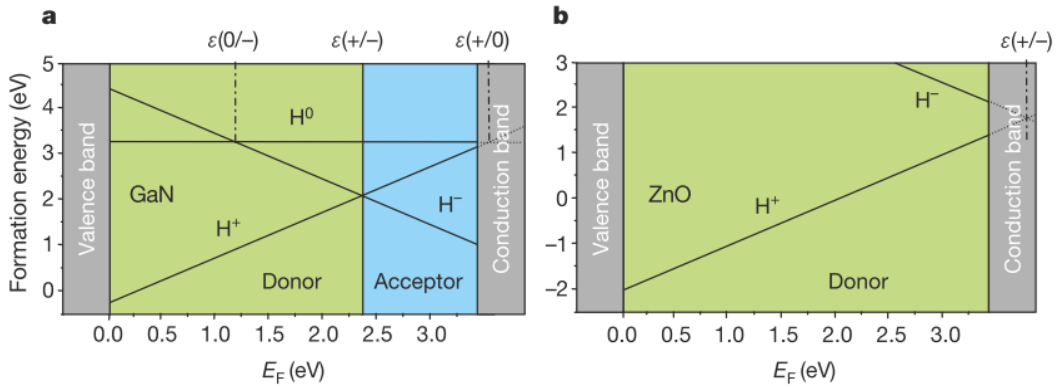

Fig. 1-9. Phenome of Hydrogen on semiconductor that usually act as both, acceptor and donor (a), while in the ZnO, the hydrogen would act always as donor (b) (After Van der Wall and Neugebauer [34])

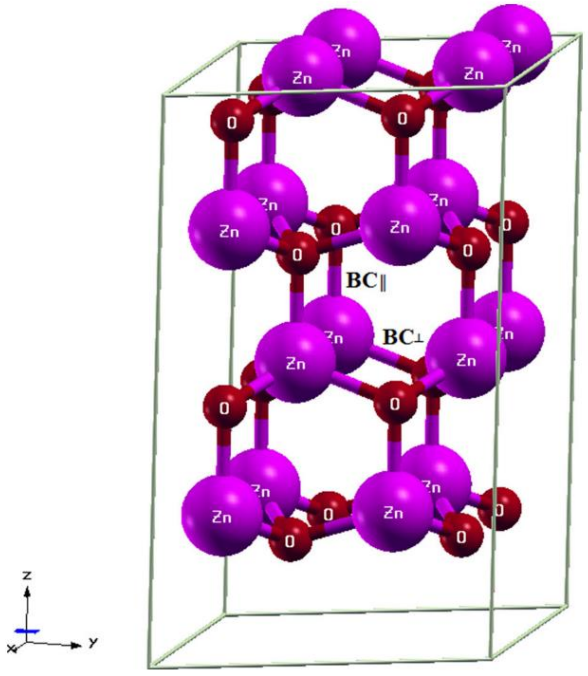

Fig. 1-10. O-H Bond center (BC) in the ZnO crystal, located in parallel ($BC_{\parallel}$) and perpendicular ($BC_{\perp}$) to the c-axis (After Bustanafruz et al.[37])

1.3. Sputtering for AZO thin-film deposition

AZO transparent electrodes are applied as thin films. Therefore, all thin film deposition techniques are capable of AZO thin film deposition, including sputtering, sol-gel dip coating, spin coating, spray pyrolysis, atomic layer deposition (ALD), chemical vapor deposition (CVD), or metal-organic CVD (MOCVD)[1,6]. Out of those many deposition techniques, Ellmer[6] and Liu et al. [4] pointed out that sputtering is one of the most capable, providing high deposition rate, capability for large deposition area, and acceptable results.

Currently, sputtering is being extensively utilized in the industry[6]. ALD is well known to produce high-quality thin films[4]. However, the slow deposition-rate of ALD limits its usability for lab-scale works[6]. Tabassum et al.[38] reported the superiority of AZO film prepared by sputtering over sol-gel dip-coating by producing relatively fewer voids to the film, contributing much more stability in the harsh environment.

During the sputtering process of AZO films, a target (or cathode) plate is bombarded by energetic ions generated in a glow discharge plasma of a sputtering gas or mixed-gasses, situated just above the target. Various targets could be used AZO film deposition by sputtering, such as a ceramic AZO target,[39] a metal alloy Zn:Al target,[40] or a metal Zn target with addition Al chips on top[41]. When a ceramic target is used, non-reactive sputtering can be conducted utilizing Ar gas. On the other hand, reactive sputtering is conducted in a reactive atmosphere of Ar and O_2 mixture when a metallic target is used. As those targets are sputtered, the bombardment causes the removal of target atoms, which may then condense on a substrate as an AZO thin film.

One of the challenges for the sputtering method is the elevated substrate temperature during the deposition, even without being intentionally heated up to 80 ºC or more[42], which limits the usage of flexible substrates. This elevated temperature is getting higher as sputtering duration becomes longer or higher radio frequency (RF) power is used. Therefore, it is very important to shorten the duration of sputtering with an RF power below 90 W to maintain an acceptable low temperature for the substrate. However, the trade-off between the thin film quality and maintaining the substrate

temperature could be an issue in this conventional sputtering method (Figure 1-11).

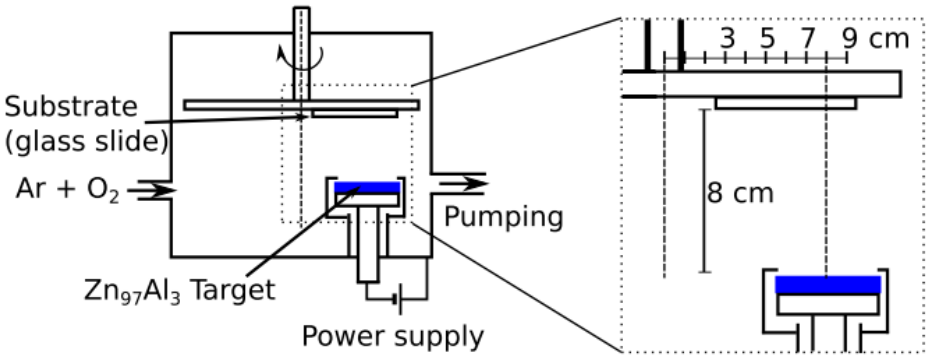

Fig. 1-11. Schematic diagram of the conventional sputtering method (After Mickan et al.[40])

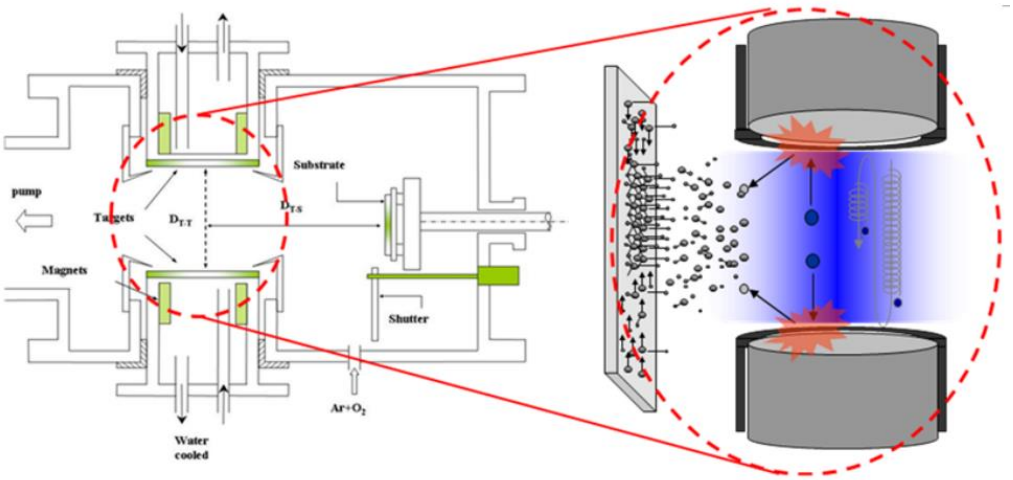

Fig. 1-12. Schematic diagram of the FTS system (After Jung et al.[42])

Concerning these issues, Jun et al.[42] proposed an unconventional sputtering method called as facing target sputtering (FTS) that could maintain substrate temperature at 50 ºC up to 80 min of sputtering. As compared to the conventional sputtering where the substrate is parallel with and put just above the target (Fig 1-11), FTS put the substrate perpendicular with and a bit away from the target (Fig. 1-12).

1.4. Usability improvement of AZO transparent electrodes

As reported by Novak,[2] under the appropriate conditions of sputtering, AZO films are able to achieve the TE quality comparable to ITO; the confirmed optimum deposition temperature of an AZO thin film is 300 ºC, and the thickness should be higher than 500 nm. These conditions are acceptable for solar cell applications, but not for touch screens or LED/OLED devices (Fig. 1-3). Minami[7] highlighted that AZO film should exhibit a resistivity in the order 10^{-4} Ωcm at the thickness of 50 nm prepared at a temperature level of 200 °C or lower in order to be suitable for display applications. Lie et al.[4] pointed out the issues of the stability of AZO films to the exposure of moisture and oxidation, which questions the applicability of AZO for any outdoor applications, including solar cells.

With the emerging flexible-wearable device[13] and space environment application, the thermal budget of these applications is lower than 200 °C, limited by the type of the utilized substrates. These emerging applications are encouraging polymer-based substrates, such as polyethylene (PET), polyimide, or a composite of polyimide (PI) film attached to polycarbonate (PC)[43].

Recyclability of LED devices has become a great interest due to ever-increasing worldwide electronic demands, which has placed Ga and In metals as supply chain critical metal[44]. Furthermore, Mickan et al.[45] suggested that the recovery of AZO films could be a great of interests.

These challenges for AZO TEs are paving the way to increase the usability of AZO films, which are:

1) Ensuring long-term stability or durability of AZO films exposed to a harsh environment to meet the expectation of outdoor applications including solar cells.

2) Proposing a recovery method for the degraded AZO films.

3) Proposing a sputtering configuration to produce high conductive and stable AZO films at low temperatures and high deposition-rate, meeting the budget of emerging flexible and space-environment applications.

4) Producing AZO films at a thickness of 50 – 150 nm with high conductivity for touch screens and LED devices.

1.5. Thesis objectives and framework

As discussed in section 1.4, the recoverability is one of the ways to extend the usability of the AZO TEs. Mickan et al. [45] reported that the recoverability of AZO TEs could be great interest, especially for a single layer of AZO devices such as antistatic films, low emissivity coatings, or transparent heaters. The reported recovery methods, however, which are post-heat treatment under nitrogen[45] and vacuum[46] annealing, were not restoring the conductivity perfectly. Therefore, a different method should be proposed for this recovery method of AZO TEs (detailed in chapter 2, section 2.1).

The durability of AZO thin films is still an issue. Therefore, the role of the crystal orientation of the film should be clarified in order to improve the AZO TEs for durability. The role of crystal orientation to the electrical property is already clarified[33], while its role for durability is not yet clear.

The reported result of comparing AZO films having different major crystal orientations was using a different method of deposition in order to produce different crystal orientations [38], which could not clarify the role of crystal

orientation since the different methods of deposition also provide different degradation rate. Therefore, the comparison should be conducted by using AZO samples deposited by the same method, where there is a paucity in the research field (detailed in chapter 2 section 2.2).

To prepare AZO thin films by a standard RF magnetron sputtering system at low temperature without post heat treatment is very important to extend the usability of AZO TEs for devices utilizing polymer-based substrates[42], which gained interest for flexible substrates[47] and outer space application[43]. Therefore, the low-temperature preparation and the durability investigation are very important for the sputtered AZO thin film on polymer-based substrates, which are not widely covered in the literature (detailed in chapter 2, section 2.3).

This thesis is focusing on the recoverability, role of crystal orientation to the durability, and the low-temperature preparation of AZO films. However, this thesis is not covering the optimization of the thickness of AZO TEs, since the durability and low-temperature preparation issue should be firstly solved before the thickness optimization, even though the thickness is a very important parameter especially for touchscreen and display application[2,48]. Nevertheless, the finding in this thesis could be utilized further for the thickness optimization of AZO-based TEs in future research.

This thesis is firstly investigating the recoverability of the electrical properties of AZO films, seeking a better recoverability method for AZO films after being degraded in the harsh environment. The hydrogen atmosphere is used in this thesis to investigate its effectiveness for the recoverability method of AZO films. The evolution of the electrical properties, including resistivity, carrier concentration, and mobility, are investigated before and after exposure to a harsh environment as well as after being recovered.

Secondly, this thesis is looking at the possibilities of extending the usability of AZO films through improved durability of the films exposed to a harsh environment. The improvement is pursued through both post-heat treatment and optimizing sputtering configuration. Producing various major crystal orientations of the AZO thin films using reactive RF magnetron sputtering method is also pursued in this thesis.

Thirdly, a low-temperature process without post-heat treatment is investigated on glass and polymer-based substrates. Finally, the lessons learned and the recommendation to meet the challenges of extending the usability of AZO films are summarized and proposed, respectively.

The framework of this thesis is presented as follows: chapter 2 reviews the literature highlighting the novelty of this thesis; chapter 3 describes the experimental, and characterization methods used in this thesis; chapter 4 investigates the evolution and the recovery of electrical properties of AZO TEs after being exposed to the harsh environment; chapter 5 studies the role of crystal orientation for the durability of AZO TEs exposed to harsh environment by preparing AZO films with various crystal growth orientations; chapter 6 proposes a method to optimize the conventional sputtering method to be suitable for a low-temperature process and test the obtained films on glass and polymer-based substrates; chapter 7 discusses several models for the durability improvement of AZO TEs; chapter 8 presents summaries of this thesis and proposes a future path for the improvement of AZO TEs.

Reference

[1] M. Morales-Masis, S. De Wolf, R. Woods-Robinson, J.W. Ager, C. Ballif, Transparent Electrodes for Efficient Optoelectronics, Adv. Electron. Mater. 3 (2017) 1600529. doi:10.1002/aelm.201600529.

[2] P. Novák, Possibilities of Increasing the Usability of Sputtered AZO Films as a Transparent Electrode, Phys. Status Solidi. 216 (2019) 1800814. doi:10.1002/pssa.201800814.

[3] C.C. Pavel, A. Marmier, E. Tzimas, T. Schleicher, D. Schüler, M. Buchert, D. Blagoeva, Critical raw materials in lighting applications: Substitution opportunities and implication on their demand, Phys. Status Solidi Appl. Mater. Sci. 213 (2016) 2937–2946. doi:10.1002/pssa.201600594.

[4] H. Liu, V. Avrutin, N. Izyumskaya, Ü. Özgr, H. Morkoç, Transparent conducting oxides for electrode applications in light emitting and absorbing devices, Superlattices Microstruct. 48 (2010) 458–484. doi:10.1016/j.spmi.2010.08.011.

[5] A. Gupta, A.D. Compaan, All-sputtered 14% CdS/CdTe thin-film solar cell with ZnO: Al transparent conducting oxide, Appl. Phys. Lett. 85 (2004) 684–686. doi:10.1063/1.1775289.

[6] K. Ellmer, Past achievements and future challenges in the development of optically transparent electrodes, Nat. Photonics. 6 (2012) 808–816. doi:10.1038/nphoton.2012.282.

[7] T. Minami, Present status of transparent conducting oxide thin-film development for Indium-Tin-Oxide (ITO) substitutes, Thin Solid Films. 516 (2008) 5822–5828. doi:10.1016/j.tsf.2007.10.063.

[8] E.M. Bomhard, The toxicology of indium tin oxide, Environ. Toxicol. Pharmacol. 45 (2016) 282–294. doi:10.1016/j.etap.2016.06.011.

[9] D.S. Ghosh, T.L. Chen, N. Formica, J. Hwang, I. Bruder, V. Pruneri, High figure-of-merit Ag/Al:ZnO nano-thick transparent electrodes for indium-free flexible photovoltaics, Sol. Energy Mater. Sol. Cells. 107 (2012) 338–343. doi:10.1016/j.solmat.2012.07.009.

[10] F. Machda, T. Ogawa, H. Okumura, K.N. Ishihara, Evolution and Recovery of Electrical Property of Reactive Sputtered Al-Doped ZnO Transparent Electrode Exposed to Harsh Environment, Phys. Status Solidi Appl. Mater. Sci. 217 (2020) 1–6. doi:10.1002/pssa.201900519.

[11] J. Juang, T. Chou, H. Lin, Y. Chou, C. Weng, Applied Surface Science Trajectory effect on the properties of large area ZnO thin films deposited by atmospheric pressure plasma jet, Appl. Surf. Sci. 314 (2014) 1074–1081. doi:10.1016/j.apsusc.2014.05.220.

[12] S. Tabassum, E. Yamasue, H. Okumura, K.N. Ishihara, Damp heat stability of AZO transparent electrode and influence of thin metal film for enhancing the stability, J. Mater. Sci. Mater. Electron. 25 (2014) 3203–3208. doi:10.1007/s10854-014-2004-1.

[13] K. Sakamoto, H. Kuwae, N. Kobayashi, A. Nobori, S. Shoji, J. Mizuno, Highly flexible transparent electrodes based on mesh-patterned rigid indium tin oxide, Sci. Rep. 8 (2018) 3–4. doi:10.1038/s41598-018-20978-x.

[14] S. Nam, M. Song, D.H. Kim, B. Cho, H.M. Lee, J.D. Kwon, S.G. Park, K.S. Nam, Y. Jeong, S.H. Kwon, Y.C. Park, S.H. Jin, J.W. Kang, S. Jo, C.S. Kim, Ultrasmooth, extremely deformable and shape recoverable Ag nanowire embedded transparent electrode, Sci. Rep. 4 (2014) 1–7. doi:10.1038/srep04788.

[15] R. Kӧnenkamp, A. Nadarajah, R.C. Word, J. Meiss, R. Engelhardt, ZnO nanowires for LED and field-emission displays, J. Soc. Inf. Disp. 16 (2008) 609. doi:10.1889/1.2918081.

[16] Z. Yu, X. Niu, Z. Liu, Q. Pei, Intrinsically Stretchable Polymer Light-Emitting Devices Using Carbon Nanotube-Polymer Composite Electrodes, (2011) 3989–3994. doi:10.1002/adma.201101986.

[17] C. Lee, C. Kim, M. Jeong, J. Kim, J. Lee, J. Oh, J. Lee, H. Kim, S. Park, J. Kim, RSC Advances Highly fl exible and transparent metal grids made of metal nanowire networks †, RSC Adv. 5 (2015) 77288–77295. doi:10.1039/C5RA14513A.

[18] K. Sakamoto, H. Kuwae, N. Kobayashi, A. Nobori, S. Shoji, J. Mizuno, Using Mesh Patterned Indium Tin Oxide for Flexible Electronic Devices, (2017) 323–326.

[19] S. You, Y.S. Park, H.W. Choi, K.H. Kim, Fabrication of Ag nanowire and Al-doped ZnO hybrid transparent electrodes, Jpn. J. Appl. Phys. 55 01AE14 (2016).

[20] C. Guillén, J. Herrero, Critical review TCO / metal / TCO structures for energy and fl exible electronics, Thin Solid Films. 520 (2011) 1–17. doi:10.1016/j.tsf.2011.06.091.

[21] Y.S. Lin, W.C. Tseng, Effect of al nanoparticles on the microstructure, electrical, and optical properties of AZO/Al/AZO trilayer thin film, J. Electron. Mater. 41 (2012) 437–441. doi:10.1007/s11664-011-1810-y.

[22] R. Chen, P. Zhu, L. Deng, T. Zhao, R. Sun, C. Wong, Effect of aluminum doping on the growth and optical and electrical

properties of ZnO nanorods, Chempluschem. 79 (2014) 743–750. doi:10.1002/cplu.201300398.

[23] F. Machda, T. Ogawa, H. Okumura, K.N. Ishihara, Damp-heat durability comparison of Al-doped ZnO transparent electrodes deposited at low temperatures on glass and PI-tape / PC substrates, Ceram. Int. (2020) 0–1. doi:10.1016/j.ceramint.2020.03.173.

[24] Y.G. Bi, Y.F. Liu, X.L. Zhang, D. Yin, W.Q. Wang, J. Feng, H.B. Sun, Ultrathin Metal Films as the Transparent Electrode in ITO-Free Organic Optoelectronic Devices, Adv. Opt. Mater. 7 (2019) 1–23. doi:10.1002/adom.201800778.

[25] M.G. Kang, L.J. Guo, Nanoimprinted semitransparent metal electrodes and their application in organic light-emitting diodes, Adv. Mater. 19 (2007) 1391–1396. doi:10.1002/adma.200700134.

[26] E.R. Rwenyagila, B. Agyei-Tuffour, M.G. Zebaze Kana, O. Akin-Ojo, W.O. Soboyejo, Optical properties of ZnO/Al/ZnO multilayer films for large area transparent electrodes, J. Mater. Res. 29 (2014) 2912–2920. doi:10.1557/jmr.2014.298.

[27] J.H. Kim, J.Y. Na, S.K. Kim, Y.Z. Yoo, T.Y. Seong, Highly Transparent and Low-Resistance Indium-Free ZnO/Ag/ZnO Multilayer Electrodes for Organic Photovoltaic Devices, J. Electron. Mater. 44 (2015) 3967–3972. doi:10.1007/s11664-015-3811-8.

[28] M.-S. Lee, K. Lee, S.-Y. Kim, H. Lee, J. Park, K. Choi, H.-K. Kim, D. Kim, D. Lee, S. Nam, J. Park, High-Performance, Transparent, and Stretchable Electrodes Using Graphene–Metal Nanowire Hybrid Structures, Nano Lett. 13 (2013) 2814–2821. doi:10.1021/nl401070p.

[29] Q. Xu, W. Shen, Q. Huang, Y. Yang, R. Tan, K. Zhu, N. Dai, W. Song, Flexible transparent conductive films on PET substrates with an AZO/AgNW/AZO sandwich structure, J. Mater. Chem. C. 2 (2014) 3750–3755. doi:10.1039/C3TC32554G.

[30] J. Zou, H.L. Yip, S.K. Hau, A.K.Y. Jen, Metal grid/conducting polymer hybrid transparent electrode for inverted polymer solar cells, Appl. Phys. Lett. 96 (2010). doi:10.1063/1.3394679.

[31] G.B. Haxel, J.B. Hedrick, G.J. Orris, Rare Earth Elements — Critical Resources for High Technology, 2002. http://geopubs.wr.usgs.gov/fact-sheet/fs087-02/.

[32] K. Ellmer, A. Klein, B. Rech, Transparent Conductive Zin Oxide Basic and Applications in Thin Film Solar Cells, 2008. doi:10.1007/978-3-540-73612-7.

[33] K. Maejima, H. Shibata, S. Niki, H. Tampo, K. Matsubara, Correlation between Electrical Properties and Crystal c -Axis Orientation of Zinc Oxide Transparent Conducting Films, Jpn. J. Appl. Phys. 51 (2013) 10NC16. doi:10.7567/jjap.51.10nc16.

[34] C.G. Van de Walle, J. Neugebauer, Universal alignment of hydrogen levels in semiconductors, insulators and solutions, Nature. 423 (2003) 626–628. doi:10.1038/nature01665.

[35] C.G. Van De Walle, Universal alignment of hydrogen levels in semiconductors and insulators, Phys. B Condens. Matter. 376–377 (2006) 1–6. doi:10.1016/j.physb.2005.12.004.

[36] V. Ondok, J. Musil, Effect of hydrogen on reactive sputtering of transparent oxide films, Plasma Process. Polym. 4 (2007) 319–324. doi:10.1002/ppap.200730901.

[37] F. Bustanafruz, M. Fazli, M.R. Mohammadizadeh, M. Jafar Tafreshi, Optical and electronic properties of H-doped ZnO, Opt. Quantum Electron. 48 (2016). doi:10.1007/s11082-016-0575-1.

[38] S. Tabassum, E. Yamasue, H. Okumura, K.N. Ishihara, Sol–gel and rf sputtered AZO thin films: Analysis of oxidation kinetics in harsh environment, J. Mater. Sci. Mater. Electron. 25 (2014) 4883–4888. doi:10.1007/s10854-014-2248-9.

[39] Q. Shi, K. Zhou, M. Dai, H. Hou, S. Lin, C. Wei, Room temperature preparation of high performance AZO films by MF sputtering,

Ceram. Int. 39 (2013) 1135–1141.
doi:10.1016/j.ceramint.2012.07.037.

[40] M. Mickan, U. Helmersson, H. Rinnert, J. Ghanbaja, D. Muller, D. Horwat, Room temperature deposition of homogeneous, highly transparent and conductive Al-doped ZnO films by reactive high power impulse magnetron sputtering, Sol. Energy Mater. Sol. Cells. 157 (2016) 742–749. doi:10.1016/j.solmat.2016.07.020.

[41] F. Machda, T. Ogawa, H. Okumura, K.N. Ishihara, Damp Heat Durability of Al-Doped ZnO Transparent Electrodes with Different Crystal Growth Orientations, ECS J. Solid State Sci. Technol. 8 (2019) Q240–Q244. doi:10.1149/2.0261912jss.

[42] Y. Sup Jung, H. Wook Choi, K. Hwan Kim, S. Joon Park, H. Hee Yoon, Properties of AZO Thin Films for Solar Cells Deposited on Polycarbonate Substrates, J. Korean Phys. Soc. 55 (2009) 1945–1949. doi:10.3938/jkps.55.1945.

[43] D.T. Peterside, J.E. Palaia, A.C. Schuerger, M.J. Correll, R.A. Bucklin, Testing of Greenhouse Cladding Materials for Space Environments, Part 2: Laminates, Appl. Eng. Agric. 34 (2018) 575–580. doi:10.13031/aea.12465.

[44] B. Swain, C. Mishra, L. Kang, K.S. Park, C.G. Lee, H.S. Hong, Recycling process for recovery of gallium from GaN an e-waste of LED industry through ball milling, annealing and leaching, Environ. Res. 138 (2015) 401–408. doi:10.1016/j.envres.2015.02.027.

[45] M. Mickan, M. Stoffel, H. Rinnert, U. Helmersson, D. Horwat, Restoring the Properties of Transparent Al-Doped ZnO Thin Film Electrodes Exposed to Ambient Air, J. Phys. Chem. C. 121 (2017) 14426–14433. doi:10.1021/acs.jpcc.7b03020.

[46] T. Tohsophon, J. Hüpkes, S. Calnan, W. Reetz, B. Rech, W. Beyer, N. Sirikulrat, Damp heat stability and annealing behavior of aluminum doped zinc oxide films prepared by magnetron sputtering, Thin Solid Films. 511–512 (2006) 673–677. doi:10.1016/j.tsf.2005.12.130.

[47] Y.S. Woo, Transparent conductive electrodes based on graphene-related materials, Micromachines. 10 (2018) 24–28. doi:10.3390/mi10010013.

[48] T. Minami, Substitution of transparent conducting oxide thin films for indium tin oxide transparent electrode applications, Thin Solid Films. 516 (2008) 1314–1321. doi:10.1016/j.tsf.2007.03.082.

2. Literature Review

As discussed in the introduction (Chapter 1), durability, recoverability, and low-temperature deposition are some of the main challenges for extending the usability of the AZO transparent electrode. In this chapter, those three challenges are comprehensively reviewed from the latest scientific literature, focusing on the recoverability of AZO transparent electrodes (TEs) (section 2.1), the role of crystal growth orientation of AZO TEs (section 2.2), low-temperature deposition (section 2.3). and damp-heat (DH) durability between AZO and other TEs. In summary (section 2.5), key findings on the reviewed literature are provided, as well as the originality or the novelty of the current thesis are highlighted among other AZO-related researches.

2.1. Recoverability of AZO transparent electrodes

Mickan et al.[1] suggested that the recovery of electrical properties of AZO films could be a great of interest, especially an annealing procedure to restore the properties of the material in applications of single-layer AZO, such as antistatic films, low emissivity coatings, or transparent heaters. However, this annealing procedure might not be feasible for heat-sensitive multilayer devices from a practical point of view. The deposition technique of AZO films is also defining whether this annealing is feasible or not. Such the degraded AZO thin film deposited via sol-gel dip-coating due to the exposure of a harsh environment where several cracks or voids were produced[2]. On the other hand, sputtered AZO thin films exhibit no cracks[2]. Even though, conductivity, carrier concentration, and Hall mobility of both, sol-gel coated and sputtered AZO films were decreased. With the produced cracks, the conductivity degraded more for AZO thin films prepared by both sol-gel, in comparison with the sputtered films, where physical and chemical damage degraded the sol-gel coated AZO thin films with even higher degradation rate.

Tohsophon et al.[3] reported that annealing in a vacuum atmosphere up to 250 °C could recover the degraded electrical property of sputtered AZO thin films after being exposed to a damp heat environment for 1000 h. Vacuum annealing at 650 ºC effectively produced very stable AZO films even after being exposed to damp-heat treatment for 1000 h, which was suggesting the effectiveness of annealing in vacuum at higher temperatures [4]. This stable AZO film was attributed to the grain boundary reconstruction, as suggested by Hüpkes et al.[4] where grains grew together and closed grain boundaries partially.

Nitrogen (N_2) annealing at 180 °C could restore the property of sputtered AZO thin films aged for six months in the ambient air, as reported by Mickan et al.[1], where out-diffusion of water molecule was suggested as the reason for the restored property of the films. This finding could confirm no physical damage during the degradation test of AZO films. Thus recoverability through annealing the films is feasible. However, in these two reports, the proposed annealing configurations with N_2 or vacuum at 180 – 250 ºC, could recover the conductivity of the degraded thin films but not as much as the original one before the degradation test.

A higher temperature of re-annealing of the degraded AZO thin film seems to be able to recover more effectively. Mickan et al.[5] reported that better electrical property and stability of AZO films are produced via a higher substrate temperature during the deposition. Tabassum et al.[6] reported similar tendencies, where high-temperature of vacuum annealing after deposition of the films produced better conductivity and stability of the films.

Besides higher temperatures, the hydrogen atmosphere for the annealing seems to be able to produce better recovery for the degraded AZO films. Tabassum et al.[2,7] reported for sputtered AZO thin films that high-temperature annealing (450 ºC or higher) in a hydrogen atmosphere was effective in enhancing the electrical stability and crystallinity property. Besides, the spontaneous formation of a very thin oxide layer as a top protective layer against moisture attack was formed via annealing at a higher temperature, providing AZO thin films with better electrical stability [6].

However, the effectiveness of annealing in hydrogen at high temperature on the electrical property recovery of the degraded films is not extensively discussed. Moreover, the characteristic of the ultra-thin layer remains elusive for this recovery route for the degraded AZO thin films.

2.2. Role of crystal orientations of AZO transparent electrodes

Crystal orientation has been reported to be very important to the property of AZO films, where the orientation (002) exhibit higher optoelectrical properties for AZO thin films, while other specific crystal orientation could act as traps for carriers[8]. Therefore, most of AZO films have been reported to have the main crystal orientation (002)[6,9], which is considered as the most effective morphology due to more reduced numbers of electron traps in comparison with other crystal orientations[8,10]. However, its role in durability is not yet widely discussed.

Tabassum et al.[2] reported that different deposition methods could produce AZO thin films with different textures, (002) and (110) respectively by the sol-gel dip-coating and the radio frequency (RF) magnetron sputtering respectively. According to this report, the sputtered AZO films with the orientation (110) was more durable, strongly suggesting the influence of deposition methods on the durability of AZO films but was not enough in attributing the role of crystal orientation for the durability of the films. Zhan et al.[9] reported that AZO films with the orientation (002) prepared by RF magnetron sputtering and zinc vapor annealing exhibited very high durability in a damp heat condition. Besides the main orientation (002), the removal of zinc vacancies by zinc vapor annealing was strongly suggested as the reason for this improved durability. With a comparison of these findings, the role of crystal orientation to the durability of sputtered AZO films remains elusive.

In order to clarify the role of crystal growth orientation, the compared AZO films should be produced with the same deposition method, which is sputtering in this thesis. However, producing different peaks of strong crystal growth orientations for AZO films via sputtering is not widely reported. Furthermore, the microstructures of the AZO films were not

extensively discussed in regard to the relation with the existence of other orientations and the mechanism of electrical conductivity degradation of AZO films.

2.3. Low-temperature preparations of the AZO thin films

Preparations of AZO films via a low-temperature configuration without annealing (post-heat treatment) are preferable for flexible optoelectronic devices, such as flexible electronics [11], electronic skin [12], and flexible solar cells [13]. This is due to the certain flexible substrates limiting the thermal budget in fabricating those devices, such as polyimide [14,15] and polycarbonate[16] materials. Those polymer-based flexible substrates cannot survive such high temperatures during the thin film deposition process or post-heat-treatment [16,17]. In comparison with glass substrates that could face high-temperature processes up to 600 °C [6], polyimide-based substrates require a process at a temperature lower than 177 °C [18].

Polyimide materials having the mold temperature range of 177 to 232 °C [18] are feasible for typical sputtering methods [19] and atomic layer deposition (ALD) [14], revealing the usability of polyimide materials as substrates for thin films deposited via conventional methods or processes.

However, polycarbonates having mold temperatures between 82 to 121 °C [20] cannot withstand those conventional processes, which usually is elevating the substrate temperature even without intentional heating[16]. Therefore, polycarbonate requires even milder deposition processes[16].

The facing-target sputtering (FTS) method could maintain the substrate temperature at room temperature up to 55 °C during the deposition of transparent-conductive AZO thin films without pos-heat treatment, opening the feasibility of polycarbonate substrates for AZO thin films[16]. In comparison with the conventional magnetron sputtering, this range of temperature is much milder. Conventional sputtering usually elevates the temperature at substrate surfaces reaching above 80 °C [16].

This feasibility of polycarbonate materials for AZO thin film deposition is very attractive since polycarbonate materials are widely utilized in several outdoor applications for their excellence in visible light transmittance, such as agricultural greenhouses [21] and tropical house roofs [22], which opens possibilities of the implementation of AZO-based devices for such applications, such as in agrivoltaics [23,24].

However, the durability of AZO thin films is very important for this kind of outdoor application, especially in a harsh environment. High-temperature processes utilizing glass substrates have been extensively reported as producing higher durability of AZO thin films when compared with lower temperature film production, especially in damp-heat conditions of a harsh environment [3,6,25]. As higher temperatures usually produced more durable AZO films, the durability performance of AZO transparent electrodes prepared at low temperature seems to be an issue.

Although successful depositions of transparent and conductive AZO films on polycarbonates or polyimide substrates have been reported [16,19], none discuss the damp-heat durability performances of deposited AZO films. The exposure of humidity for the AZO film of polyimides had been tested by Marques et al. [14], in which the test excluded the high temperature or heat of the harsh environment. Therefore, damp-heat durability of low-temperature prepared AZO thin films with the exposure of both humidity and high temperature is not widely discussed in the literature for AZO films deposited on glass, polyimide, and polycarbonate substrates.

Furthermore, polymer-based materials are attracting the application for the outer space, suggesting the importance of applicability of AZO films deposited on those substrates, which emphasize the low-temperature processes. Polyimide films attached to various polymers, such as acrylic, polyvinyl chloride (PVC), or polycarbonates, are proposed as protective films for cladding materials of agricultural greenhouses to withstand ultraviolet damage when exposed to a high ultraviolet condition in the space environment such as the Moon or Planet Mars [26]. The composite of polyimide-polymer materials, such as polyimide-polycarbonate, is not yet widely discussed in the literature for transparent electrode materials, including gallium-doped zinc oxide (GZO) and AZO thin films.

2.4. DH-durability comparisons of AZO, GZO and ITO TEs

To know the durability issue of AZO TEs, the durability of the ITO and GZO transparent conducting oxides are reviewed and compared. The ITO TEs, as the industrial standard of TE materials, exhibited excellent durability in DH condition (Fig. 2-1). On the other hand, ZnO-based TE materials such as AZO and GZO are significantly degraded, with AZO as the most degraded one (Fig. 2-2).

The degradation of GZO seemed to involve the decrease of mobility, rather than the decrease in carrier concentration, where GZO exhibited excellent carrier concentration (Fig. 2-3) as exposed to the DH condition, while AZO showed significant decrease in both, carrier concentration and Hall mobility in the DH condition (Fig 2-4).

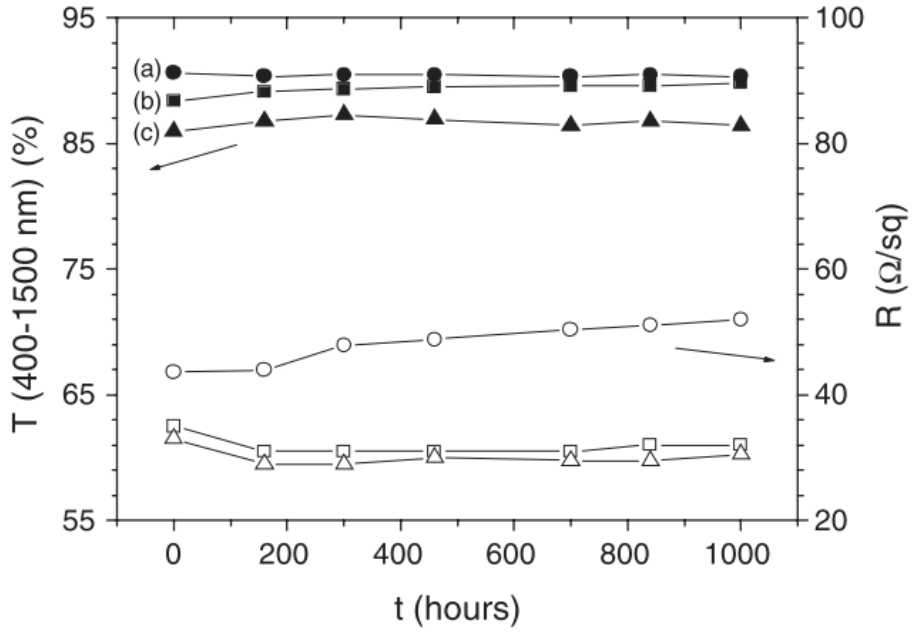

Fig. 2-1. DH-durability of ITO TEs (after Guillén and Herrero[27])

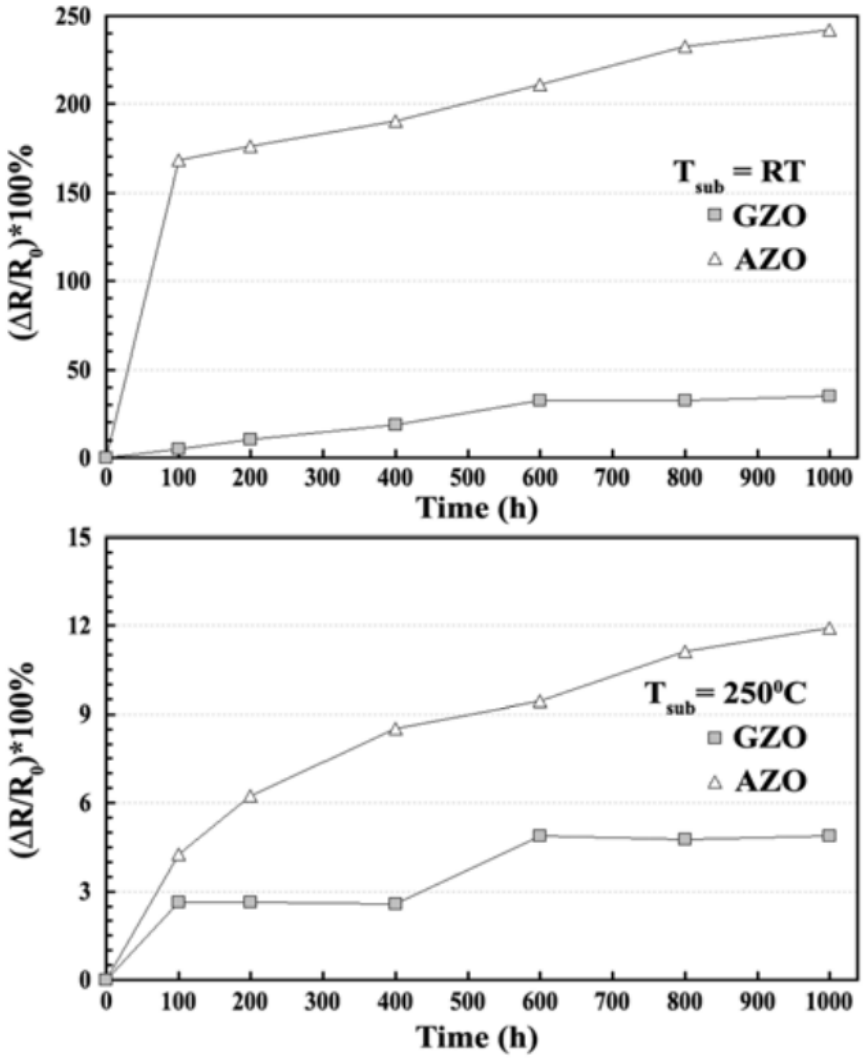

Fig. 2-2. DH-durability of AZO and Gallium-doped ZnO (GZO) TEs with annealing (top) and no annealing (bottom) (after Asvarov et al.[28])

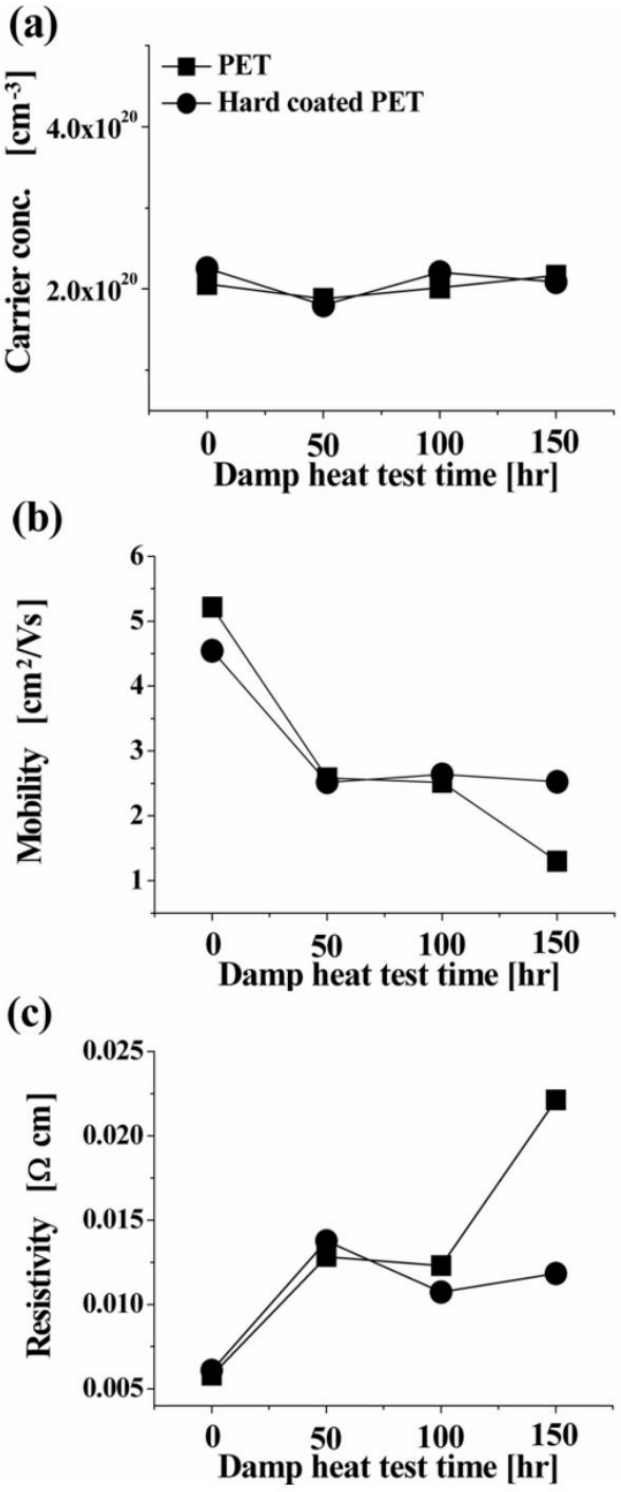

Fig. 2-3. DH-durability and Hall effect measurement of GZO on PET substrates (Lim et al.[29])

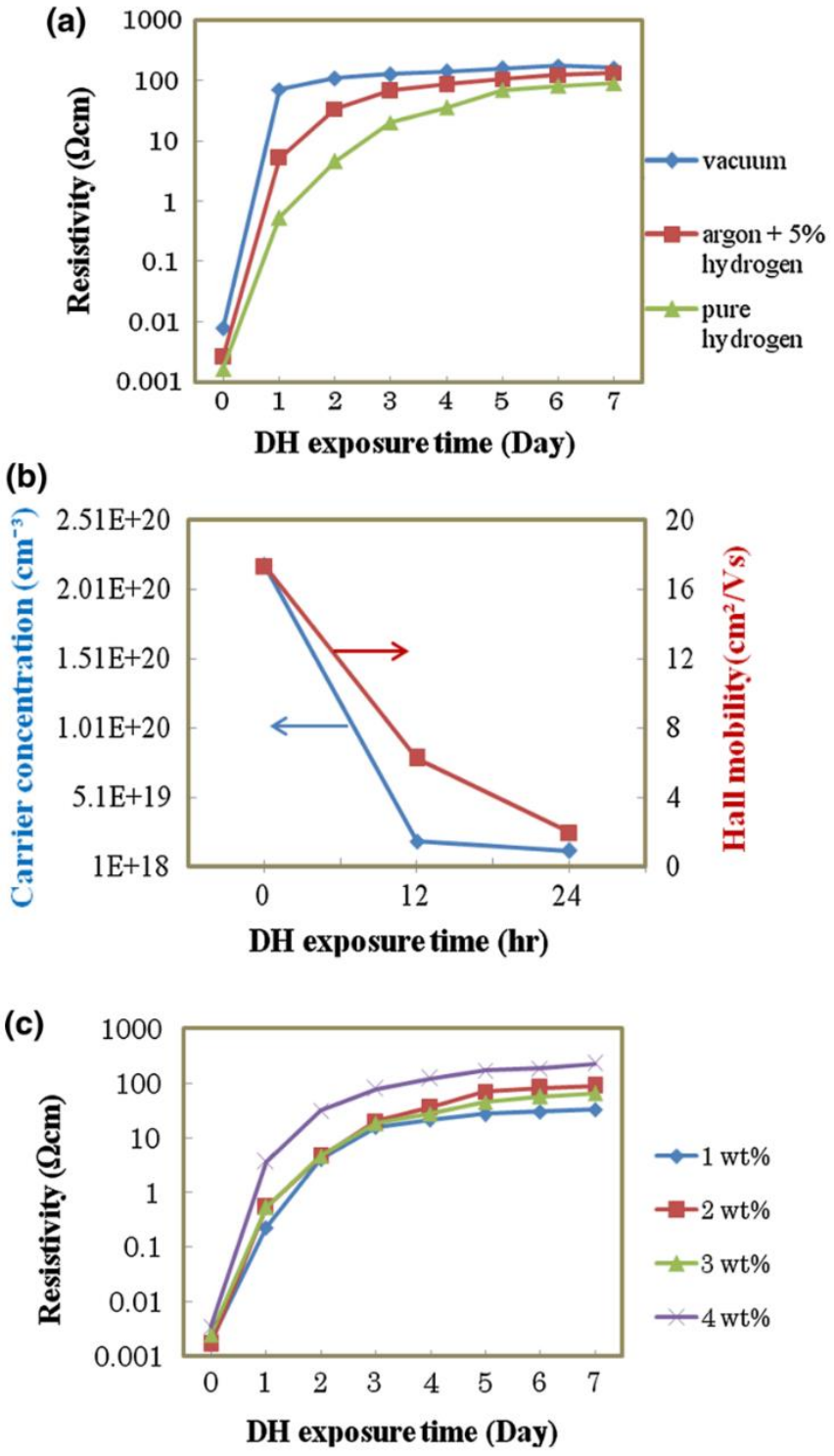

Fig. 2-4. DH-durability and Hall effect measurement of AZO on glass substrates (Tabassum et al.[7])

2.5. Summary

This literature review has been discussed to highlight several findings and issues to further explored in extending the usability of AZO transparent electrodes through sputtering deposition, which are:

1. Sputtered AZO thin films exhibit no cracks during as exposed to a harsh environment, suggesting the possibility of recovery of the electrical properties by re-annealing. N_2 and vacuum annealing at 180-250 ^oC have been reported to recover the conductivity of AZO films. However, the conductivity was not perfectly recovered

2. Role of crystal growth orientations to the durability sputtered AZO thin films are not yet clear since the comparison of the reported results was based on different deposition method. Moreover, there is a paucity in the literature on producing different crystal orientations for the films through sputtering

3. Low-temperature preparation of AZO thin films through a standard RF magnetron sputtering system is still challenging to open for the applicability of the films to the polymer-based substrates. Moreover, the degradation mechanism of AZO thin films deposited at low temperature on polymer-based substrates are not widely covered.

By addressing the above-mentioned three points, this thesis differs from the available literature in proposing a route and an insight into the perfect recovery of degraded AZO thin films. Besides, a simple method to produce different crystal growth orientation via sputtering has been reported and the role of crystal orientations for the durability of the films has been compared comprehensively in this thesis.

Furthermore, a method of low-temperature deposition of highly conductive-durable AZO films has been proposed and the difference in degradation mechanisms between AZO deposited on glass and polymer-based substrates has been clarified in this thesis.

Reference

[1] M. Mickan, M. Stoffel, H. Rinnert, U. Helmersson, D. Horwat, Restoring the Properties of Transparent Al-Doped ZnO Thin Film Electrodes Exposed to Ambient Air, J. Phys. Chem. C. 121 (2017) 14426–14433. doi:10.1021/acs.jpcc.7b03020.

[2] S. Tabassum, E. Yamasue, H. Okumura, K.N. Ishihara, Sol–gel and rf sputtered AZO thin films: Analysis of oxidation kinetics in harsh environment, J. Mater. Sci. Mater. Electron. 25 (2014) 4883–4888. doi:10.1007/s10854-014-2248-9.

[3] T. Tohsophon, J. Hüpkes, S. Calnan, W. Reetz, B. Rech, W. Beyer, N. Sirikulrat, Damp heat stability and annealing behavior of aluminum doped zinc oxide films prepared by magnetron sputtering, Thin Solid Films. 511–512 (2006) 673–677. doi:10.1016/j.tsf.2005.12.130.

[4] J. Hüpkes, J.I. Owen, M. Wimmer, F. Ruske, D. Greiner, R. Klenk, U. Zastrow, J. Hotovy, Damp heat stable doped zinc oxide films, Thin Solid Films. 555 (2014) 48–52. doi:10.1016/j.tsf.2013.08.011.

[5] M. Mickan, U. Helmersson, D. Horwat, Effect of substrate temperature on the deposition of Al-doped ZnO thin films using high power impulse magnetron sputtering, Surf. Coatings Technol. 347 (2018) 245–251. doi:10.1016/j.surfcoat.2018.04.089.

[6] S. Tabassum, E. Yamasue, H. Okumura, K.N. Ishihara, Electrical stability of Al-doped ZnO transparent electrode prepared by sol-gel method, Appl. Surf. Sci. 377 (2016) 355–360. doi:10.1016/j.apsusc.2016.03.133.

[7] S. Tabassum, E. Yamasue, H. Okumura, K.N. Ishihara, Damp heat stability of AZO transparent electrode and influence of thin metal film for enhancing the stability, J. Mater. Sci. Mater. Electron. 25 (2014) 3203–3208. doi:10.1007/s10854-014-2004-1.

[8] K. Maejima, H. Shibata, S. Niki, H. Tampo, K. Matsubara, Correlation between Electrical Properties and Crystal c -Axis

Orientation of Zinc Oxide Transparent Conducting Films, Jpn. J. Appl. Phys. 51 (2013) 10NC16. doi:10.7567/jjap.51.10nc16.

[9] Z. Zhan, J. Zhang, Q. Zheng, D. Pan, J. Huang, F. Huang, Z. Lin, Strategy for Preparing Al-Doped ZnO Thin Film with High Mobility and High Stability, Cryst. Growth Des. 11 (2011) 21–25. doi:10.1021/cg101216z.

[10] F. Claeyssens, C.L. Freeman, N.L. Allan, Y. Sun, M.N.R. Ashfold, J.H. Harding, Growth of ZnO thin films - Experiment and theory, J. Mater. Chem. 15 (2005) 139–148. doi:10.1039/b414111c.

[11] H. Kang, S. Jung, S. Jeong, G. Kim, K. Lee, flexible electronics, Nat. Commun. 6 (2015) 1–7. doi:10.1038/ncomms7503.

[12] T. Yokota, T. Someya, Electronic skin for healthcare monitoring, in: 2019 26th Int. Work. Act. Flatpanel Displays Devices, IEEE, 2019: pp. 1–2. doi:10.23919/AM-FPD.2019.8830621.

[13] E. Lee, J. Ahn, H. Kwon, S. Ma, K. Kim, S. Yun, J. Moon, All-Solution-Processed Silver Nanowire Window Electrode-Based Flexible Perovskite Solar Cells Enabled with Amorphous Metal Oxide Protection, Adv. Energy Mater. 8 (2018) 1702182. doi:10.1002/aenm.201702182.

[14] A.C. Marques, J. Faria, P. Perdigão, B.M.M. Faustino, R. Ritasalo, K. Costabello, R.C. da Silva, I. Ferreira, Stability under humidity, UV-light and bending of AZO films deposited by ALD on Kapton, Sci. Rep. 9 (2019) 17919. doi:10.1038/s41598-019-54451-0.

[15] X. Hao, J. Ma, D.-H. Zhang, Y. Yang, H. Ma, C.-F. Cheng, X.-D. Liu, Comparison of the properties for ZnO:Al films deposited on polyimide and glass substrates, Mater. Sci. Eng. B. 90 (2002) 50–54. doi:10.1016/S0921-5107(01)00828-5.

[16] Y. Sup Jung, H. Wook Choi, K. Hwan Kim, S. Joon Park, H. Hee Yoon, Properties of AZO Thin Films for Solar Cells Deposited on Polycarbonate Substrates, J. Korean Phys. Soc. 55 (2009) 1945–1949. doi:10.3938/jkps.55.1945.

[17] M.Y. Zhang, Q. Nian, G.J. Cheng, Room temperature deposition of alumina-doped zinc oxide on flexible substrates by direct pulsed laser recrystallization, Appl. Phys. Lett. 100 (2012) 151902. doi:10.1063/1.3702460.

[18] RTP, General Processing Conditions RTP 4285 Thermoplastic Polyimide (TPI) Carbon Fiber, (2005). http://web.rtpcompany.com/info/data/4200/RTP4285.htm (accessed January 6, 2020).

[19] P. Prepelita, R. Medianu, F. Garoi, A. Moldovan, Growth of ZnO:Al thin films onto different substrates, AIP Conf. Proc. 1292 (2010) 213–216. doi:10.1063/1.3518300.

[20] RTP, General Processing Conditions RTP 300 Polycarbonate (PC) Unreinforced, (2004). http://web.rtpcompany.com/info/data/0300/RTP300.htm (accessed January 6, 2020).

[21] M.C. Subin, J.S. Lourence, R. Karthikeyan, C. Periasamy, Analysis of materials used for Greenhouse roof covering - Structure using CFD, IOP Conf. Ser. Mater. Sci. Eng. 346 (2018). doi:10.1088/1757-899X/346/1/012068.

[22] K.M. Al-Obaidi, M. Ismail, A.M. Abdul Rahman, Design and performance of a novel innovative roofing system for tropical landed houses, Mod. Lang. Q. 85 (2014) 488–504. doi:10.1016/j.enconman.2014.05.101.

[23] A. Leon, K.N. Ishihara, Assessment of new functional units for agrivoltaic systems, J. Environ. Manage. 226 (2018) 493–498. doi:10.1016/j.jenvman.2018.08.013.

[24] A. Leon, K.N. Ishihara, Resources , Conservation & Recycling In fl uence of allocation methods on the LC-CO 2 emission of an agrivoltaic system, Resour. Conserv. Recycl. 138 (2018) 110–117. doi:10.1016/j.resconrec.2018.06.017.

[25] F. Machda, T. Ogawa, H. Okumura, K.N. Ishihara, Evolution and Recovery of Electrical Property of Reactive Sputtered Al-Doped ZnO

Transparent Electrode Exposed to Harsh Environment, Phys. Status Solidi. 1900519 (2019) 1900519. doi:10.1002/pssa.201900519.

[26] D.T. Peterside, J.E. Palaia, A.C. Schuerger, M.J. Correll, R.A. Bucklin, Testing of Greenhouse Cladding Materials for Space Environments, Part 2: Laminates, Appl. Eng. Agric. 34 (2018) 575–580. doi:10.13031/aea.12465.

[27] C. Guillén, J. Herrero, Stability of sputtered ITO thin films to the damp-heat test, Surf. Coatings Technol. 201 (2006) 309–312. doi:10.1016/j.surfcoat.2005.11.114.

[28] A. Asvarov, A. Abduev, A. Akhmedov, A. Abdullaev, Effects of a high humidity environment and air anneal treatments on the electrical resistivity of transparent conducting ZnO-based thin films, Phys. Status Solidi Curr. Top. Solid State Phys. 7 (2010) 1553–1555. doi:10.1002/pssc.200983158.

[29] Y.S. Lim, D.W. Kim, J.-H. Kang, M.-H. Lee, W.-S. Seo, H.-H. Park, K.H. Seo, M.G. Park, Effect of a Hard Coating Layer on the Damp Heat Stability of Ga-doped ZnO Thin Films on Polyethylene Terephthalate Substrates, J. Korean Phys. Soc. 57 (2010) 1045–1048. doi:10.3938/jkps.57.1045.

3. Methods

3.1. Sample Preparation

This research used radio frequency (RF) magnetron sputtering for AZO layer deposition which had been the first choice for thin-film industries due its high growth-rate and the acceptable quality of the produced film as well as proven to produce better and more stable AZO transparent electrodes in comparison with sol-gel methods[1,2].

Prior to the thin-film deposition by sputtering, a glass[3,4] substrate was cleaned in an ultrasonic bath using acetone as the cleaning agent then dried through wiping by lab-experimental tissues. For the investigation of polymer-based substrates in this thesis, PI-tape is used and attached to polycarbonate (PC). As polymer-based substrate is fragile to the exposure of acetone, the PI-tape is cleaned by ethanol-wiping.

The AZO films deposited on the hard glass substrates ($48 \times 28 \times 1.3$ mm^3) were used for comparison with the films deposited on the very flexible polyimide tapes ($48 \times 28 \times 0.04$ mm^3) attached to the surface of the polycarbonates ($48 \times 28 \times 1$ mm^3) labeled “PI-tape/PC” substrates[5]. This PI-tape/PC was cleaned through ethanol-wiping by lab-experimental tissues. An air duster was used to remove all the remained dust caused by the wiping step on the substrate (Fig. 3-1).

Inside the sputtering chamber, the cleaned substrate was put 7 cm above the target. A zinc metal target (diameter of 75 mm and a thickness of 5 mm with 99.99% purity) was used together with three aluminum chips (size of 5×5 mm with 99.99% purity). The three aluminum chips were arranged with a triangle shape.

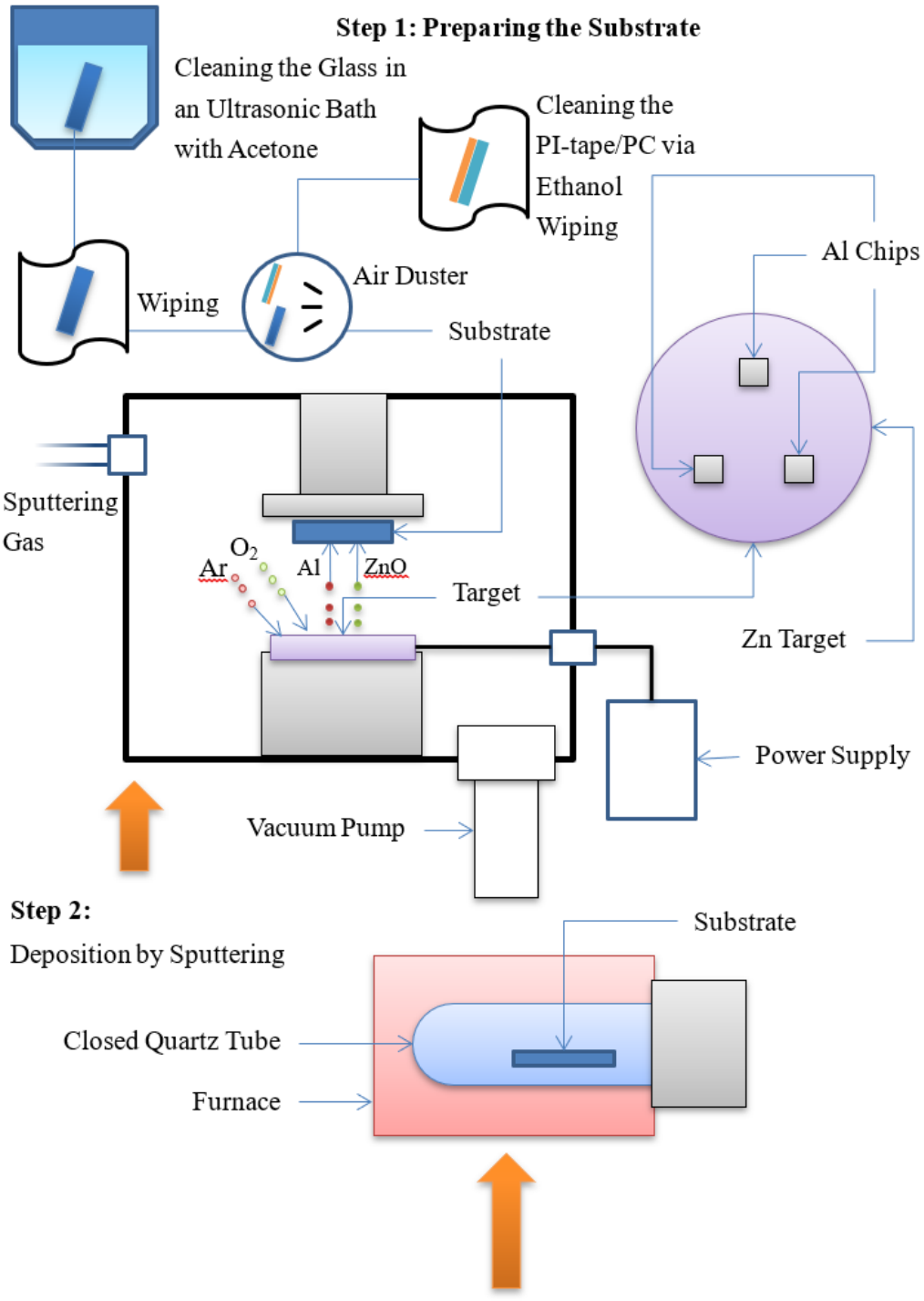

Fig. 3-1. Overall steps of the sample preparation

The chamber was then made into a vacuum with a base pressure at 10^{-3} Pa or less. With this base pressure, a mixture of Ar and O_2 gases with various ratios were flowed into the sputtering chamber to bombard the target (Fig. 3-1). This mixture of Ar and O_2 gasses would provide a reactive atmosphere inside the sputtering chamber[6]. For a high O_2-to-Ar ratio, the O_2 was set 30 or 60 sccm while the Ar gas was varied from 3 to 60 sccm[3,4]. For a low O_2-to-Ar ratio, O_2 was set at 3 sccm, while the Ar gas set was fixed at 90 sccm[5].

As RF power was applied at 80 - 100 W, the plasma was generated while the substrate was spinning at room temperature. The substrate temperature was elevated without intentional heating as the thin film was being deposited[7]. During the plasma generation, the pressure at the chamber was increased from 10^{-3} Pa to be around 1 Pa of working pressure for the sputtering deposition. Then, the sputtered target-atoms would condense on substrates as thin films[1]. The deposition duration was 30 to 60 min.

After the deposition of AZO layers by sputtering was accomplished, post-heat treatment was conducted by an electric furnace in a hydrogen atmosphere at 0.06 MPa at 400 – 550 °C inside a closed quartz tube (Fig. 3-1). The hydrogen atmosphere was chosen to even reduce the resistivity to the AZO films[8]. Depending on the research goal and the substrate requirement, the post-heat treatment is conducted only for the glass substrate[3,4] and no post-heat treatment for the low-temperature thin-film preparation on both the glass and the PI-tape/PC substrates[5].

As for the re-annealing of the AZO films after being degraded as exposed to a harsh environment, the temperature is set to be as same as temperature of the post-heat treatment prior to the degradation test. For example, samples labelled AZO-400 °C are post-heat treated and re-annealed at 400 °C and samples labelled AZO-550 °C are post-heat treated and re-annealed at 550 °C.

3.2. Characterization Apparatus

3.2.1. Temperature Measurement Sticker

Temperature measurement stickers HEAT LABEL MICRON CORP 10R-49 or 6R-65 were used in this work to investigate the development of the surface temperature during the sputtering deposition. Considering that the substrate is put inside the chamber and facing the generated plasma, these temperature labels are the most accurate one for investigating the temperature development on the substrate surface because these temperature stickers are put directly on top of the substrate surface.

The stickers monitor the temperatures by several small heat-sensitive indicators sealed under transparent, heat-resistant windows. When the surface temperature rises due to the bombardment of sputtering plasma, then the heat indicator shown on the label will change from white to black irreversibly according to the associated reached-temperature level. The blackened indicators would then register the temperature history of the surface substrates during the film deposition.

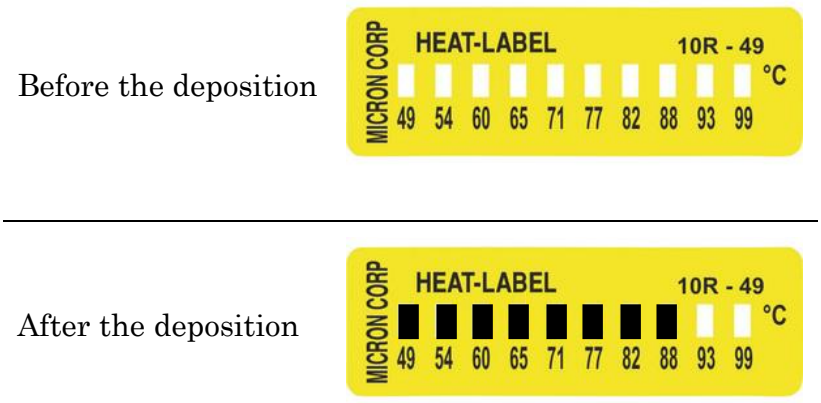

Fig. 3-2. Temperature measurement stickers

3.2.2. UV-Vis-NIR Spectrometer

For transparency of the prepared AZO samples, a UV-Vis-NIR spectrometer Perkin Elmer Lambda 750S was used in this work. The transparency of the samples was checked in between 300 - 2500 nm. By this range of wavelength, the wavelength in the visible (400 to 700 nm) and near infra-red (NIR) spectrum, are all included in the measurement. The average transparency in the visible wavelength range is considered as the overall transparency of the sample. When the values of transparency and sheet resistance are known, the figure of merit of AZO samples could be defined by equation 1.1. The measurement is also conducted in the NIR range of wavelength to confirm the difference of carrier concentrations between the sample, where the sample with more carrier concentrations will have less transmittance in the NIR range due to the unwanted free carrier absorption in the IR range[9].

The UV-Vis-NIR spectrophotometry can measure the transmittance of a sample as a function of the wavelength of the incident light. It uses light in the visible and adjacent, near UV and NIR ranges. The spectrometer consists of a light source, sample, spectrometer, and detector. The light source can emit light of wavelength 250-2500 nm. After passing through the sample, the transmitted light is passed through a spectrometer, which disperses the light onto the photodiode detector.

3.2.3. Four-point Probe

The sheet resistance of the prepared samples is measured by four-point probe measurement, where the four probes were pressed adequately to the surface of the thin films. The two outer probes are connected to the current generator and ammeter, while the two inner probes are connected to a voltmeter (Fig. 3-3). By this measurement, the sheet resistance of the thin film is defined exclusively with a unit of Ω/□ which describes a resistance across a uniform-square sheet regardless of the size of the square.

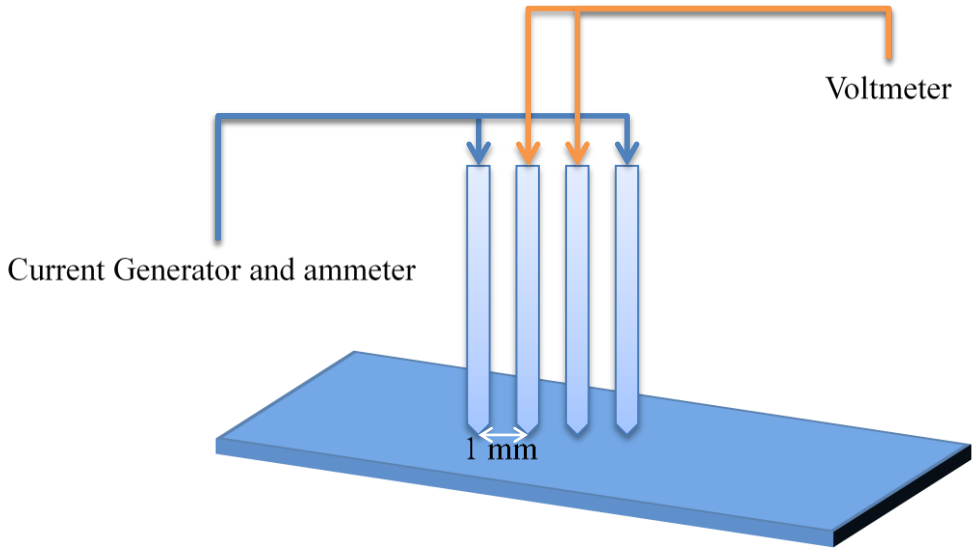

Fig. 3-3. Schematic diagram of sheet resistance measurement by four-point probe method

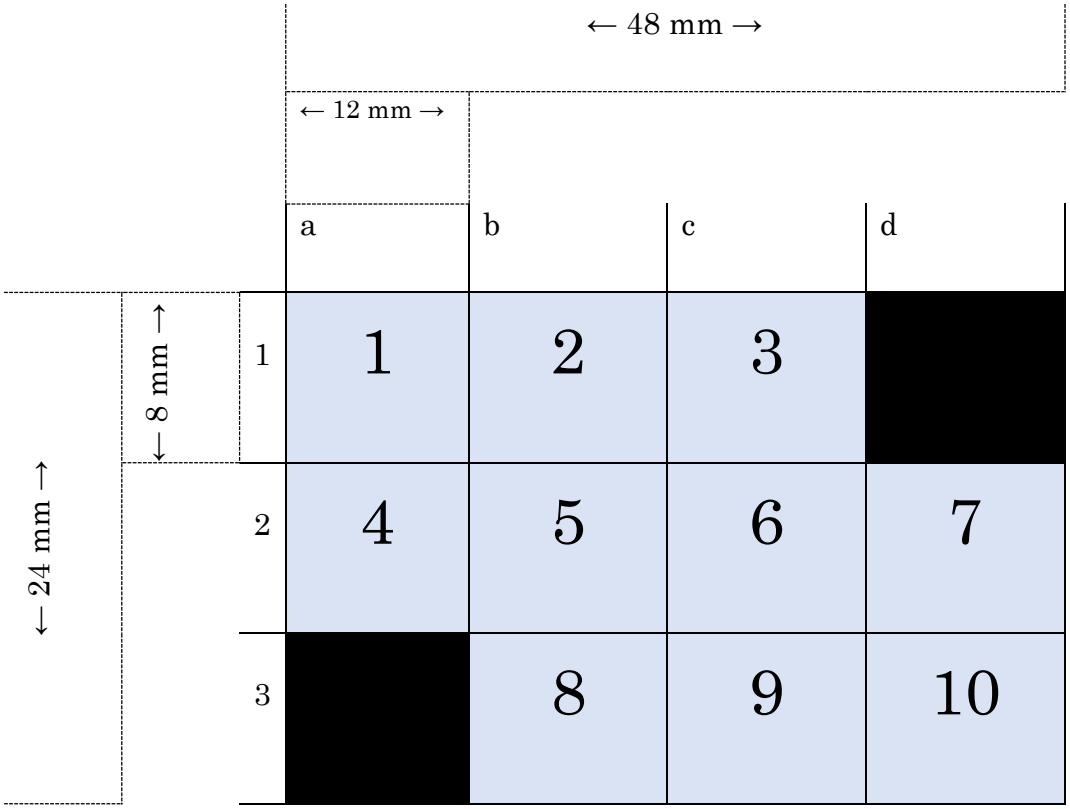

Fig. 3-4. Schematic diagram on the surface of the AZO thin films where 10 points were selected for sheet resistance measurement. The black squares are the square where the parts of the glasses are held on to the substrate holder of the sputtering system where the film is not deposited.

For each AZO sample, 10 points are selected, and each point was measured for its sheet resistance (Fig. 3-4.). The overall sheet resistance of a sample is the average of these 10 points. When the thickness d and sheet resistance R_s of the sample are known, bulk resistivity ρ of a sample with a unit Ωcm could be defined by this equation:

$$\rho = R_s \times d \tag{3.1}$$

Sheet resistance and resistivity represent two different kinds of conductivity. When the term sheet resistance is used, the discussed current is along the plane of the sheet, not vertical to it. While for resistivity, the current is not only along the plane but also along the perpendicular of the films representing the inherent conductivity of the deposited AZO layer.

3.2.4. Hall Measurement System

In this thesis, the carrier concentration and Hall mobility of the AZO thin films were measured by a Hall measurement system Resitest 8308. In this measurement system (Fig. 3-5), three steps of measurements are conducted, which are the Van der Paw method for sheet resistance measurement, carrier concentration through Hall effect, and finally, the calculation of Hall mobility.

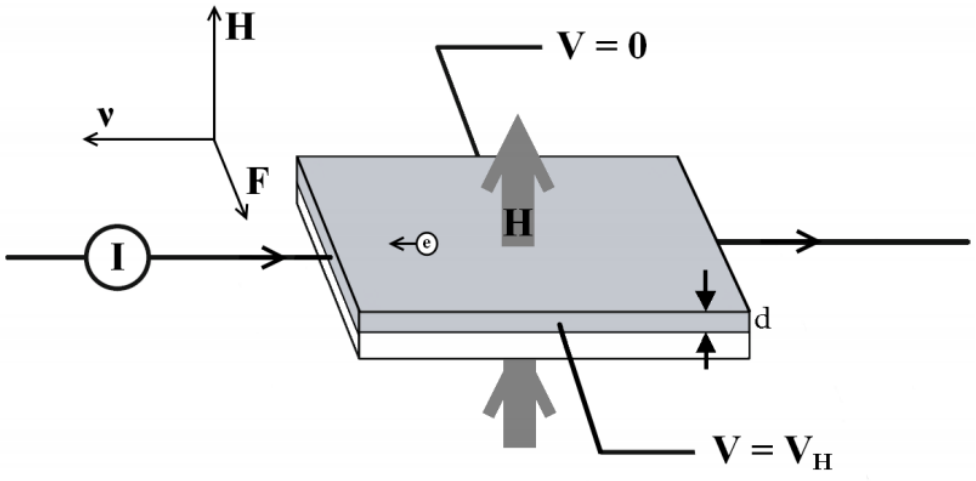

Fig. 3-5. Diagram of the Hall measurement system (after Tabassum [10])

Firstly, the sheet resistance R_S is measured by the van der Pauw method. The measurement is conducted by four small contacts, which are put at the periphery of a square-shaped (10 x 10 mm) of an AZO sample. This square shape is obtained by cutting the AZO films, where AZO films on the glass are cut by the diamond cutter while the films on PI-tape/PC is cut by the flush scissors for plastics. In measuring the sheet resistance, a current I is passed from one contact to adjacent contact, while the corresponding voltage difference V is measured across the two contacts on the opposite side. The measured sheet resistance, $R_S = V/I$ by this van der paw method is complementary, mainly used for measuring carrier concentration and the Hall mobility at 26 °C in this research.

Secondly, the carrier concentration (n) is measured through the Hall effect, which is the voltage difference (V_H) from the deflection of the charged carriers by the Lorentz force. As V_H is determined, the carrier concentration is calculated as:

$$n = {}^{IH}/_{eV_H d} \tag{3.2}$$

where I is current input (5×10^{-3} A), H is the magnetic field (0.42 T), e is the electronic charge, and d is the thickness of the film.

Thirdly, the Hall mobility μ_H is deduced from the determined value of R_S and V_H through:

$$\mu_H = (enR_s d)^{-1} \tag{3.3}$$

3.2.5. X-ray Diffractometer (XRD)

This thesis work investigated the crystallinity of the samples, trough X-ray diffraction (XRD) data measured with Rigaku RINT2100CMJ in terms of crystal orientation and crystallite size. XRD data of AZO samples were compared to preferred crystal orientation (002) of ZnO at $2\theta = 34.4°$[11] that represents wurtzite hexagonal crystal structure[12], the optimal morphology of ZnO in terms of optoelectrical properties[13,14].

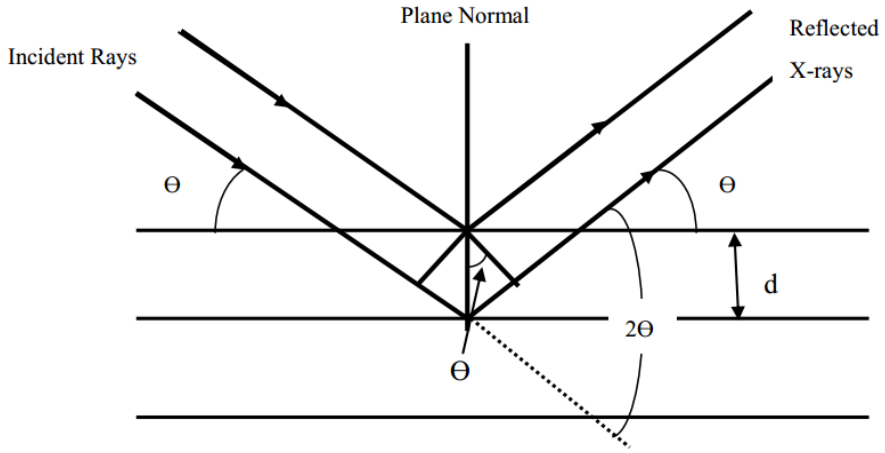

Fig. 3-6. A schematic image of XRD measurement (After Tabassum [10])

For crystallite size, full width at half maximum (FWHM) was firstly measured along the highest peak of XRD data of each AZO sample. By this FWHM, crystallite d size is estimated by Scherrer's equation as following [2]:

$$d = \frac{0.9\lambda}{\beta \cos\theta} \tag{3.4}$$

where λ is the x-ray wavelength (0.15405 nm), β is the measured FWHM, and θ is the angle of the diffraction of the highest peak at the XRD data.

3.2.6. X-ray Photoelectron Spectrometer (XPS)

X-ray photoelectron spectrometer (XPS) Jeol JPS-9030 was used in this research work to confirm the chemical elements of AZO film, at the surface and beneath the surface of the films. This one is the most widely used surface analysis technique because of its accuracy data interpretation and simplicity in use. The measurement is conducted by a square-shaped (10 x 10 mm) of an AZO sample. This square shape is obtained by cutting the AZO films, where AZO films on the glass are cut by the diamond cutter while the films on PI-tape/PC are cut by the flush scissors for plastics. It works by irradiating a sample with an x-ray beam and then quantifying the kinetic energy and number of electrons that are ejected from the material.

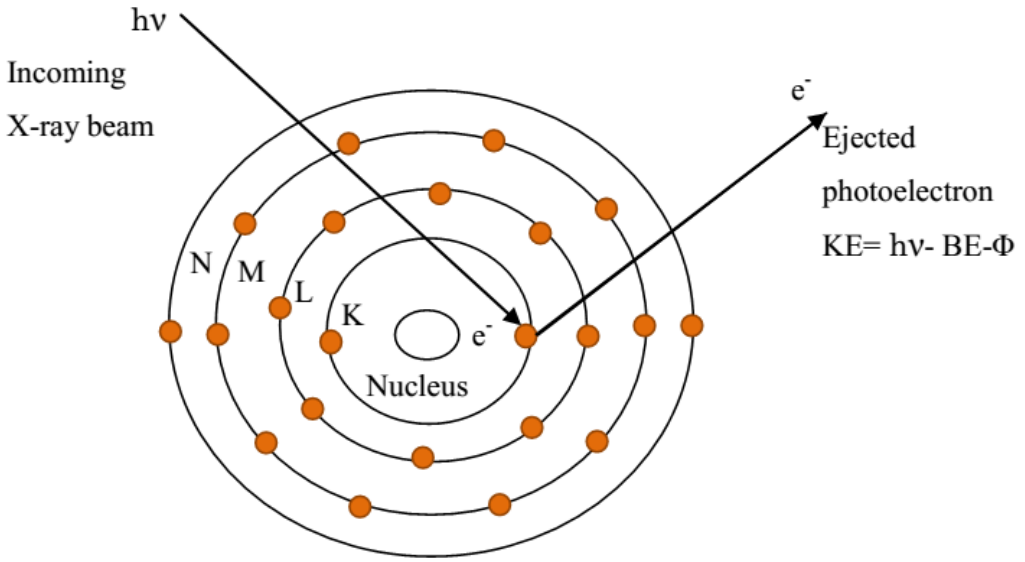

Fig. 3-7. A schematic image of measurement process in the XPS (After Tabassum [10])

This technique works by having a high energy X-ray beam and using it to excite the surface of the desired sample. The XPS measures the kinetic energy and number of electrons that escape from the top 0 to 10 nm of the material being analyzed. If the incoming X-ray has enough energy and is absorbed by an atom in the surface, then the innermost electron will be ejected. This phenomenon is known as the photoelectric effect. Because the energy of an X-ray with a particular wavelength is known, the ejected photoelectron has kinetic energy that can be calculated to be equal to the energy of the incident X-ray minus the binding energy and the work function of the element.

By detecting and measuring the energy of this electron that is unique for each element, one is able to determine the composition of the sample. XPS can be used as a surface analysis technique and depth profiling analysis. For the depth profiling analysis, the sample is firstly etched by ion beam etching then the measurement of the elemental composition as a function of depth becomes feasible as a chemical characterization beneath the surface.

3.2.7. Scanning Electron Microscope (SEM)

This research work used a scanning electron microscope (SEM) HITACHI SU6600. The SEM uses a focused beam of high-energy electrons, which generates a variety of signals at the surface of the samples. The derived signals from electron-sample interactions are then collected over a selected area of the surface of the sample, and an associated 2-dimensional image is generated. These signals include secondary electrons, backscattered electrons, diffracted backscattered electrons, photons, visible light, and heat.

The secondary electrons and backscattered electrons are commonly used for imaging samples, where secondary electrons are most valuable for showing morphology and topography on samples, and backscattered electrons are most valuable for illustrating contrasts in composition in multiphase samples. In this work, the SEM analysis was used to confirm the thickness of the films, the surface condition of the films, as well as the grain boundary of the films.

3.2.8. Surface Profilometer

This thesis used a surface profilometer Surfcorder ET3000 to measure the exact thickness of the prepared AZO thin films. Profilometry is a simple and accurate, offering a non-destructive measurement technique for the sample. Due its reliability, this technique is frequently used for the determination of the thickness of thin films[10].

The surface profilometer employs a diamond stylus or probe in contact with the AZO thin film surface. This probe is then moved laterally to detect and measure small vertical variations. To have the accurate thickness, there should be a clear step between the surface of the substrate and the surface of the AZO films.

In order to provide this clear step, the sample should be clear from the dust, which the air duster can offer the function very well. Then, the probe was moved from the AZO thin film surface to the uncoated parts of the substrate. The height difference between the film and the uncoated substrate was then investigated in three locations or points, and the average of the difference is considered as the thickness of the AZO films.

3.2.9. Constant Damp Heat Chamber

The durability of the samples was observed in a damp heat (DH) test condition using an electronic constant temperature/humidity chamber Advantec THR030FA. This durability is represented by the degradation of sheet resistance of the AZO samples during the observation duration. If the sheet resistance degrades more, the AZO layer is not durable. The damp heat test condition is set at 85°C and 85% relative humidity to represent a harsh environment.

This sheet resistance degradation index *DI* was then presented as a ratio between the sheet resistance as prepared R_{S0} and the sheet resistance at the completed duration x of DH test R_{Sx} using the following equation:

$$DI = \frac{R_{Sx}}{R_{S0}} \tag{3.5}$$

By considering the relation of thickness, resistivity, sheet resistance, carrier concentration, and Hall mobility in the Equation 3.1 and 3.3, the role of the carrier concentration and Hall mobility during this sample durability observation was further elaborated by the log of DI (Eq. 3.6)[4], the decrease percentage of carrier concentration n (Eq. 3.7)[3], and the decrease percentage of Hall mobility (Eq 3.8)[3].

$$\log\left(\frac{\rho_x}{\rho_0}\right) = \log\left(\frac{n_0}{n_x}\right) + \log\left(\frac{\mu_0}{\mu_x}\right) \tag{3.6}$$

$$D\%_n = (n_0 - n_1)/n_0 \times 100\% \tag{3.7}$$

$$D\%_\mu = (\mu_0 - \mu_1)/\mu_0 \times 100\%, \tag{3.8}$$

Reference

[1] P.J. Kelly, R.D. Arnell, Magnetron sputtering: A review of recent developments and applications, Vacuum. 56 (2000) 159–172. doi:10.1016/S0042-207X(99)00189-X.

[2] S. Tabassum, E. Yamasue, H. Okumura, K.N. Ishihara, Sol–gel and rf sputtered AZO thin films: Analysis of oxidation kinetics in harsh

environment, J. Mater. Sci. Mater. Electron. 25 (2014) 4883–4888. doi:10.1007/s10854-014-2248-9.

[3] F. Machda, T. Ogawa, H. Okumura, K.N. Ishihara, Evolution and Recovery of Electrical Property of Reactive Sputtered Al-Doped ZnO Transparent Electrode Exposed to Harsh Environment, Phys. Status Solidi Appl. Mater. Sci. 1900519 (2019) 1–6. doi:10.1002/pssa.201900519.

[4] F. Machda, T. Ogawa, H. Okumura, K.N. Ishihara, Damp Heat Durability of Al-Doped ZnO Transparent Electrodes with Different Crystal Growth Orientations, ECS J. Solid State Sci. Technol. 8 (2019) Q240–Q244. doi:10.1149/2.0261912jss.

[5] F. Machda, T. Ogawa, H. Okumura, K.N. Ishihara, Damp-heat durability comparison of Al-doped ZnO transparent electrodes deposited at low temperatures on glass and PI-tape / PC substrates, Ceram. Int. (2020) 0–1. doi:10.1016/j.ceramint.2020.03.173.

[6] K. Ellmer, Past achievements and future challenges in the development of optically transparent electrodes, Nat. Photonics. 6 (2012) 808–816. doi:10.1038/nphoton.2012.282.

[7] Y. Sup Jung, H. Wook Choi, K. Hwan Kim, S. Joon Park, H. Hee Yoon, Properties of AZO Thin Films for Solar Cells Deposited on Polycarbonate Substrates, J. Korean Phys. Soc. 55 (2009) 1945–1949. doi:10.3938/jkps.55.1945.

[8] S. Tabassum, E. Yamasue, H. Okumura, K.N. Ishihara, Damp heat stability of AZO transparent electrode and influence of thin metal film for enhancing the stability, J. Mater. Sci. Mater. Electron. 25 (2014) 3203–3208. doi:10.1007/s10854-014-2004-1.

[9] H. Liu, V. Avrutin, N. Izyumskaya, Ü. Özgr, H. Morkoç, Transparent conducting oxides for electrode applications in light emitting and absorbing devices, Superlattices Microstruct. 48 (2010) 458–484. doi:10.1016/j.spmi.2010.08.011.

[10] S. Tabassum, Investigation and improvement of environmental stability of Al-doped ZnO transparent electrode, Kyoto University, 2015. doi:10.14989/doctor.k18698.

[11] X. Zhao, H. Shen, Y. Zhang, X. Li, X. Zhao, M. Tai, J. Li, J. Li, X. Li, H. Lin, Aluminum-Doped Zinc Oxide as Highly Stable Electron Collection Layer for Perovskite Solar Cells, ACS Appl. Mater. Interfaces. 8 (2016) 7826–7833. doi:10.1021/acsami.6b00520.

[12] Ü. Özgür, Y.I. Alivov, C. Liu, A. Teke, M.A. Reshchikov, S. Doğan, V. Avrutin, S.-J. Cho, H. Morkoç, A comprehensive review of ZnO materials and devices, J. Appl. Phys. 98 (2005) 041301. doi:10.1063/1.1992666.

[13] E. Arakelova, A. Khachatryan, A. Kteyan, K. Avjyan, S. Grigoryan, ZnO fi lm deposition by DC magnetron sputtering : Effect of target con fi guration on the fi lm properties, Thin Solid Films. 612 (2016) 407–413. doi:10.1016/j.tsf.2016.06.030.

[14] K. Maejima, H. Shibata, S. Niki, H. Tampo, K. Matsubara, Correlation between Electrical Properties and Crystal c -Axis Orientation of Zinc Oxide Transparent Conducting Films, Jpn. J. Appl. Phys. 51 (2013) 10NC16. doi:10.7567/jjap.51.10nc16.

4. Evolution and Recovery of Electrical Property of Reactive Sputtered Al-Doped ZnO Transparent Electrode Exposed to Harsh Environment

4.1. Introduction

The electrical stability of AZO thin films is still questionable, especially after exposure to high humidity and temperature[1]. This electrical stability of AZO films is quite important since its degradation would lead to the decreased efficiency of the devices such as the degradation of AZO layer in Cu(In, Ga)Se2 (CIGS)-based thin film photovoltaic (PV) would decrease the efficiency of this PV device as exposed to damp heat environment as reported by Lee et al.[2].

Tabassum et al.[1] reported that a harsh environment could produce several cracks or voids for AZO thin films coated on glass substrates prepared by sol-gel methods, while no cracks were found for sputtered AZO thin films. The high dense surface of the sputtered films seems the reason for this stable surface protecting the film from the oxygen or water-molecule-derived species. However, both carrier concentration and Hall mobility were decreased. Thus, the conductivity degraded for AZO thin

films prepared by both sol-gel and sputtering methods. Physical and chemical damage could be the reason that the sol-gel methods produce higher degradation rate of AZO thin films in comparison with the sputtering.

Tohsophon et al.[3] reported that the recovery of the electrical property of sputtered AZO thin films by annealing in vacuum atmosphere up to 250 °C after being exposed to a damp heat environment for 1000 h. Hüpkes et al.[4] reported that annealing at 650 °C in vacuum atmosphere effectively produced very stable AZO films in comparison with the as-deposited AZO films even after being exposed to damp heat treatment for 1000 h, which was suggesting the effectiveness of annealing at higher temperature.

A grain boundary reconstruction of AZO films was suggested by Hüpkes et al.[4] where grains grew together and closed grain boundaries partially on the cost of other areas due to the annealing. Mickan et al.[5] reported that annealing in a nitrogen atmosphere at 180 °C could restore the property of sputtered AZO thin films aged for six months in the ambient air, where out-diffusion of water molecule was suggested as the reason for the restored property of the films. This evidence might suggest no physical damage during the degradation test of AZO films. In these two reports, the films were not annealed (post-heat treated) prior to the degradation test. Moreover, the annealing configurations, which were conducted only after the degradation test, could recover the conductivity of the degraded thin films but not as much as the original one before the degradation test.

Mickan et al.[6] reported that higher substrate temperature produced better electrical property and stability of AZO films. The similar tendencies produced by high temperature trough heated substrates during deposition or annealing after deposition of the films showed the importance of high temperature treatment for highly stable and conductive AZO films. Besides the substrate temperature, Greiner et al.[7,8] reported that AZO films deposited on smooth surface by non-reactive sputtering are more durable than on rough substrates by avoiding smaller grains growth with non-orientated c-axis and a higher area fraction of grain boundaries (extended grain boundaries).

Moreover, high-temperature annealing (450 °C or higher) in a hydrogen atmosphere had been reported to be effective by Tabassum et al.[1,9] for sputtered AZO thin films to enhance its electrical stability and crystallinity property. However, its effectiveness on the electrical property recovery of

the degraded films is not extensively discussed. Besides, annealing at a higher temperature after sputtering deposition could produce AZO thin films with better electrical stability by the spontaneous formation of a very thin oxide layer as a top protective layer against moisture attack[10].

However, the characteristic of the ultra-thin layer remains elusive yet. Moreover, the relation of carrier concentration evolution to the recoverability and durability of ZnO-based transparent electrodes exposed to the harsh environment is not clear, despite its direct relation to annealing conditions and Hall mobility such as by the creation of oxygen vacancies[9] and ionized impurity scattering respectively[11].

In this chapter, AZO thin films were deposited on glass substrates by reactive sputtering with 30 sccm for both, Ar and O_2 gasses at 100 W of RF power, for an hour then annealed at higher temperatures (400 – 550 °C) under a hydrogen (0.06 MPa) atmosphere for 30 min, both before and after the durability test of harsh environmental exposure. Durability of the films were evaluated by the electrical property evolution, including carrier concentration and Hall mobility as a function of annealing temperature.

The conductivity recovery of the AZO thin films was investigated by re-annealing for each sample at its respective initial annealing temperature in a hydrogen atmosphere after the degradation test. The re-annealing for each AZO sample was conducted at the same condition as before the damp heat test of each sample where hydrogen annealing at the same temperature for the same duration as the initially associated annealing temperature and duration of each sample was applied to recover the conductivity as much as before the degradation test. Scanning Electron Microscopy (SEM) was used to confirm the difference of the surface images before and after the exposure to the harsh environment.

4.2. Results and Discussions

The resistivity of AZO thin films deposited with similar sputtering condition decreased from 1.3 to 0.4 × 10^{-3} Ω·cm with the increase of annealing temperature from 400 – 550 °C (Fig. 4-1). Due to the similar condition of the deposition, all samples exhibited similar thickness at 0.5 μm as measured by a surface profilometer.

The higher annealing temperature induced the higher carrier concentration, which confirmed the effectiveness of annealing AZO thin films as reported by Tabassum et al.[9] that suggested the creation of more oxygen vacancies by higher annealing temperature in a hydrogen atmosphere.

Hall mobility was generally increased by higher annealing. However, a slight decrease was exhibited at 550 ºC annealing, which could be attributed to the electron scattering due to ionized impurity[11,12].

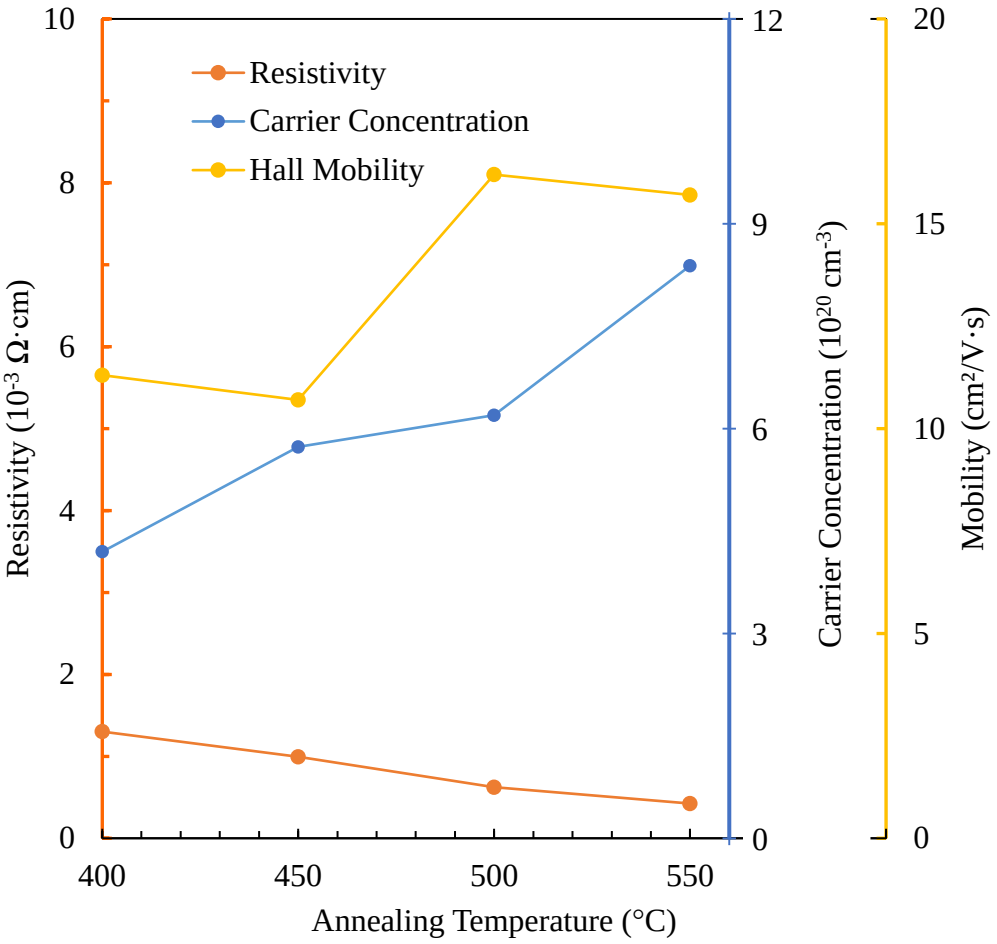

Fig. 4-1. Electrical property of AZO thin films as a function of annealing temperature.

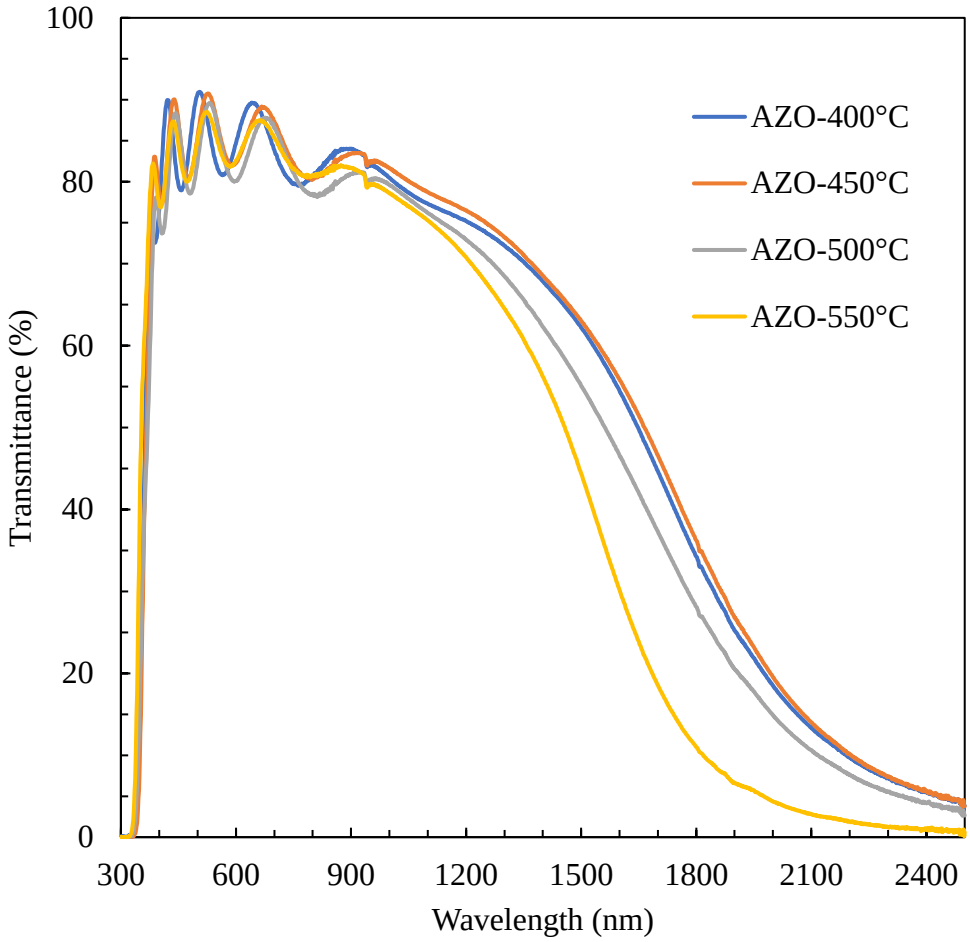

Fig. 4-2. Transmittance spectra of AZO thin films in the visible and near infrared range of wavelength.

All samples showed the excellent quality of more than 80% of transmittance in the wavelength of the visible range (Fig. 4-2) confirming the high transparency of AZO materials applied as thin films. Conversely, the transmittance appears to be decreasing with the annealing temperature in the near infrared range (Fig. 4-2), suggesting an increase in the charge carrier concentration. These results are in line with findings reported by Mickan et al.[6] and Lee et al.[12] where the transmittance in the near infrared range decreased with the higher applied substrate temperature.

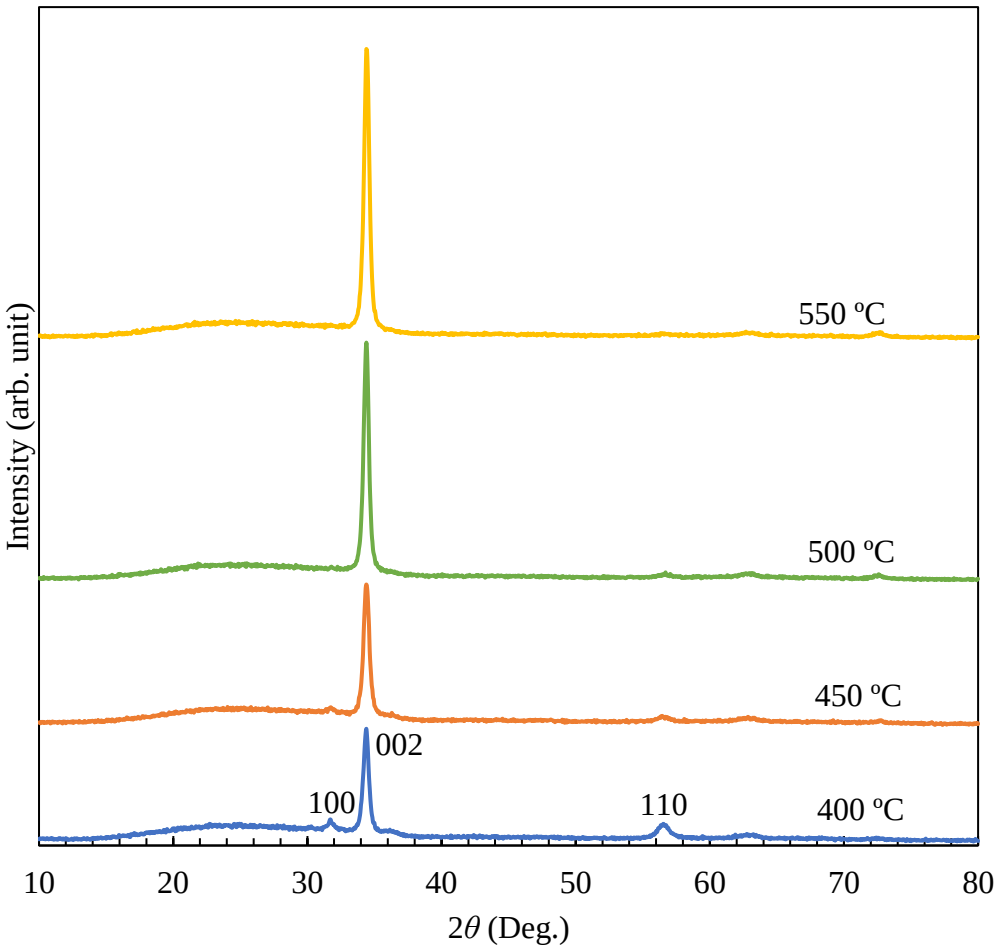

Fig. 4-3. XRD patterns of AZO thin film in respective to the annealing temperature.

XRD patterns of AZO (Fig. 4-3) shows that the intensity increased with higher annealing temperature, which might suggest the crystallinity improvement due to the formation of larger grain size by higher annealing temperature as extensively studied[10,13,14].

Although the crystallite size was not significantly different as investigated by Scherrer's equation (Table 4-1), it can be speculated that the grains might agglomerate to form larger grains thus the intensity increased by higher annealing temperature with (002) orientation.

Table 4-1. Crystallite Size of AZO thin films through (002) crystal orientation

Sample	Before damp heat test (nm)	As Reannealed after DH test (nm)
AZO 400 ºC	17	18
AZO 450 ºC	16	16
AZO 500 ºC	18	19
AZO 550 ºC	17	18

As purposed by Hüpkes et al.[4], a grain boundary reconstruction might happen as the films heated where the grains grow together and these connections close the gap or boundaries between the grains partially reducing environmental species such as water and carbon dioxide that could penetrate and thus degradation of the AZO film is reduced. This (002) crystal orientation is the optimal crystal growth orientation for optical and electrical properties of ZnO, respectively due to *c*-axis growth and the reduced number of traps for electrons[15,16].

The degradation of AZO thin films as a function of damp heat test duration for each annealing temperature exhibited that AZO thin films annealed at 400°C showed far more considerable degradation in comparison with AZO samples annealed at 450 °C or higher (Fig. 4-4). After 15 days, the degradation of AZO samples annealed at 400 °C became more extensive while samples annealed at 450 °C or higher, started to show stable resistivity. Table 4-2 provides detailed resistivity before and after damp heat where higher temperature annealing maintained the lowest resistivity even after damp heat test.

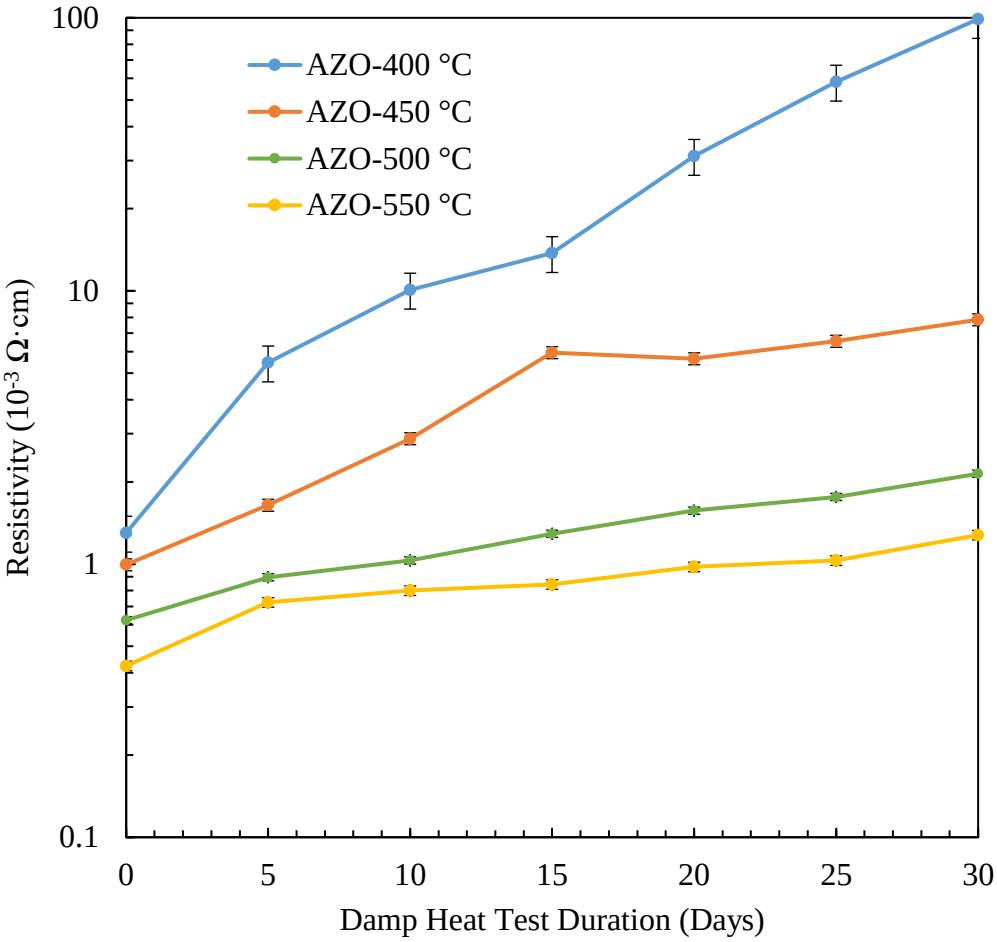

Fig. 4-4. Resistivity of AZO thin films on a logarithmic scale as exposed to harsh environment.

The comparison of degradation index (Eq. 3.5) and carrier concentration loss (Eq. 3.7) showed similar tendencies as a function of annealing temperature (Fig. 4-5). The samples annealed at 400 °C and 550 °C show 76- and 3-times higher resistivity, respectively, which suggests the higher temperature annealing produced the more durable thin films.

However, the comparison of Hall mobility before and after damp heat test (Fig. 4-5) showed equivalent results for samples annealed at 400- 550 °C where the difference is around 7-9 $cm^2/V{\cdot}s$ between the mobility before and after damp heat test. Despite, a clear difference in electrical stability of annealed AZO samples at 450-550 °C in comparison with the samples of 400 °C annealing temperature.

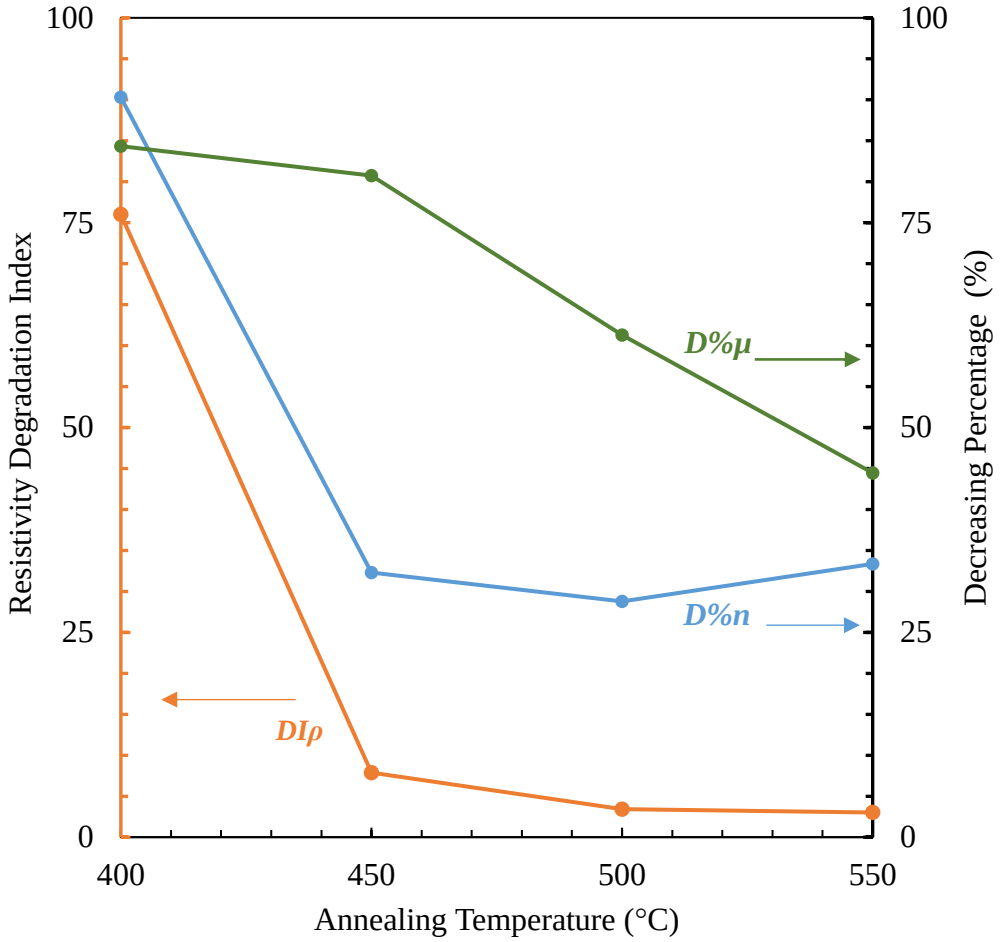

Fig. 4-5. Degradation index DI_{ρ} (Eq. 3.5) in comparison with the decreasing percentage of carrier concentration $D\%_{n}$ (Eq 3.7) and Hall mobility $D\%_{\mu}$ (Eq. 3.8).

On the other hand, the degradation index of AZO samples annealed at 450 °C or higher exhibited comparable value despite a clear significant decline in the decreasing percentage of Hall mobility. It could show the more significant influence of carrier concentration evolution during the exposure of harsh environment to the electrical stability of AZO thin films where the less decrease of carrier concentration would contribute to the less degradation index, in other words, more durable AZO thin films[17].

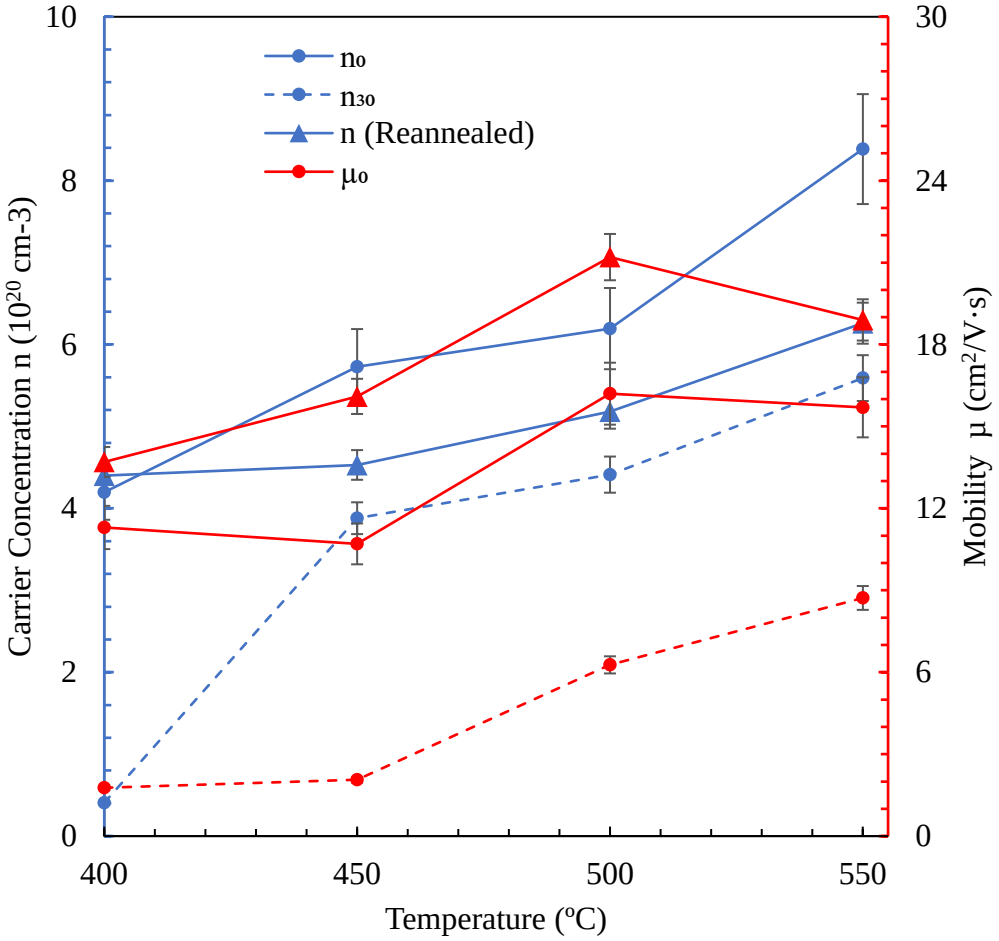

Fig. 4-6. Carrier concentration and Hall mobility before and after damp heat test compared to both evolution after re-annealing as a function of annealing temperature.

A decrease of Hall mobility was comparably exhibited by all samples (Fig. 4-6), which indicated the diffusion of water-molecule-derived species or oxygen molecules to the AZO thin films increasing the electron scattering at grain boundaries as reported by Mickan et al.[5]. After the damp heat test, carrier concentration and Hall mobility decreased for all samples where the highest carrier concentration and Hall mobility were maintained at AZO samples annealed at 550 °C.

Reannealing was conducted and effectively able to restore the conductivity, Hall mobility, and carrier concentration of AZO samples exposed to a harsh environment (Fig. 4-6). Despite the excellent conductivity recovery by re-annealing (Table 4-2), evolution and recovery of carrier concentration showed slightly different tendencies between samples annealed at 400°C and samples annealed at 450 °C or higher.

Although the conductivity is perfectly recovered (Table 4-2), the carrier concentration and Hall mobility as a function of annealing temperature of each sample before the damp heat test shows different value as compared to the recovered results (Fig. 4-6).

Table 4-2. Resistivity Development of AZO thin films

Temperature	ρ_0 (10^{-3} Ω·cm)	ρ_{30} (10^{-3} Ω·cm)	ρ - Reannealed (10^{-3} Ω·cm)
AZO-400 ºC	1.3	98.9	1
AZO-450 ºC	1	7.8	0.9
AZO-500 ºC	0.6	2.1	0.6
AZO-550 ºC	0.4	1.3	0.5

The carrier concentration of samples annealed at 400 °C could be comparably restored as much as the initial one while samples annealed at 450 °C or higher temperature were also recovered but slightly lower than the initial carrier concentration before damp heat test. On the other hand, re-annealing produced slightly higher Hall mobility as compared to the original one.

Firstly, re-annealing could contribute to the out-diffusion of water-molecule-derived species coming from exposure to the harsh environment. Secondly, as re-annealing produced a slight decrease of carrier concentration to be below the concentration before the degradation test, the ionized impurity scattering was then decreased that contributed to the slightly higher Hall mobility.

This less scattering could show the direct influence of carrier concentration evolution to the development of Hall mobility as reported by Liu et al.[18], about this trade-off of high carrier concentration and mobility through ionized impurity scattering.

More removal of chemisorbed OH^- could also be attributed to higher annealing temperature that would contribute to less scattering centers thus increased the Hall mobility as reported by Kim et al.[19].

For crystallite size after re-annealing, no significant changes in crystallite size (Table 1) were found, which could show that the maximum crystallinity had been achieved during the initial annealing and no crystallinity improvement after the re-annealing conducted. The same annealing condition for this re-annealing step as the initially associated annealing temperature could be the reason of this insignificant effect.

As reported by Calnan et al.[20], the applied higher temperature produced more oxygen vacancies, which was improving the carrier concentration of the thin films in consequence. Thus, conductivity improved by higher annealing temperature. Tabassum et al.[10] reported oxygen concentration was reported dominantly detected at the surface of AZO samples annealed at 450-600 °C and significantly decreased just beneath the surface of the films, which could show the formation of an ultra-thin oxide layer on top of the AZO layer after the first annealing.

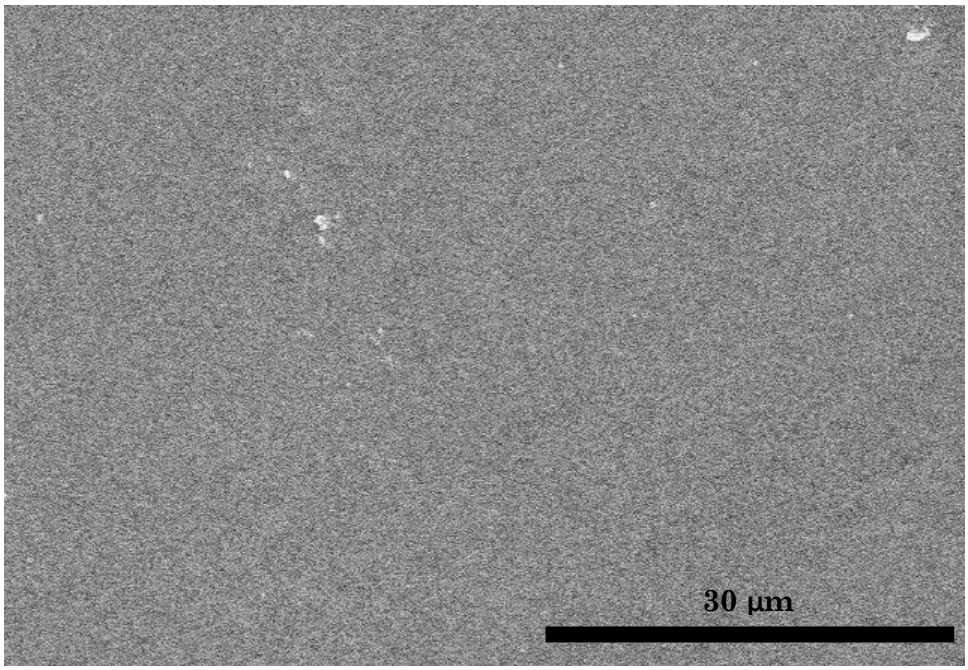

Fig. 4-7. AZO thin film annealed at 400 ºC before DH test.

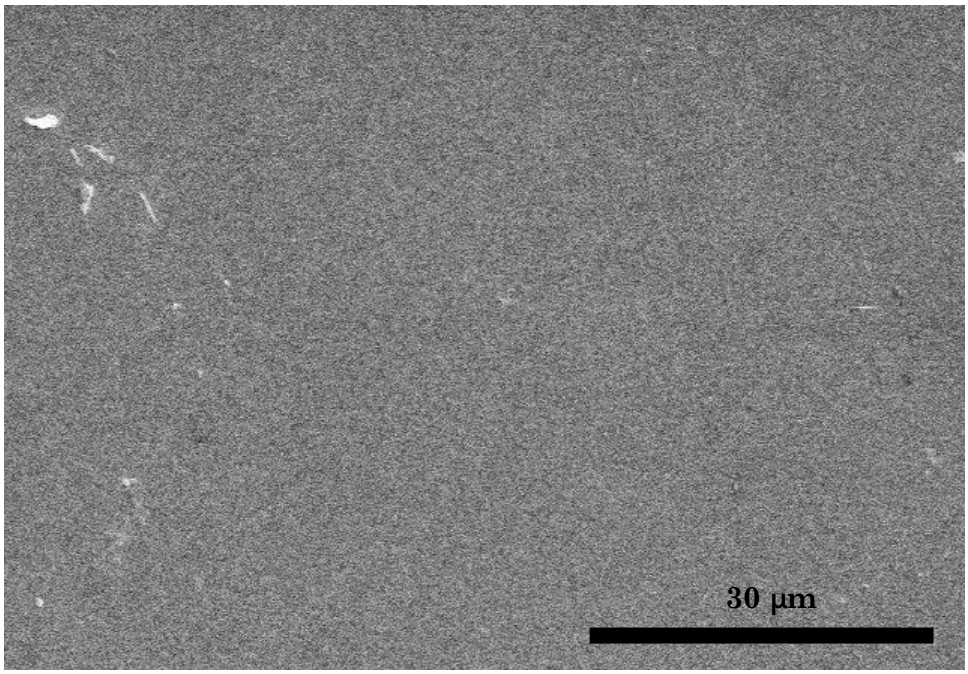

Fig. 4-8. AZO thin film annealed at 400 ºC after DH test.

In addition to higher crystallinity of the samples annealed at 450-550 °C (Fig. 4-3), this ultra-thin layer could act as passivation or protective layer[9,21] especially for samples annealed at 450 °C or higher while maintaining the conductivity of AZO layer beneath thus durability of AZO films improved in the harsh environment. As the formation of the ultra-thin oxide layer, the carrier concentration could be protected from the diffusion of water-molecule-derived species or removal of oxygen vacancies.

However, the 400 °C-annealed sample showed severe degradation compared to other samples, which could suggest the incomplete formation of an ultra-thin oxide layer on the surface. Moreover, 400 °C-annealed samples exhibited lower overall crystallinity in comparison with samples annealed at 450 °C or higher (Fig. 4-3). Thus, the carrier concentration could be easily decreased through the diffusion of oxygen molecule or water-molecule-derived species of the high humidity condition.

Besides the recoverability of Hall mobility and carrier concentration, this recoverability could also be attributed to the stable physical property of sputtered AZO samples coated on the hard substrate such as glass substrates. As showed by the image of SEM prior to the damp heat test (Fig. 4-7), there were similarly no cracks or voids found at the surface of AZO thin films after the damp heat test even for 400 °C-annealed sample, which was the most degraded one (Fig. 4-8 AZO thin film annealed at 400 °C after DH test.), confirming the findings of Tabassum et al.[1].

Glass substrates as hard substrate might support this stability since AZO thin films tend to be easily cracked with the physical deformation of the substrate such as by bending it physically as reported by Xu et al.[22].

4.3. Conclusion

Various AZO thin films have been prepared by reactive sputtering and annealed in the hydrogen atmosphere at 400 to 550 °C. Damp heat test was performed at 85 °C and 85% relative humidity to examine the durability of the films.

Re-annealing was then conducted and successfully able to recover the initial conductivity of the degraded thin films as exposed to a harsh environment with high temperature and humidity showing that the degradation is due to chemical aspects in the harsh environment such as

diffusion of oxygen or water molecules. The physical strength of the films supported by hard glass substrate could also contribute to this recoverability preventing the films from physical damage such as voids or cracks.

The evolution of electrical property of the films has been investigated before and after the damp heat test as well as after the recovery as a function of annealing temperature where improvement was exhibited by samples with higher annealing temperature. During the damp heat test, the evolution of carrier concentration exhibited similar tendencies to the electrical stability or durability differences despite the comparable decrease in Hall mobility of all samples, which suggested that the durability difference among the samples was rather caused by a reduced carrier concentration than a decreased Hall mobility.

Reference

[1] S. Tabassum, E. Yamasue, H. Okumura, K.N. Ishihara, Sol–gel and rf sputtered AZO thin films: Analysis of oxidation kinetics in harsh environment, J. Mater. Sci. Mater. Electron. 25 (2014) 4883–4888. doi:10.1007/s10854-014-2248-9.

[2] D.W. Lee, W.J. Cho, C.I. Jang, J.K. Song, C.H. Park, K.E. Park, J.S. Ryu, H. Lee, Y.N. Kim, Damp heat and thermal cycling-induced degradation mechanism of AZO and CIGS films in Cu(In,Ga)Se2 photovoltaic modules, Curr. Appl. Phys. 15 (2015) 285–291. doi:10.1016/j.cap.2014.12.023.

[3] T. Tohsophon, J. Hüpkes, S. Calnan, W. Reetz, B. Rech, W. Beyer, N. Sirikulrat, Damp heat stability and annealing behavior of aluminum doped zinc oxide films prepared by magnetron sputtering, Thin Solid Films. 511–512 (2006) 673–677. doi:10.1016/j.tsf.2005.12.130.

[4] J. Hüpkes, J.I. Owen, M. Wimmer, F. Ruske, D. Greiner, R. Klenk, U. Zastrow, J. Hotovy, Damp heat stable doped zinc oxide films, Thin Solid Films. 555 (2014) 48–52. doi:10.1016/j.tsf.2013.08.011.

[5] M. Mickan, M. Stoffel, H. Rinnert, U. Helmersson, D. Horwat, Restoring the Properties of Transparent Al-Doped ZnO Thin Film Electrodes Exposed to Ambient Air, J. Phys. Chem. C. 121 (2017) 14426–14433. doi:10.1021/acs.jpcc.7b03020.

[6] M. Mickan, U. Helmersson, D. Horwat, Effect of substrate temperature on the deposition of Al-doped ZnO thin films using high power impulse magnetron sputtering, Surf. Coatings Technol. 347 (2018) 245–251. doi:10.1016/j.surfcoat.2018.04.089.

[7] D. Greiner, S.E. Gledhill, C. Köble, J. Krammer, R. Klenk, Damp heat stability of Al-doped zinc oxide fi lms on smooth and rough substrates, Thin Solid Films. 520 (2011) 1285–1290. doi:10.1016/j.tsf.2011.04.190.

[8] D. Greiner, N. Papathanasiou, A. P, F. Ruske, R. Klenk, In fl uence of damp heat on the optical and electrical properties of Al-doped zinc oxide, 517 (2009) 2291–2294. doi:10.1016/j.tsf.2008.10.107.

[9] S. Tabassum, E. Yamasue, H. Okumura, K.N. Ishihara, Damp heat stability of AZO transparent electrode and influence of thin metal film for enhancing the stability, J. Mater. Sci. Mater. Electron. 25 (2014) 3203–3208. doi:10.1007/s10854-014-2004-1.

[10] S. Tabassum, E. Yamasue, H. Okumura, K.N. Ishihara, Electrical stability of Al-doped ZnO transparent electrode prepared by sol-gel method, Appl. Surf. Sci. 377 (2016) 355–360. doi:10.1016/j.apsusc.2016.03.133.

[11] H.Y. Liu, V. Avrutin, N. Izyumskaya, Ü. Özgür, A.B. Yankovich, A. V. Kvit, P.M. Voyles, H. Morkoç, Electron scattering mechanisms in GZO films grown on a-sapphire substrates by plasma-enhanced molecular beam epitaxy, J. Appl. Phys. 111 (2012) 103713. doi:10.1063/1.4720456.

[12] H. Lee, Electron scattering mechanisms in indium–tin-oxide thin films prepared at the various process conditions, Appl. Surf. Sci. 252 (2006) 3428–3435. doi:10.1016/j.apsusc.2005.03.203.

[13] M.-C. Jun, J.-H. Koh, Effects of Annealing Temperature on Properties of Al-Doped ZnO Thin Films prepared by Sol-Gel Dip-

Coating, J. Electr. Eng. Technol. 8 (2013) 163–167. doi:10.5370/JEET.2013.8.1.163.

[14] S. Jian, Y. Lin, W. Ke, Effects of Thermal Annealing on the Structural, Electrical and Mechanical Properties of Al-Doped ZnO Thin Films Deposited by Radio-Frequency Magnetron Sputtering, Sci. Adv. Mater. 5 (2013) 7–13. doi:10.1166/sam.2013.1424.

[15] F. Claeyssens, C.L. Freeman, N.L. Allan, Y. Sun, M.N.R. Ashfold, J.H. Harding, Growth of ZnO thin films - Experiment and theory, J. Mater. Chem. 15 (2005) 139–148. doi:10.1039/b414111c.

[16] K. Maejima, H. Shibata, S. Niki, H. Tampo, K. Matsubara, Correlation between Electrical Properties and Crystal c -Axis Orientation of Zinc Oxide Transparent Conducting Films, Jpn. J. Appl. Phys. 51 (2013) 10NC16. doi:10.7567/jjap.51.10nc16.

[17] F. Machda, T. Ogawa, H. Okumura, K.N. Ishihara, Evolution and Recovery of Electrical Property of Reactive Sputtered Al-Doped ZnO Transparent Electrode Exposed to Harsh Environment, Phys. Status Solidi Appl. Mater. Sci. 217 (2020) 1–6. doi:10.1002/pssa.201900519.

[18] H. Liu, V. Avrutin, N. Izyumskaya, Ü. Özgür, H. Morkoç, Transparent Conducting Oxides for Electrode Applocations in Light Emitting and Absorbing Devices, Superlattices Microstruct. 48 (2010) 458–484. doi:10.1016/j.spmi.2010.08.011.

[19] J.I. Kim, W. Lee, T. Hwang, J. Kim, S.Y. Lee, S. Kang, H. Choi, S. Hong, H.H. Park, T. Moon, B. Park, Quantitative analyses of damp-heat-induced degradation in transparent conducting oxides, Sol. Energy Mater. Sol. Cells. 122 (2014) 282–286. doi:10.1016/j.solmat.2013.12.014.

[20] S. Calnan, A.N. Tiwari, High mobility transparent conducting oxides for thin fi lm solar cells, Thin Solid Films. 518 (2010) 1839–1849. doi:10.1016/j.tsf.2009.09.044.

[21] P. Poodt, A. Lankhorst, F. Roozeboom, K. Spee, D. Maas, A. Vermeer, High-Speed Spatial Atomic-Layer Deposition of Aluminum Oxide Layers for Solar Cell Passivation, Adv. Mater. 22 (2010) 3564–3567. doi:10.1002/adma.201000766.

[22] Q. Xu, W. Shen, Q. Huang, Y. Yang, R. Tan, K. Zhu, N. Dai, W. Song, Flexible transparent conductive films on PET substrates with an AZO/AgNW/AZO sandwich structure, J. Mater. Chem. C. 2 (2014) 3750–3755. doi:10.1039/C3TC32554G.

5. Damp Heat Durability of Al-Doped ZnO Transparent Electrodes with Different Crystal Growth Orientations

5.1. Introduction

The crystal growth orientation plays an important role to the conductivity of AZO films, where specific crystal orientation could act as traps for carriers[1]. Most of AZO films have been reported to have the main crystal orientation (002),[2,3] which is considered as the most effective morphology due to more reduced numbers of electron traps in comparison with other crystal orientations[1,4].

As well as conductivity, durability in a harsh environment such as a damp heat condition is still questionable for those ZnO-based transparent electrodes. This durability issue becomes more crucial when considering the implementation of durable and outdoor devices such as automotive displays and photovoltaics respectively since the degradation of transparent electrodes will degrade the overall performances of the device.

Tabassum et al.[5] reported the preparation of AZO thin films with different textures of (002) and (110) by two different deposition methods: the sol-gel dip-coating and the radio frequency (RF) magnetron sputtering respectively. According to this report, the samples prepared by sputtering having the orientation (110) was more durable, strongly suggesting the influence of deposition methods on the durability of AZO films. However, the influence of different crystal growth orientation is not clear yet, especially for the samples prepared by the sputtering methods with crystal orientation other than (110). As reported by Zhan et al.[3], AZO films with the orientation (002) prepared by RF magnetron sputtering and zinc vapor annealing exhibited very high durability in a damp heat condition. Besides the main orientation (002), the removal of zinc vacancies by zinc vapor annealing was strongly suggested as the reason for this improved durability.

Furthermore, methods to produce different crystal growth orientations other than (002) through sputtering were not widely reported [6]. Hence, there is also a paucity of research evaluating an influence of crystal growth orientation on the durability.

The study in this chapter prepared AZO thin films by varying argon gas flow (3 – 60 sccm) amidst a fixed oxygen gas flow rate (60 sccm) of one-hour RF-magnetron sputtering using 100 W of RF power. The deposited films are then annealed at 550 °C in a hydrogen atmosphere (0.06 MPa for 30 min) before characterizing the difference in the crystal growth orientation and the effectiveness of each crystal orientation for the durability of sputtered AZO films in a harsh environment represented by a damp heat condition.

The durability was evaluated in terms of electrical conductivity degradation as a function of argon gas flow. Moreover, surface conditions of AZO samples were then compared to clarify on how the physical aspects of AZO samples were affected by these variations of crystal orientations and how these physical aspects would influence the degradation mechanism of AZO films. The investigated samples are labeled as "AZO-x/y", where "x" and "y" represent argon and oxygen gas flow respectively.

5.2. Results and Discussion

Figure 5-1 shows XRD patterns of the prepared AZO films with different main crystal growth orientations according to the working gas condition during the sputtering as confirmed by the data in the Inorganic Crystal Structure Database (ICSD). AZO-3/60 and AZO-15/60 samples exhibited (110) plane as the strongest peak along with other lower peaks of crystal orientations such as (100) and (002).

As the argon gas flow was increased along with the fixed oxygen gas flow of 60 sccm for AZO-30/60 and AZO-60/60 samples, a transition of the main peak from (110) to (002) texture was clearly exhibited along with lower peak of crystal orientations of (101), (100), and (004). As argon gas flow increased to 15 sccm, (002) texture started to appear. When argon gas flow is 30 sccm, which weakens the peak of the orientation (110), the orientation (002) becomes the orientation with the highest peak.

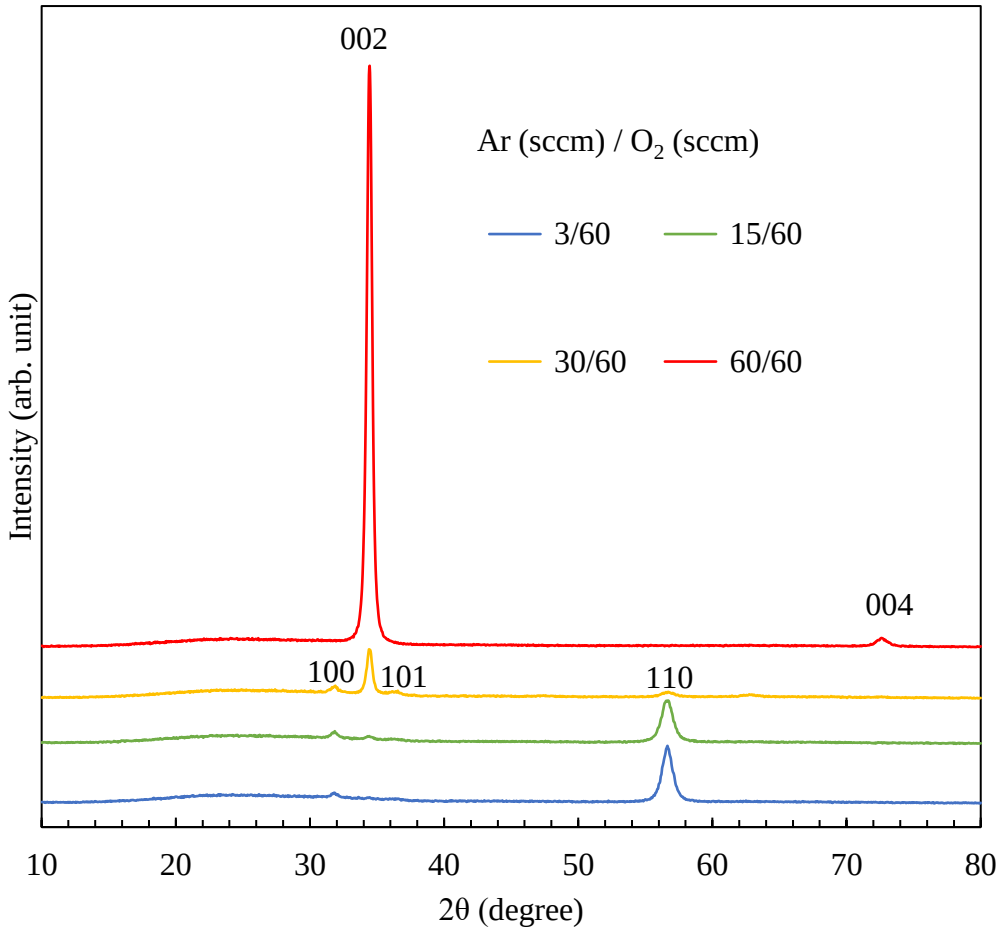

Fig. 5-1. A transition of main crystal growth orientations of the AZO films according to the applied argon gas flow rate as checked by XRD.

In comparison with the results of AZO films deposited by a ceramic target and incorporating only argon gas, which showed no transition as reported by Han et al.[7], these transitions of (110) to (002) showed different tendencies. This could suggest the different influences between ceramic and metallic targets onto the sputtered films.

As evaluated by Eq. 3.4, AZO samples with (002) as the main crystal orientation obtained almost doubled crystallite size (17-18 nm) in comparison with the crystallite size of films having (110) texture (9-10 nm).

This tendency showed similar results reported by Han et al.[7] that applying higher argon gas could lead to bigger crystallite size. This bigger crystallite size and higher peak indicated increased crystallinity of the films prepared by a higher rate of argon gas flow.

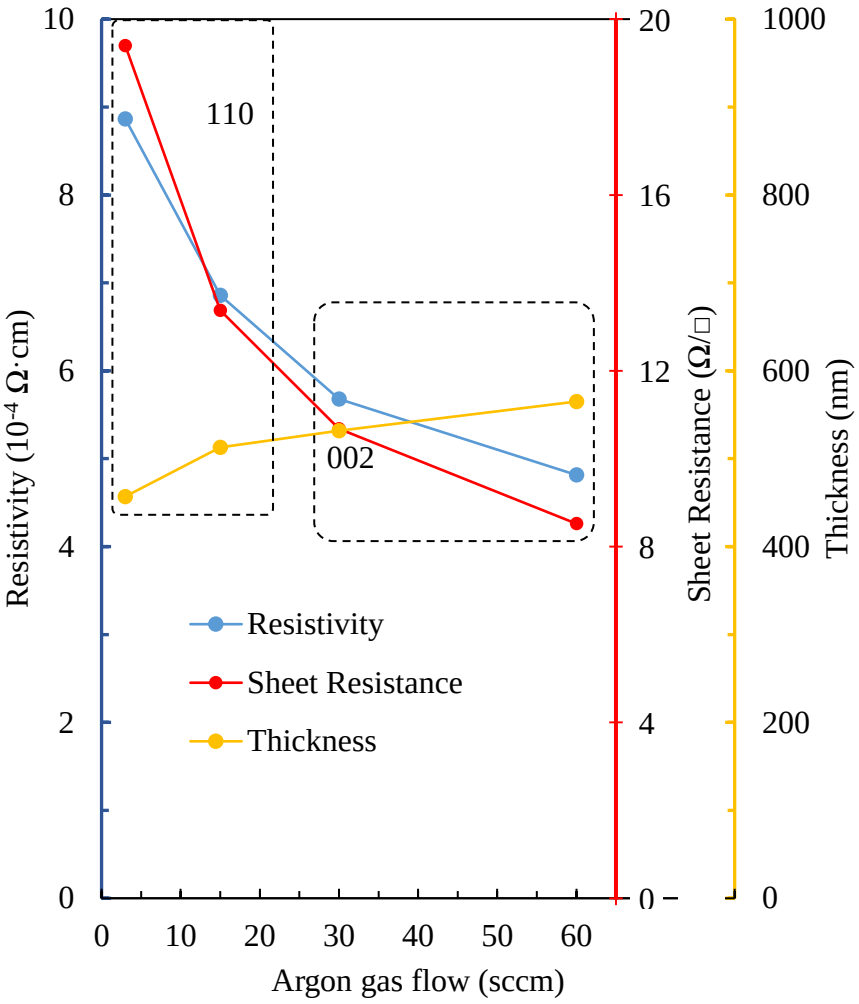

Fig. 5-2. Resistivity, sheet resistance, and thickness of the AZO films as prepared.

The thickness of AZO films increased slightly with higher argon gas flow (Fig. 5-2). It indicates that higher rate of argon gas flow would lead to slightly more rapid deposition rate which confirmed the results reported by Jafarzadeh et al.[8] As the higher rate of argon gas flow was applied, a transition of the orientation (110) to (002) contributed to the decrease of

sheet resistance and resistivity (Fig. 5-2), indicating that texture (002) contributed to better conductivity of AZO films in comparison with films with (110). As reported by Maejima et al.[1], the growth of such c-oriented films in wurtzite-type crystals of (002) could decrease the number of defects and traps for the electrons, which contributed to the higher carrier density and mobility.

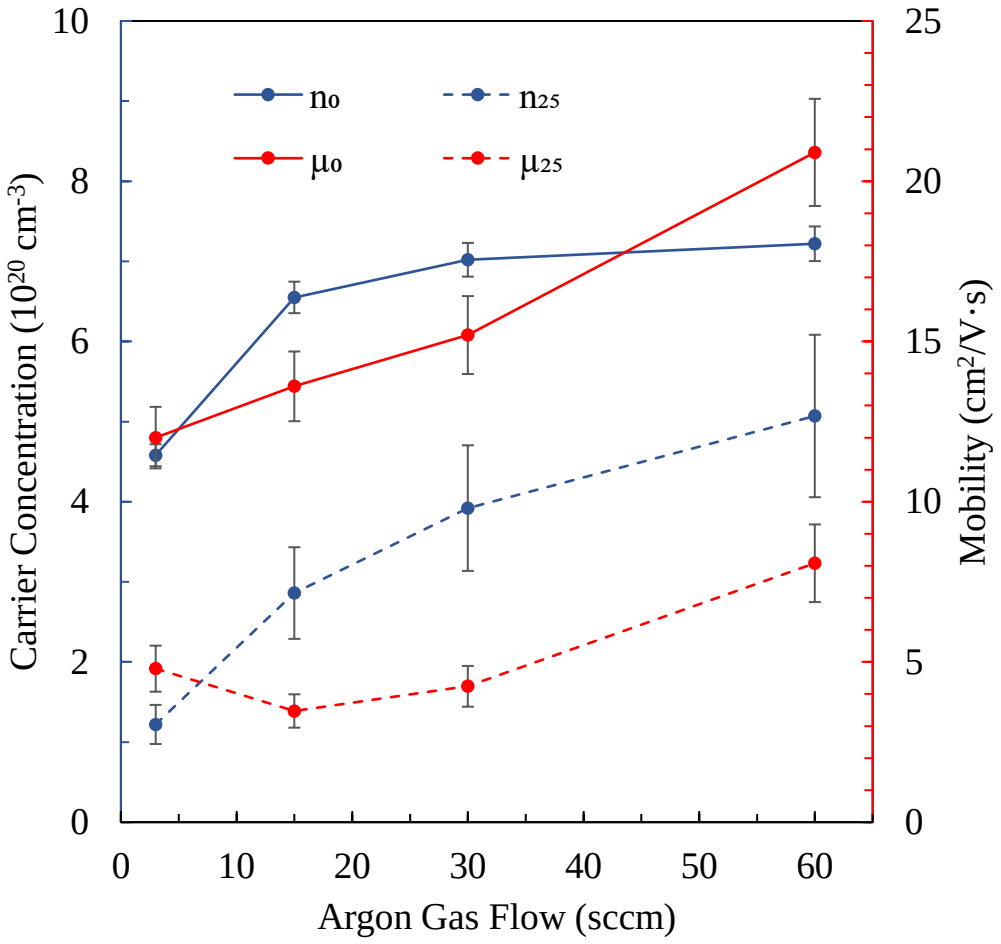

Fig. 5-3. Comparison between as prepared and after damp heat test of carrier concentration (n) and Hall mobility (μ) as a function of the argon gas flow.

Figure 5-3 confirmed this correlation where carrier concentration and Hall mobility were increased with higher argon (or total) gas flow in sputtering with crystal growth orientation (002). The increased thickness could also contribute to the less interface scattering as reported by Look et al.[9] thus the mobility increased with a higher rate of applied argon gas flow.

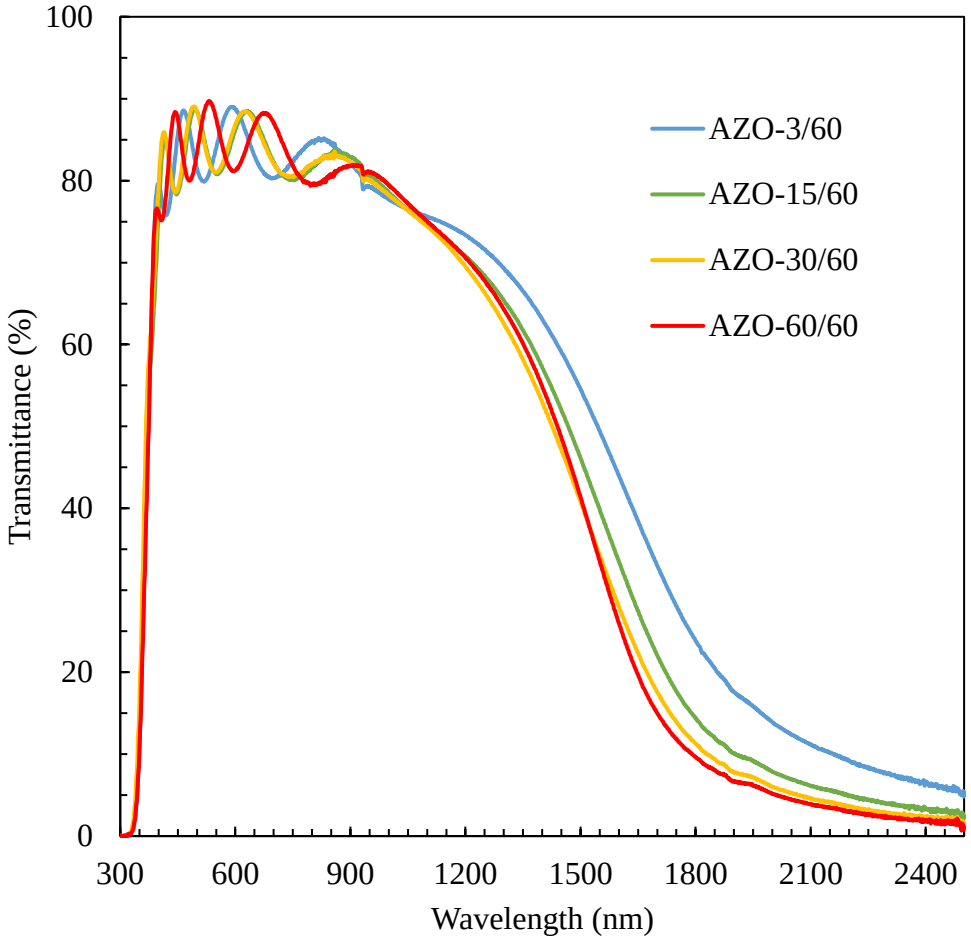

Fig. 5-4. The transmittance of AZO thin films in the visible and near-infrared range of wavelength

Figure 5-4 showed that all prepared samples demonstrated similarly the average transmittance of around 85% in the wavelength range of visible light (400-700 nm) regardless of the difference of the sputtering gas condition or crystal orientation as measured by UV/Vis/NIR spectrometer. It confirmed the high quality of transparency of AZO thin films as TE materials in general in the visible range of wavelength[10]. However, higher transmittance is exhibited in the near-infrared range of wavelength

by samples prepared by lower argon gas corresponding to lower carrier concentrations of the films (Fig. 5-4). As reported by Liu et al.[11], transparent electrodes with higher carrier concentration tend to show lower transmittance in near-infrared wavelength due to free carrier absorption, which is confirmed by this result.

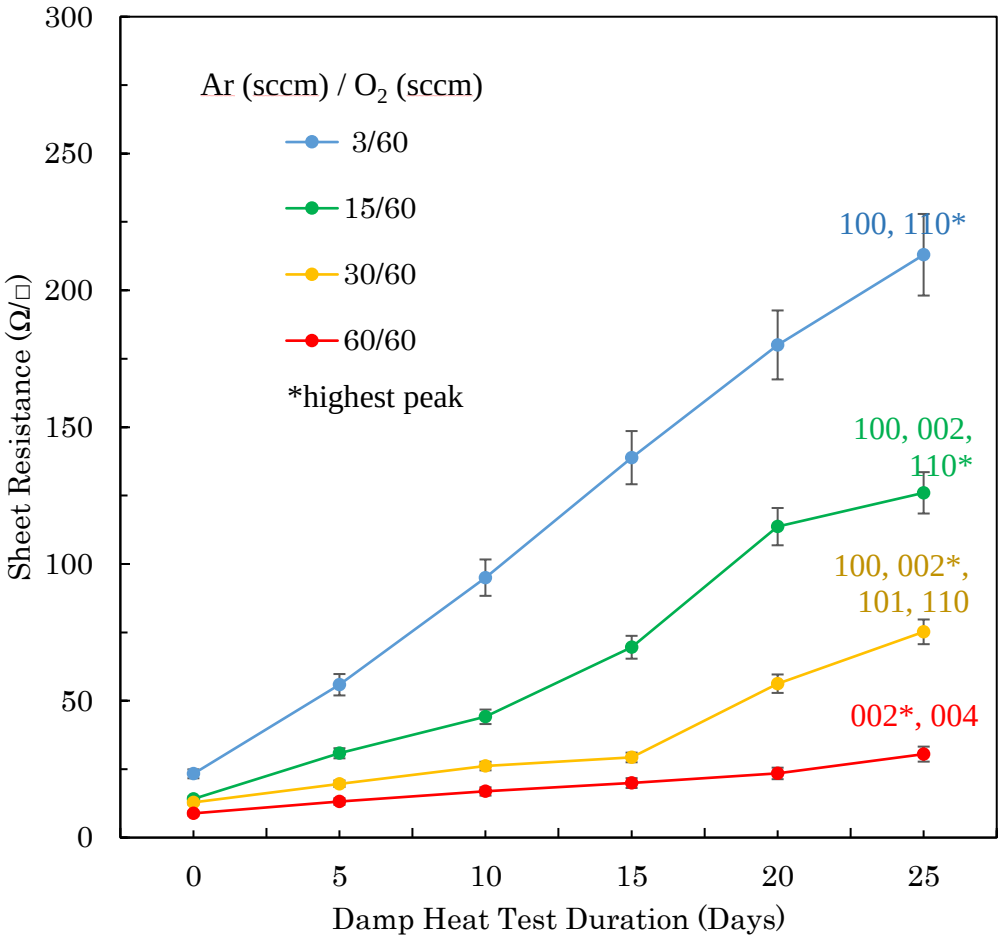

Fig. 5-5. Degradation of AZO films during the damp heat test according to the applied argon gas flow rate.

As exposed to the damp heat condition of 85% of relative humidity at 85 °C for 25 days, carrier concentrations and mobility of all samples reduced (Fig. 5-5). In consequence, the conductivity of all samples degraded (Fig. 5-5). In comparison with AZO films with orientation (110), AZO films with orientation (002) showed less degradation.

As a function of argon gas flow, carrier concentration as prepared (n_0) and after 25 days (n_{25}) exhibited a monotonically increasing function. On the other hand, mobility as prepared (μ_0) and after 25 days (μ_{25}) showed different tendencies. As a function of argon gas flow, μ_0 exhibited a monotonically increasing function while μ_{25} showed a function that was not monotonic.

AZO-15/60 and AZO-30/60 showed more decreased mobility in comparison with AZO-3/60 and AZO-60/60. AZO-15/60 and AZO-30/60 have both different main crystal orientations, which are (110) and (002) respectively but have comparably more numbers of crystal orientation variations in comparison with AZO-3/60 and AZO 60/60. More variations of crystal orientation seemed to lead to more decreased Hall mobility for AZO films. Conversely, less variation of crystal orientation would lead to less decreased Hall mobility.

As evaluated by equation 3.5, different values are shown in the degradation index of AZO films even for films with the same main crystal orientations where lower degradation index represents more durable films (Fig. 5-6). As compared within the pair of orientation (110), AZO-3/60 showed less durability than AZO-15/60.

The appearance of orientation (002) in AZO-15/60 samples could contribute to the more protected carrier concentration thus it became more durable. Even though the mobility of AZO-15/60 is more decreased, the overall degradation is less for AZO-15/60 in comparison with AZO-3/60 indicating that the different degradation index is rather caused by the reduced carrier concentration.

For the comparison within the pairs of orientation (002), AZO-60/60 showed more durability than AZO-30/60 (Fig 5-6). Fewer variations of crystal orientation of AZO-60/60 (Table 5-1 and Fig 5-5 - 5-7) could lead to more stable Hall mobility (Fig. 5-7).

Table 5-1. Crystal orientation and crystallite size of AZO films

Ar (sccm) / O_2 (sccm)	**Plane**	**FWHM (deg.)**	**Crystallite size (nm)**
60/60	002*	0.4756	17
	004	0.9832	10
30/60	100	0.5873	14
	002*	0.474	18
	101	0.8367	10
	110	1.153	8
15/60	100	0.5704	14
	002	0.7096	12
	110*	1.0041	9
3/60	100	0.5142	16
	110*	0.8718	10

*Crystal orientations with the highest peak in the samples

Furthermore, the existence of several crystal orientations other than (002), such as (110) in AZO-30/60 samples could lead to less protected carrier concentration in comparison with AZO-60/60 where the orientation (110) disappeared. The nature of polycrystalline of the films where variations of many crystal orientations exist (Fig. 5-1 and Table 5-1) contributed to this different degree of degradation or durability between the films[5].

As a function of argon gas flow, the degraded conductivity showed monotonous tendencies, which was similar to the reduced carrier concentration (Fig. 5-7). Besides crystal orientations, the influence of the higher working pressure due to the higher rate of applied argon gas flow during the sputtering which could contribute to the bigger crystal size as reported by Park et al.[12]. This influence clarified the importance of total working pressure on structural property and durability of sputtered AZO films.

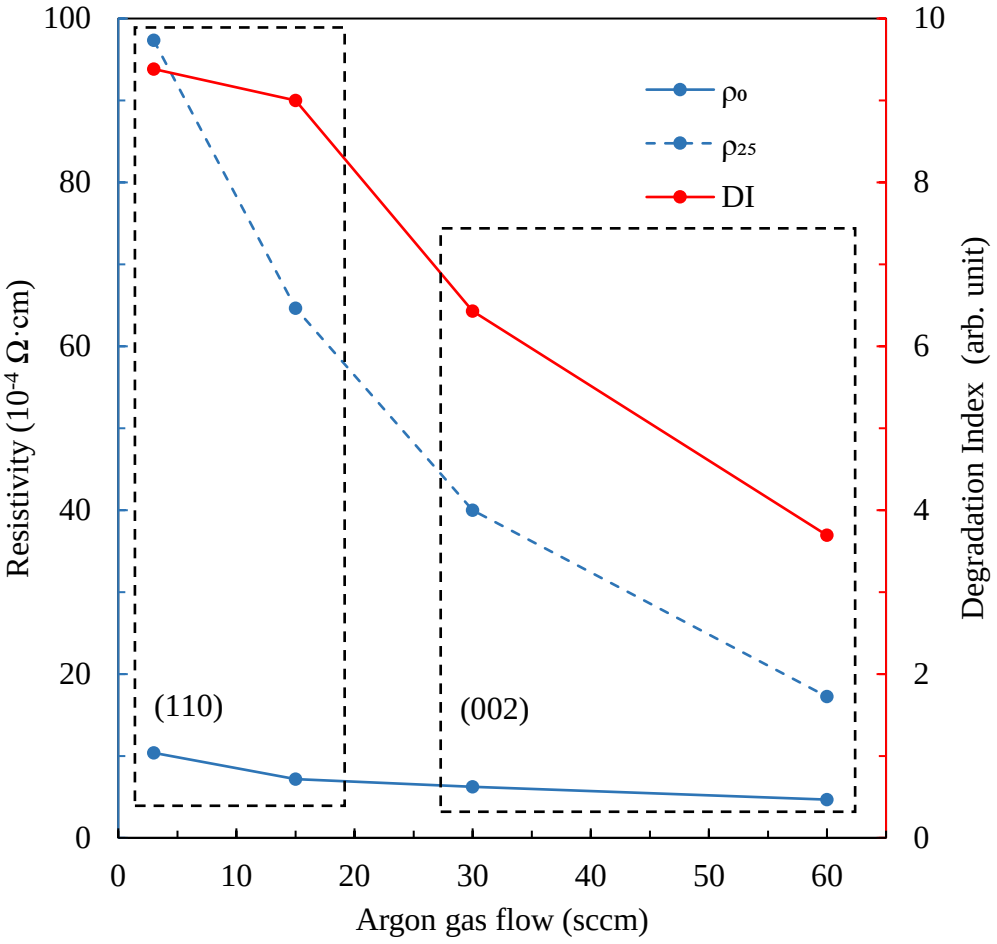

Fig. 5-6. Degradation index (DI) and a comparison between resistivity (ρ) of AZO films as prepared and after 25 days in the damp heat test.

By looking at each sample individually, the decrease of Hall mobility contributes more than the decrease of carrier concentration for degradation index for each sample (Eq. 3.6 and Fig. 5-7). However, by comparing between the prepared samples, the different degree of conductivity degradation index seemed more caused by the significant difference in the decrease of carrier concentration since both of them are monotonous as a function of argon gas flow along with the comparable decrease of Hall mobility of all prepared samples.

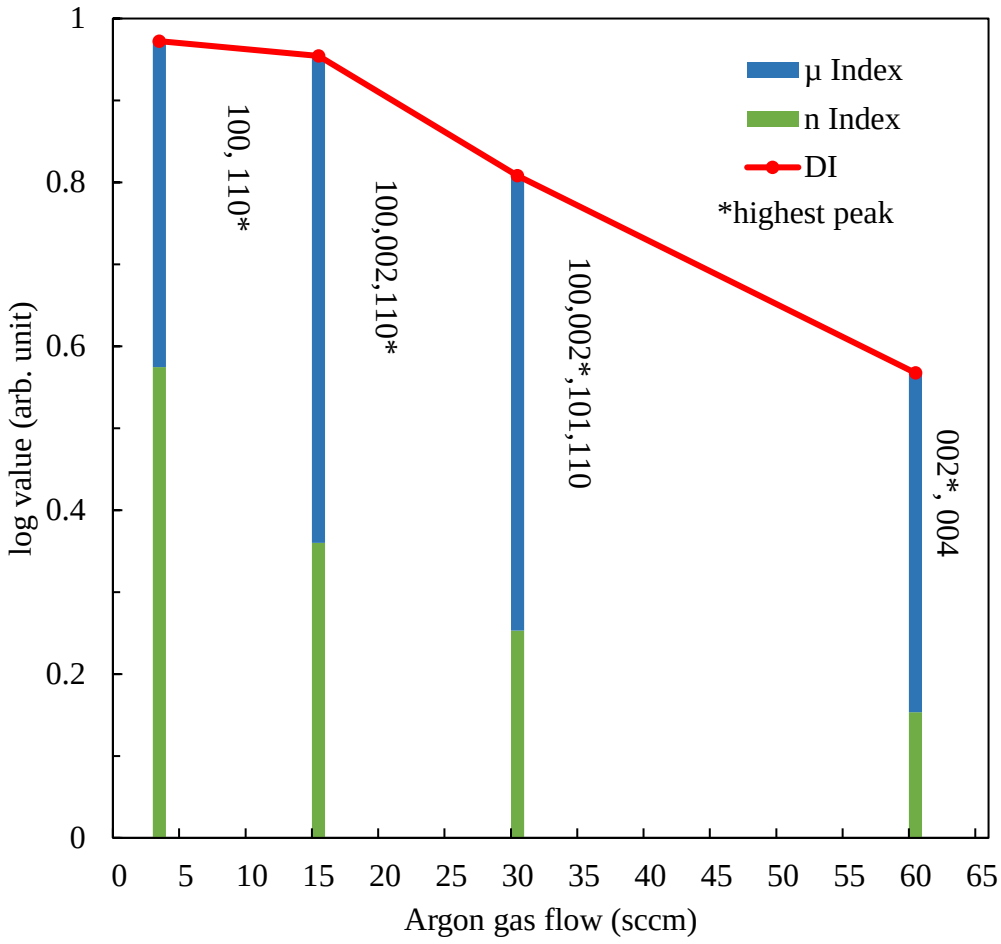

Fig. 5-7. Log of the decrease-index of carrier concentration (n) and mobility (μ) in comparison with the log of degradation index (DI) (Eq. 3.6).

During the damp heat test, oxygen vacancies might be removed due to the chemisorption of oxygen or water molecule at the surface and grain boundaries, contributing to the decrease in carrier concentration as reported by Tabassum et al.[2]. Besides the removal of oxygen vacancies, water vapor of a damp heat condition could act as a trap for free carriers when adsorbed at the grain boundaries as reported by Tohsophon et al.[13] thus reduced carrier concentration.

Furthermore, Mickan et al.[14] reported that as the water molecules adsorbed, the formation of hydroxyl groups such as $Zn(OH)_2$ could happen and act as trap states, decreasing the carrier concentration thus the conductivity degraded. However, AZO films with crystal orientation (002) were more durable which could be attributed to the better protection of carrier concentration, preventing removal of oxygen vacancies and the creation of hydroxyl groups.

The log of decrease-index of Hall mobility (Eq. 3.6) showed different tendencies with the log of degradation index, which could be attributed to an almost comparable decrease of Hall mobility between the prepared samples regardless of the difference in main crystal orientations. However, a slightly different decrease-index of Hall mobility is in line with the numbers of existing crystal orientation on the films (Fig. 5-7). Kang et al.[15] attributed this decrease of Hall mobility due to the increase in barrier height at the grain boundaries caused by the permeation of chemisorbed oxygen through defects such as the boundaries or voids as the films exposed to a damp heat condition. Tohsophon et al.[13] attributed the reduced mobility to the carrier scatterings enhanced by the adsorption of water vapor at grain boundaries.

As investigated by the SEM, the samples having more crystal orientations showing more voids than the samples with less crystal orientation (Fig. 5-8) regardless of the main crystal orientations owned by the samples. These less dense grains or more voids could suggest that the more crystal orientations exist, the more defects could exist in the film. Therefore, with more defects, water vapor of a damp heat condition could adsorb more into the film causing more scattering centers for the free carriers, leading to more decreased Hall mobility for the samples being exposed to a damp heat condition.

For instance, these defects are very comparable between AZO-3/60 and AZO-60/60. Even though these two samples having different main crystal orientation, the numbers of existing crystal orientations are similar, therefore the decrease-index of Hall mobility is likewise comparable. Despite this comparable decrease of Hall mobility of both samples (Fig 5-7), the conductivity degradation index (Fig. 5-6) and the decrease-index of carrier concentrations (Fig. 5-7) between AZO-3/60 and AZO-60/60 are significantly different along with the difference in the main crystal orientations, i.e. (110) for AZO-3/60 samples and (002) for AZO-60/60 samples.

As compared with AZO-3/60 samples, the less degraded films of AZO-60/60 samples were mainly due to the less-decreased carrier concentration along with the existence of the main crystal orientation (002). Therefore, the crystal orientation (002) seems to be more effective in protecting the films from the diffusion of hydroxyl groups than the orientation (110), which could be attributed to the more homogenous atomic crystal plane structure of the orientation (002) than of the orientation (110) as reported by Bach et al.[16].

For a comparison of another pair of main orientation (110), AZO-15/60 samples exhibited better durability than AZO-3/60 samples (Fig. 5-5 and Fig. 5-6) due to the less decreased carrier concentrations of AZO-15/60 samples (Fig. 5-7), which could be attributed to the appearance of minor orientation (002) in AZO -15/60 samples (Table 5.1) leading to the less-diffusion of hydroxyl groups[17]. Even though, the mobility of AZO-15/60 was more decreased (Fig. 5-7) due to more variations of crystal orientations, which could lead to more voids on the surface (Fig. 5-8) in comparison with AZO-3/60 samples.

Furthermore, before the damp heat test, the carrier concentration of AZO-15/60 was higher than AZO-3/60 that could lead to higher durability. This result is in line with the findings indicated in the chapter 4 where higher carrier concentration contributes to better durability of AZO films[18]. Despite that both are having main crystal orientation (110), fewer crystal orientations of AZO-3/60 as compared to AZO-15/60 could contribute to this different level of decrease in Hall mobility. However, the interdependence between the crystal orientations and the magnetic field causing magnetic anisotropy and polarization might affect the Hall measurement[19].

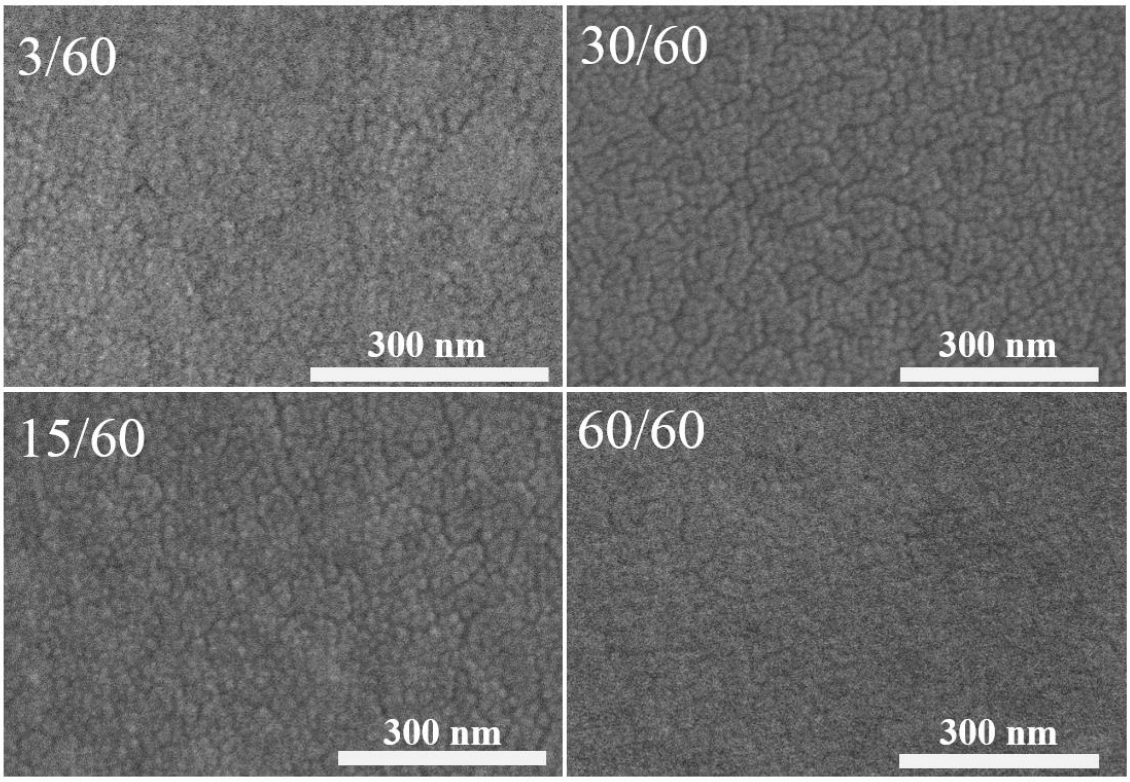

Fig. 5-8. SEM images showing the variations of voids and grain boundaries of the AZO films according to the applied argon-to-oxygen gas flow ratio conditions

However, the significant difference is exhibited in the decrease of carrier concentration in the comparison between both samples where AZO-15/60 exhibited less-decreased carrier concentration (Fig. 5-7) thus obtained conductivity that is more durable (Fig. 5-6). The appearance of crystal orientation (002) could contribute to the protection of carrier concentration of AZO-15/60 samples thus made it more durable conductivity as compared with AZO-3/60.

Consequently, AZO-60/60 exhibited the most durable film in this research Fig. 5-5) by having the main crystal orientation (002) and comparably fewer crystal orientations (Fig. 5-1 and Table 5-1). As respectively compared with the carrier concentration and mobility of other samples in this research, the crystal orientation (002) would provide more homogenous atomic crystal plane structure[16] leading to the less-decreased carrier concentrations (Fig.

5-3) and fewer crystal orientations would lead to fewer voids on the surface (Fig 5-8) thus, the mobility was less-decreased (Fig. 5-3 and Fig. 5-7).

Both of less-decreased carrier concentration and mobility of AZO-60/60 samples could indicate that as exposed to damp heat test, AZO films with orientation (002) could be less diffused by hydroxyl groups, which could act as traps for charge carriers reducing carrier concentration and mobility of AZO films as reported by Mickan et al.[14].

The crystal orientation (002) protects the films from the oxidation, and thus the carrier concentration is relatively protected as compared to other crystal orientations. Moreover, thin films with fewer variations of crystal orientations tend to have fewer defects, which would contribute to more stable Hall mobility of thin films exposed to a damp heat condition such as in a harsh environment.

5.3. Conclusions

AZO films with various crystal growth orientations were prepared by varying argon gas flow against consistent flow rate of oxygen gas in reactive sputtering. A transition of crystal growth orientation from (110) to (002) was exhibited when argon gas flow was increased during thin film deposition. During the damp heat test, films with the main crystal growth of orientation (002) were more durable in electrical conductivity than those films with orientation (110). Electrical conductivity degraded monotonously with decreasing carrier concentration as a function of argon gas flow.

Conversely, the decrease in Hall mobility seemed more affected by physical surface structures such as defects or voids, where more variations in crystal orientations would lead to more defects, leading to more decreased Hall mobility. Despite this tendency being observed for both orientations of AZO films, the degradation index differences among AZO films seemed to be rather caused by the effectiveness of major crystal orientations of each sample in protecting the films from oxidations and maintaining carrier concentrations. Crystal orientation (002) was more effective in maintaining carrier concentration of the film, leading to better durability of thin-film electrical conductivity, than crystal orientation (110).

As the ratio argon gas flow was increased in the mixture of argon and oxygen gasses, the orientation (002) was strengthened resulting an increased durability. From this point, the result of this research suggests that ratio of argon gas flow should as high as possible to obtain the most durable of AZO. Another way of increasing of argon gas flow ratio is to reduce the flow of oxygen gas, which will be very interesting to be investigated (discussed in the chapter 6).

Reference

[1] K. Maejima, H. Shibata, S. Niki, H. Tampo, K. Matsubara, Correlation between Electrical Properties and Crystal c -Axis Orientation of Zinc Oxide Transparent Conducting Films, Jpn. J. Appl. Phys. 51 (2013) 10NC16. doi:10.7567/jjap.51.10nc16.

[2] S. Tabassum, E. Yamasue, H. Okumura, K.N. Ishihara, Electrical stability of Al-doped ZnO transparent electrode prepared by sol-gel method, Appl. Surf. Sci. 377 (2016) 355–360. doi:10.1016/j.apsusc.2016.03.133.

[3] Z. Zhan, J. Zhang, Q. Zheng, D. Pan, J. Huang, F. Huang, Z. Lin, Strategy for Preparing Al-Doped ZnO Thin Film with High Mobility and High Stability, Cryst. Growth Des. 11 (2011) 21–25. doi:10.1021/cg101216z.

[4] F. Claeyssens, C.L. Freeman, N.L. Allan, Y. Sun, M.N.R. Ashfold, J.H. Harding, Growth of ZnO thin films - Experiment and theory, J. Mater. Chem. 15 (2005) 139–148. doi:10.1039/b414111c.

[5] S. Tabassum, E. Yamasue, H. Okumura, K.N. Ishihara, Sol–gel and rf sputtered AZO thin films: Analysis of oxidation kinetics in harsh environment, J. Mater. Sci. Mater. Electron. 25 (2014) 4883–4888. doi:10.1007/s10854-014-2248-9.

[6] F. Machda, T. Ogawa, H. Okumura, K.N. Ishihara, Effects of Sputtering Gas on Crystal Growth Orientations and Durability of Al-doped ZnO Transparent Electrodes in Harsh Environment, in:

2019 26th Int. Work. Act. Flatpanel Displays Devices, IEEE, Kyoto, Japan, 2019: pp. 1-4 (3–3). doi:10.23919/AM-FPD.2019.8830628.

[7] S.I. Han, H.B. Kim, A Study on Properties of RF-sputtered Al-doped ZnO Thin Films Prepared with Different Ar Gas Flow Rates, Appl. Sci. Converg. Technol. 25 (2016) 145–148. doi:10.5757/ASCT.2016.25.6.145.

[8] M. Jafarzadeh, K. Khojier, H. Savaloni, Influence of Nitrogen Gas Flow on Mechanical and Tribological Properties of Sputtered Chromium Nitride Thin Films, Adv. Mater. Res. 829 (2013) 497–501. doi:10.4028/www.scientific.net/amr.829.497.

[9] D.C. Look, K.D. Leedy, A. Kiefer, B. Claflin, N. Itagaki, K. Matsushima, I. Suhariadi, Model for thickness dependence of mobility and concentration in highly conductive zinc oxide, Opt. Eng. 52 (2013) 033801. doi:10.1117/1.OE.52.3.033801.

[10] J.H. Shi, S.M. Huang, J.B. Chu, H.B. Zhu, Z.A. Wang, X.D. Li, D.W. Zhang, Z. Sun, W.J. Cheng, F.Q. Huang, X.J. Yin, Effect of ZnO buffer layer on AZO film properties and photovoltaic applications, J. Mater. Sci. Mater. Electron. 21 (2010) 1005–1013. doi:10.1007/s10854-009-0028-8.

[11] H. Liu, V. Avrutin, N. Izyumskaya, Ü. Özgür, H. Morkoç, Transparent Conducting Oxides for Electrode Applocations in Light Emitting and Absorbing Devices, Superlattices Microstruct. 48 (2010) 458–484. doi:10.1016/j.spmi.2010.08.011.

[12] H. Park, S. Qamar Hussain, S. Velumani, A.H. Tuan Le, J. Yi, S. Ahn, S. Kim, Influence of working pressure on the structural, optical and electrical properties of sputter deposited AZO thin films, Mater. Sci. Semicond. Process. 37 (2015) 29–36. doi:10.1016/j.mssp.2014.12.076.

[13] T. Tohsophon, J. Hüpkes, S. Calnan, W. Reetz, B. Rech, W. Beyer, N. Sirikulrat, Damp heat stability and annealing behavior of aluminum doped zinc oxide films prepared by magnetron sputtering, Thin Solid Films. 511–512 (2006) 673–677. doi:10.1016/j.tsf.2005.12.130.

[14] M. Mickan, M. Stoffel, H. Rinnert, U. Helmersson, D. Horwat, Restoring the Properties of Transparent Al-Doped ZnO Thin Film Electrodes Exposed to Ambient Air, J. Phys. Chem. C. 121 (2017) 14426–14433. doi:10.1021/acs.jpcc.7b03020.

[15] D.-W. Kang, J.-Y. Kwon, D.-J. Lee, M.-K. Han, Boron and Aluminum Codoped ZnO Transparent Conducting Films with High Electrical Stability, J. Electrochem. Soc. 159 (2011) H61–H65. doi:10.1149/2.002202jes.

[16] L.G. Bach, N.G. Nguyen, V.T.T. Ho, Enhanced Light Scattering by Preferred Orientation Control of Ga Doped ZnO Films Prepared through MOCVD, Int. J. Photoenergy. 2016 (2016) 1–7. doi:10.1155/2016/1217576.

[17] F. Machda, T. Ogawa, H. Okumura, K.N. Ishihara, Damp Heat Durability of Al-Doped ZnO Transparent Electrodes with Different Crystal Growth Orientations, ECS J. Solid State Sci. Technol. 8 (2019) Q240–Q244. doi:10.1149/2.0261912jss.

[18] F. Machda, T. Ogawa, H. Okumura, K.N. Ishihara, Evolution and Recovery of Electrical Property of Reactive Sputtered Al-Doped ZnO Transparent Electrode Exposed to Harsh Environment, Phys. Status Solidi. 1900519 (2019) 1900519. doi:10.1002/pssa.201900519.

[19] P. Zhou, Y. Qi, C. Yang, Z. Mei, A. Ye, K. Liang, Z. Ma, Z. Xia, T. Zhang, Magnetic anisotropy of epitaxial La2/3Sr1/3MnO3 thin films on SrTiO3 with different orientations, AIP Adv. 6 (2016). doi:10.1063/1.4972955.

6. Damp-heat durability comparison of Al-doped ZnO transparent electrodes deposited at low temperatures on glass and PI-tape / PC substrates

6.1. Introduction

With emerging flexible optoelectronic devices, such as flexible electronics [1], electronic skin [2], and flexible solar cells [3], certain flexible substrates are required for fabricating those devices, such as polyimide [4,5] and polycarbonate[6] materials. Compared to hard-transparent substrates such as glass materials that could survive high-temperature processes between 450 to 600 °C [7], for example, polymer-based flexible substrates cannot survive such high temperatures during the thin film deposition process or post-heat-treatment [6,8]. Therefore, a low-temperature process or no post-heat-treatment is more preferable for this kind of polymer-based flexible device; such a process at a temperature lower than 177 °C [9] is required for polyimide-based substrates.

Prepelita et al. [10] and Marques et al. [4] both reported being able to deposit AZO thin films on polyimide (Kapton) substrates via non-reactive radio frequency (RF) magnetron sputtering and atomic layer deposition (ALD), respectively, revealing the usability of polyimide materials as substrates for thin films deposited via typical methods or processes. Polyimide materials having the mold temperature range of 177 to 232 °C [9] are adequate for such typical ALD and sputtering methods, while polycarbonates having mold temperatures between 82 to 121 °C [11] cannot withstand those typical processes and thus require even milder deposition processes [6].

Jung et al. [6] reported that a facing-target sputtering (FTS) method could produce transparent-conductive AZO thin films on polycarbonate

substrates by maintaining temperatures at 20 to 55 °C for two hours of deposition with no post-heat-treatment. This range of temperature is much lower in comparison with the deposition temperatures of typical magnetron sputtering, which could make substrate surfaces reach temperatures above 80 °C [6]. This capability to deposit AZO thin films on polycarbonate materials is very attractive, since polycarbonate materials are utilized in several outdoor applications for their excellence in visible light transmittance, such as agricultural greenhouses [12] and tropical house roofs [13], which opens possibilities of the implementation of AZO-based devices for such applications, such as in agrivoltaics [14,15].

However, this kind of outdoor application requires highly stable performances of devices, especially when exposed to damp-heat conditions of a harsh environment. This issue would call into question the durability performance of AZO transparent electrodes prepared at low temperatures on both polyimide and polycarbonate substrates. High-temperature processes utilizing glass substrates have been extensively reported as producing a higher durability of AZO thin films when compared with lower temperature film production, especially in damp-heat conditions of a harsh environment [7,16,17].

Although successful depositions of transparent and conductive AZO films on polycarbonates or polyimide substrates have been reported [6], none discuss the damp-heat durability performances of deposited AZO films. On the other hand, Marques et al. [4] reported on a durability test of AZO films deposited on polyimide substrates via the ALD method, in which the test included exposure to humidity, UV light, or bending but did not consider the high temperature or heat of the harsh environment. Therefore, there is a paucity of literature on the damp-heat durability performances of AZO films deposited on polyimide and polycarbonate substrates.

Peterside et al. [18] reported attaching a polyimide film as a protective layer on various polymers, such as acrylic, polyvinyl chloride (PVC), or polycarbonates, to help cladding materials of agricultural greenhouses withstand ultraviolet damage when exposed to a high ultraviolet condition, such as in the space environment.

This combination of polyimide-polymer materials, such as polyimide-polycarbonate, may open another interesting pathway toward their

usability and durability as substrates, which are not yet widely covered in the literature for transparent electrode materials including ITO, gallium-doped zinc oxide (GZO), and AZO thin films[19].

In this chapter 6, the combination of polyimide-polycarbonate materials is represented by polyimide (PI)-tape attached to polycarbonate (PC) materials labeled "PI-tape/PC", which is used as a substrate. The AZO thin films were deposited by reactive 30-min RF magnetron sputtering of 80 – 90 W of RF power with 90 sccm of Ar gas and 3 sccm of O_2 gas for both, the glass and the PI-tape/PC without intentional heating. Neither post heat-treatment nor annealing was conducted for both substrates. The optical and electrical properties are comprehensively compared with those of AZO films deposited on hard glass substrates sputtered by the same configuration.

Durability comparisons of the AZO films on both substrates were investigated via the degradation of the electrical properties of the films exposed to a harsh environment with higher temperatures and humidity. The samples were then labeled as AZO/glass and AZO/PI-tape/PC to represent the AZO films deposited on the glass and PI-tape/PC substrates, respectively.

6.2. Results and Discussion

Table 6-1 and figure 6-1 show the thickness and optoelectrical properties of AZO thin films prepared via sputtering with 83 to 90 W of RF power. The thicknesses of the prepared AZO films were similar and range around 0.9 to 1.3 μm. However, the samples prepared at 83 W of RF power exhibited very low conductivity (6689 Ω/□), and the samples deposited at 87 and 90 W exhibited an average transmittance below 80% in the visible wavelength range.

Moreover, only the samples prepared by sputtering at 85 W could produce AZO thin films with an acceptable conductivity 10 Ω/□ and average visual transmittance of 80%. Therefore, to further investigate the mechanism of the DH-durability performance of AZO films on glass and PI-tape/PC substrates, detailed experiments were carried out for the AZO films prepared by sputtering with 85 W of RF power.

Figure 6-2 shows the schematic images of the prepared samples on glass and PI-tape/PC substrates. As investigated by a surface profilometer, the thickness of the AZO films deposited with 85 W of RF power for 30 min was 1.1 μm, confirmed by the SEM investigation (Fig. 6-3).

This deposition rate producing 1.1 μm in 30 min with a. 3/90 of oxygen-to-argon gas ratio is approximately four times faster than those with higher oxygen flow: One hour deposition at 100 W with 30/30 [16,20] or 60/3 [21] oxygen-to-argon gas ratios has been reported to produce around 0.5 μm of AZO film thickness, confirming the lower deposition rate of sputtering with the higher oxygen [22] and lower argon gas flow of sputtering gas [21].

Table 6-1. Thickness and optoelectrical properties of AZO thin films coated on glass substrates with a variation in RF power.

RF Power (W)	**Thickness (nm)**	**Average Visual Transparency (%)**	**Sheet Resistance (Ω/□)**
83	957	84	6689
85	1134	80	10
87	1291	63	9
90	1346	5	9

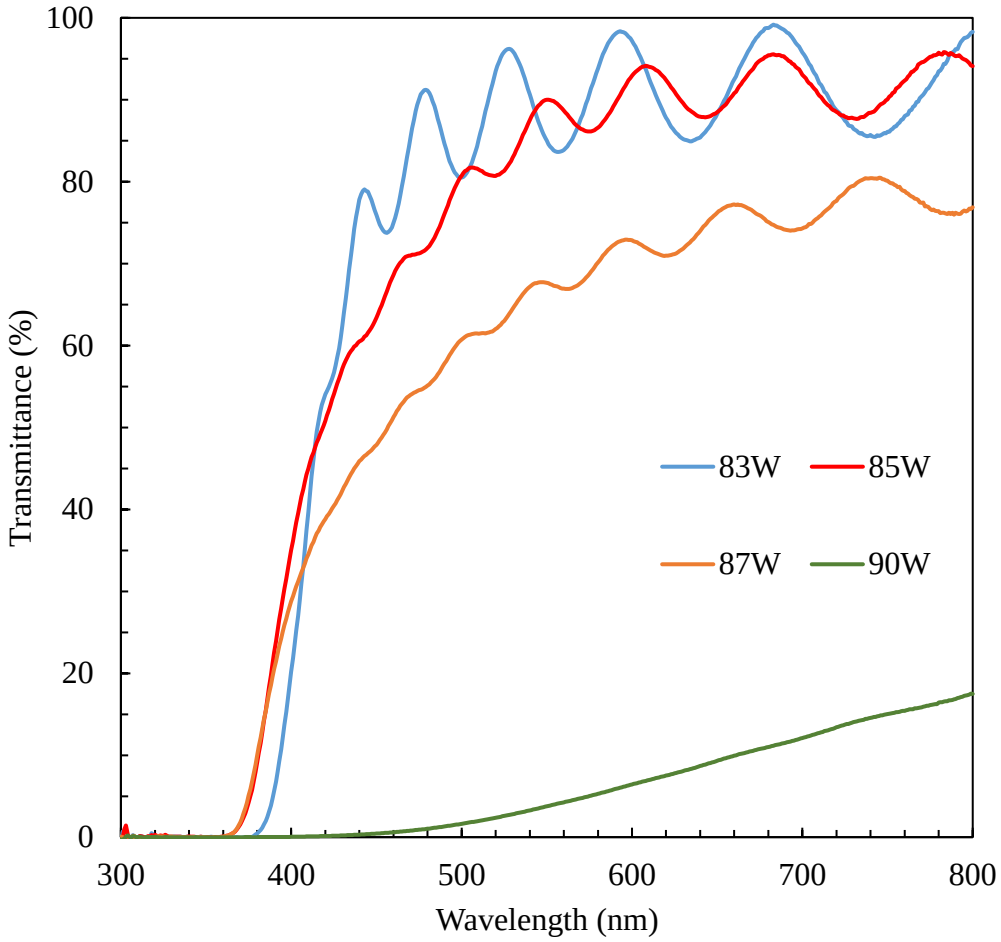

Fig. 6-1. Transmittance of AZO thin films coated on the glass substrate within the visible wavelength range with varied RF power between 83 to 90 W.

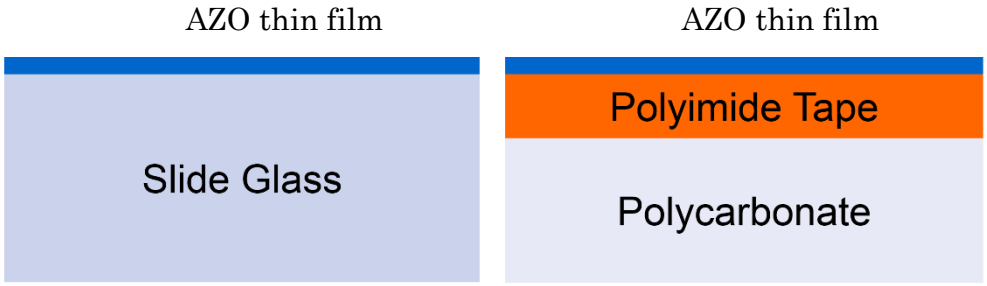

Fig. 6-2. Schematic set-up of the AZO thin films (top blue line) deposited on both the glass (right) and PI-tape/PC substrates (left)

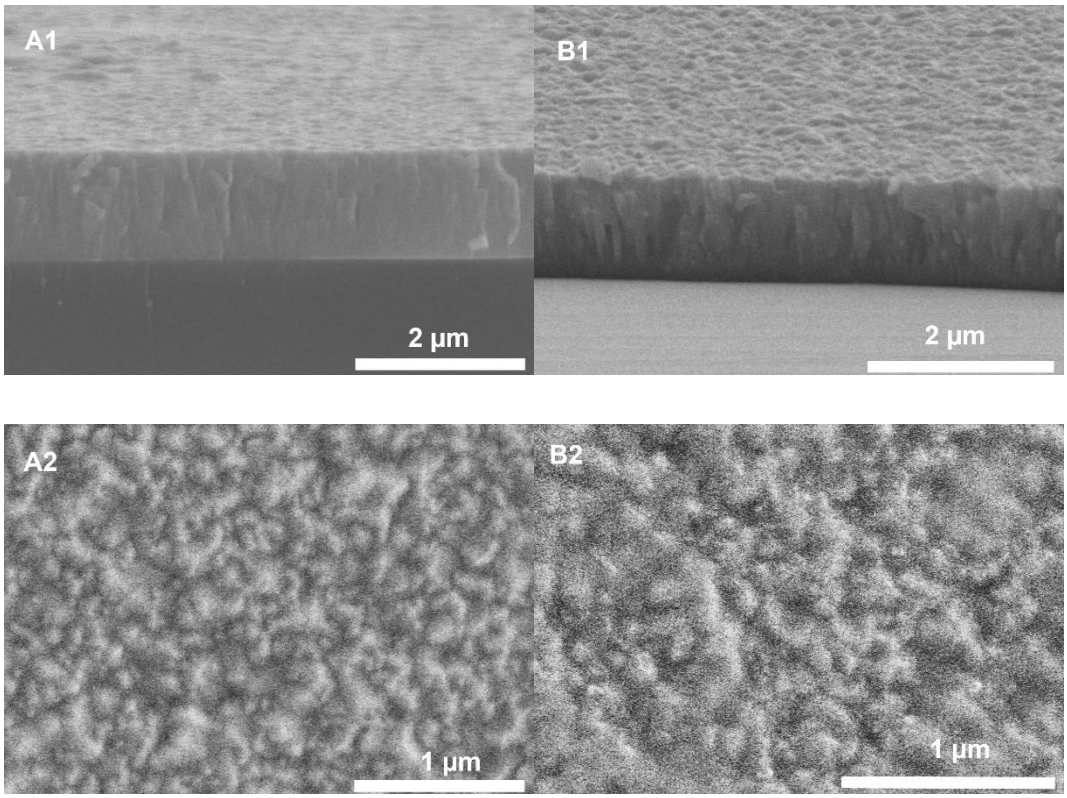

Fig. 6-3. SEM images of the cross-sections of the AZO thin films deposited on the glass (A1) substrate compared with the PI-tape/PC substrate (B1) and the surface of the films deposited on the glass (A2) substrate when compared with the PI-tape/PC substrate (B2).

Confirmed by the temperature measurement sticker, the surface temperature of the substrates, which was positioned at 15 cm above the target, raised from room temperature to 88 ºC after 30 min of sputtering deposition without intentional heating. A shorter duration of sputtering could be purposed to reduce this temperature increase at the substrate surface, as reported by Jung et al. [6]. This temperature of 88 °C is considered a low-temperature process and suitable for thin film deposition on polyimide (PI) substrates.

Therefore, this reactive sputtering configuration of 85 W of RF power for 30 min in the argon-rich process was suitable for depositing AZO thin films on both the glass and PI-tape/PC substrates. Without the PI-tape, this temperature of 88 °C is still too high for PC materials, which is in the range of the mold temperature for PCs [11].

As tested throughout the experiment, this configuration of sputtering was unable to deposit the AZO films on the PC substrates without the PI-tape layer, on which many cracks were visible, and the cracked films were easily delaminated. This confirmed the possibility of PI materials being applied as a protective layer for PC materials against one-direction heat, such as the heat generated by the plasma of the sputtering, which supports the method purposed by Peterside et al. [18] on using the PI-film as a protective layer for polymer materials including PCs against space environment.

As investigated by the UV-Vis spectrometer, the transmittance of the samples was greatly affected by the transmittance of the substrates (Fig. 6-4). By considering the transmittance of the substrates, the AZO/PI-tape/PC sample shows that its overall transmittance is limited by the transmittance of the PI-tape, showing almost no transmittance at wavelengths of 445 nm or lower.

Conversely, by examining the AZO thin film individually without considering the substrates, a high transmittance average of 80% in the range of visible light (400 to 700 nm) was observed. However, this transmittance is slightly lower than the transmittance of the AZO films prepared under high oxygen-to-argon ratios, which could reach more than 85% of the average transmittance, as reported by Machda et al [16,21].

This slight difference is likely caused by a greater number of oxygen vacancies and zinc interstitials, produced by sputtering with a low oxygen-to-argon gas ratio at 85 W of RF power, which would deteriorate the transmittance of AZO films [23].

As tested throughout experiment, the optoelectrical properties of the deposited films were very sensitive to the RF power with this reactive sputtering configuration. At 90 W of RF power, the deposited films were not transparent. However, at 83 W of RF power, the films were transparent but had very low conductivity (Table 6-1 and Fig. 6-1).

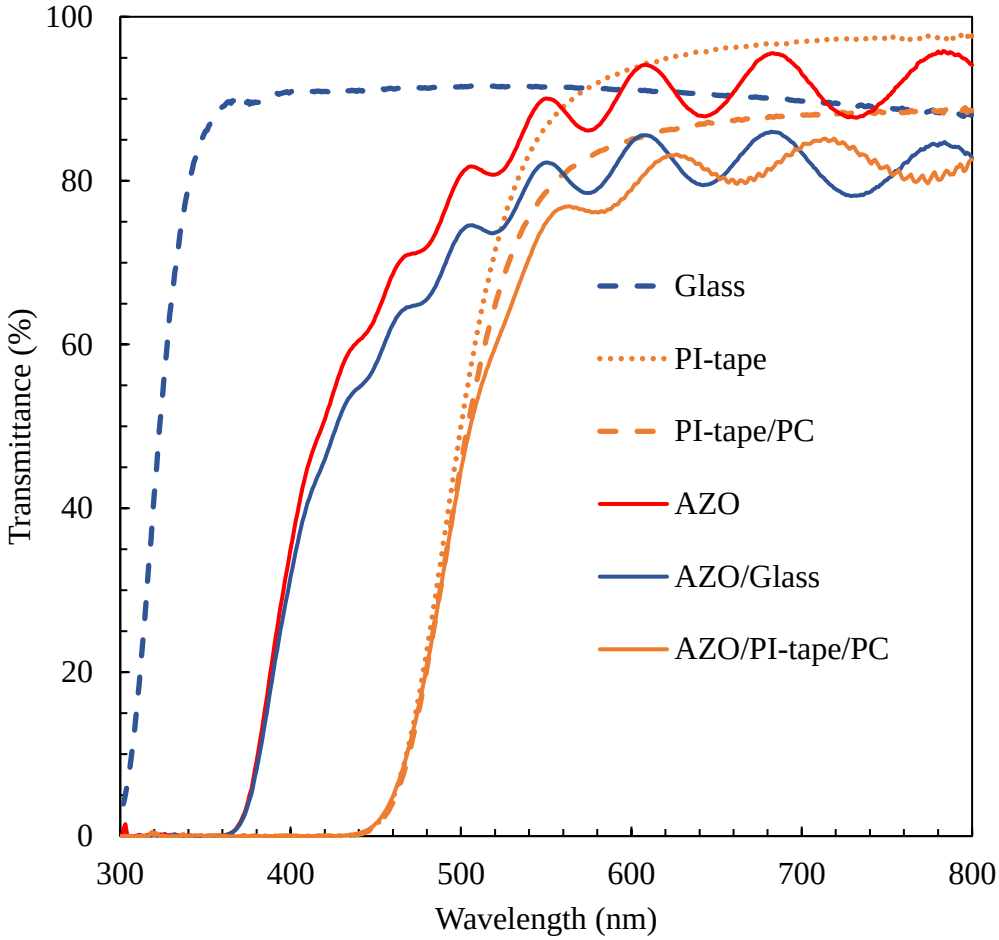

Fig. 6-4. Transmittance of the glass substrate, PI-tape/PC substrate, AZO thin films, AZO/glass, and AZO/PI-tape/PC samples.

As deposited, both AZO samples exhibited (002) as their major crystal orientation while having different intensities along with its second order (004) (Fig. 6-5). In evaluating the (002) orientation using Scherrer's equation (Eq. 3.4), the average crystallite-column dimension of the AZO/glass and AZO/PI-tape/PC are estimated to be 25 nm and 26 nm, respectively, which are very similar for both samples.

As the strain-broadening effect is not included in the estimation, the value is shown as the lower limit of the coherently-diffracting domain, which is

consistent with SEM observations (Fig. 6-3). Moreover, the 2θ values of the AZO/glass and AZO/PI-tape/PC for (002) diffraction peaks are, respectively, 34.11° and 34.30°, and for (004) 72.028° and 72.286°, respectively.

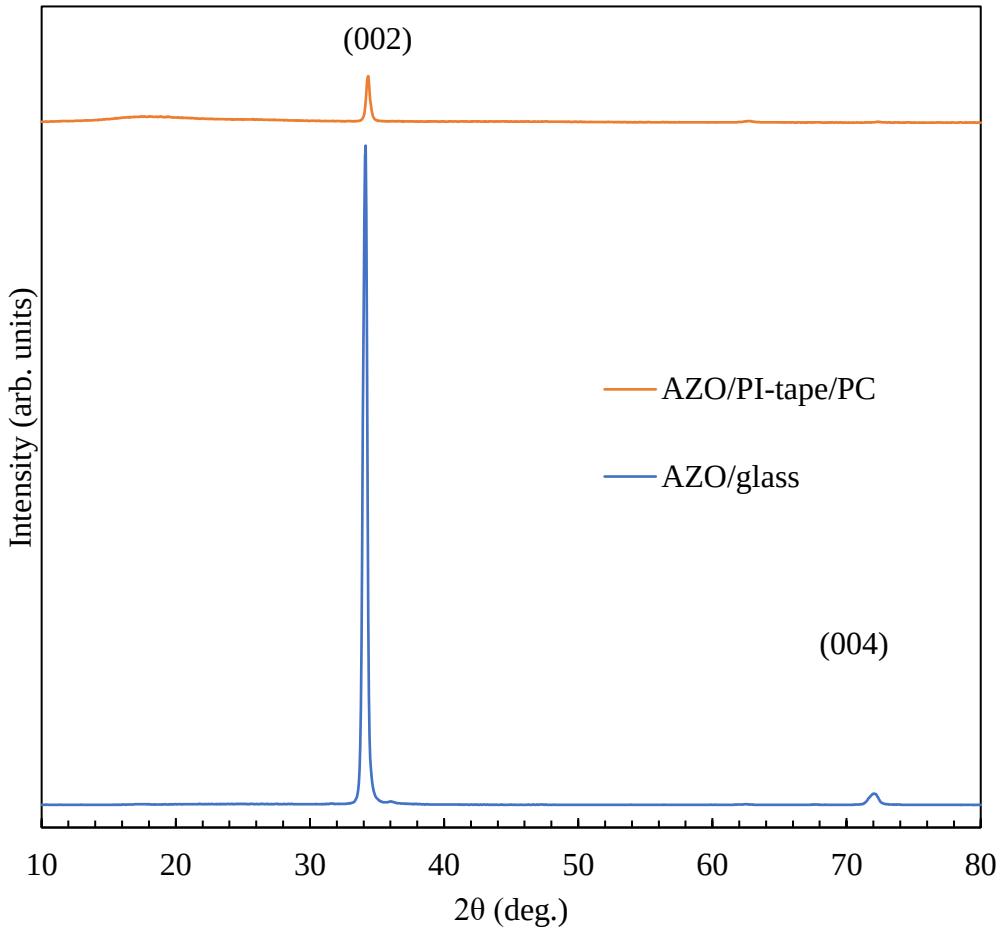

Fig. 6-5. XRD patterns of AZO thin films coated on the glass and the PI-tape/PC substrates.

The XRD pattern of the AZO/glass samples shifted to a lower angle in comparison with the standard ZnO crystal (34.45° for 002, 72.49° for 004), which means higher interlayer distance between basal planes in the c-axis

direction in comparison with the standard ZnO[23]. This shift in the AZO films to lower angle is in line with the results reported by Novak et al [23]. The grains are also similarly comparable for both samples, as investigated by SEM (Fig. 6-3). These comparable results of crystallite column dimensions, grain sizes, and crystal orientations strongly indicate the similarity of the AZO thin films on both substrates, which implied that aluminum replaced zinc in the hexagonal lattice [24].

However, the XRD pattern shows that the (002) peak for the AZO/glass film is broadened and becoming significantly more intense in comparison with the peak for the AZO/PI-tape/PC sample. This could suggest higher crystallinity of the AZO/glass samples, a finding in line with results reported by Hao et al. [5] confirming the influence of polyimide and glass substrates on the differences in the crystallinity of the films. This peak with higher intensity could suggest the increased crystallinity of AZO/glass samples due to more perfect alignment of crystal columns as relatively compared to the AZO/PI-tape/PC samples[5], including the possibly larger strain effect in the latter film.

As investigated by XPS, the AZO/glass and AZO/PI-tape/PC samples exhibited a similar pattern, in which the oxygen (O 1s) element was highly detected on the surface of both samples (Fig. 6-6), suggesting that the films were immediately oxidized when exposed to the atmosphere. The aluminum (Al 2p3/2) content was revealed to be slightly higher on the surface than the bulk (under the surface), which could be attributed to the formation of aluminum compounds, such as alumina (Al_2O_3) or zinc aluminate ($ZnAl_2O_4$), formed on the surface, causing a slightly higher aluminum content [7] when naturally oxidized in the ambient.

As prepared, prior to the DH test, the sheet resistance of the AZO/PI-tape/PC samples exhibited a similar sheet resistance as the 10Ω/□ sheet resistance of the AZO/glass samples (Fig. 6-7), which was due to the similarly applied configurations of the thin film deposition method for both samples. However, the AZO/PI-tape/PC samples exhibited slightly lower carrier concentrations when compared with the AZO/glass (Fig. 6-8).

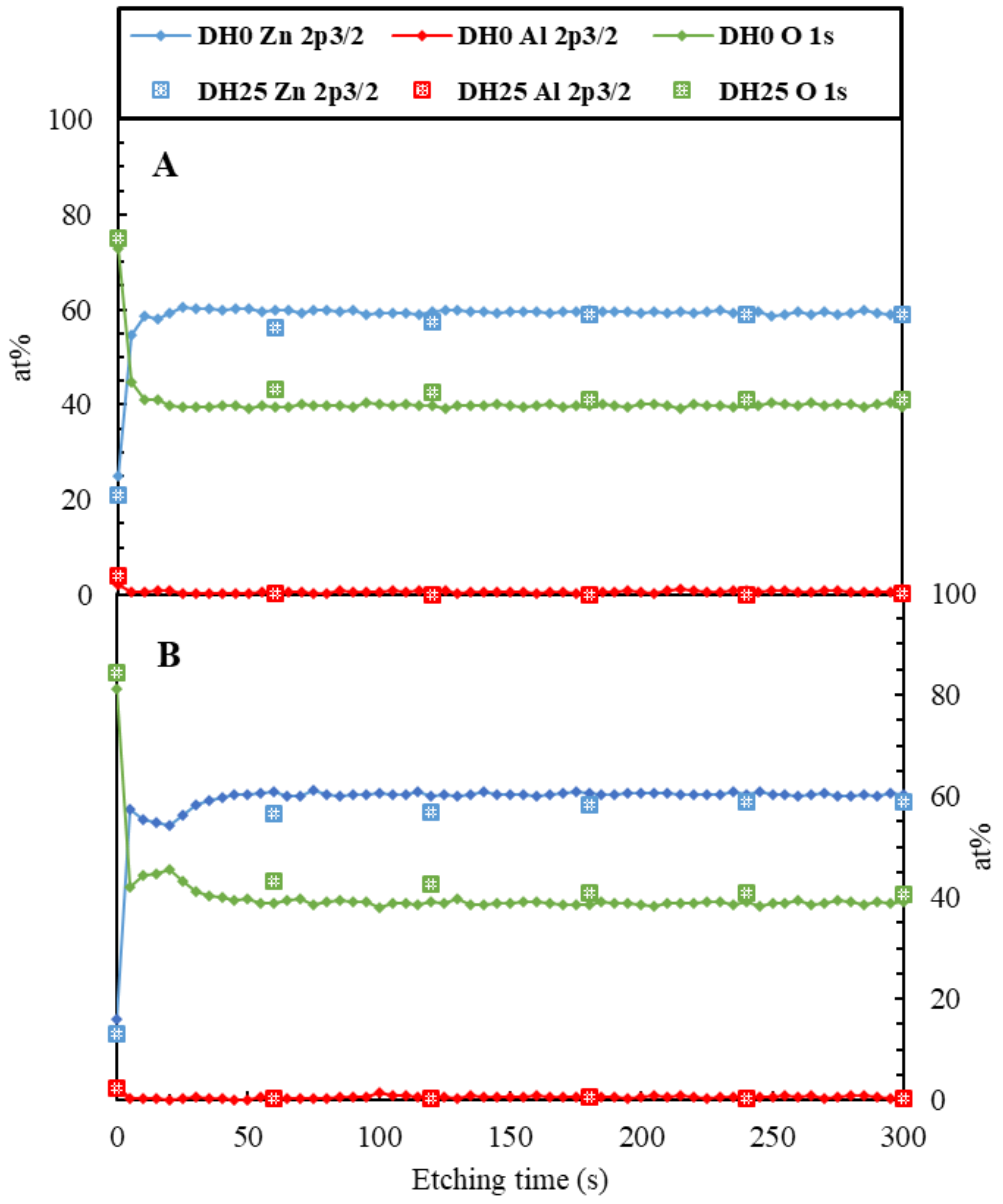

Fig. 6-6. Quantification of the Zn 2p3/2, Al 2p3/2, and O elements via XPS for the AZO/glass (A) and AZO/PI-tape/PC (B) samples before (line with diamonds) and after (squares) the damp-heat (DH) test.

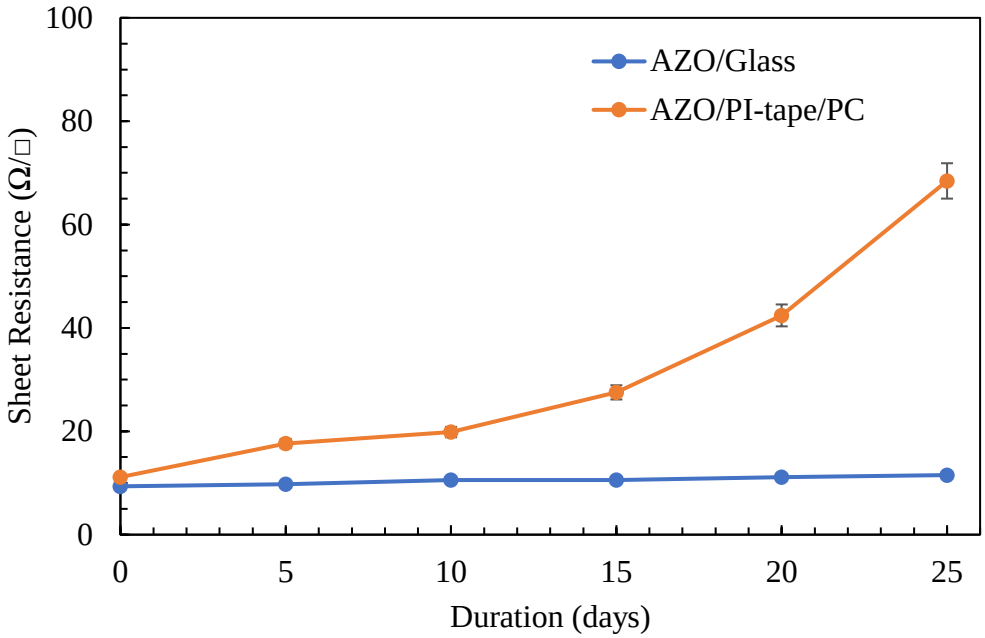

Fig. 6-7. Degradation of AZO films deposited on both the glass and PI-tape/PC substrates when exposed to the damp-heat (DH) test.

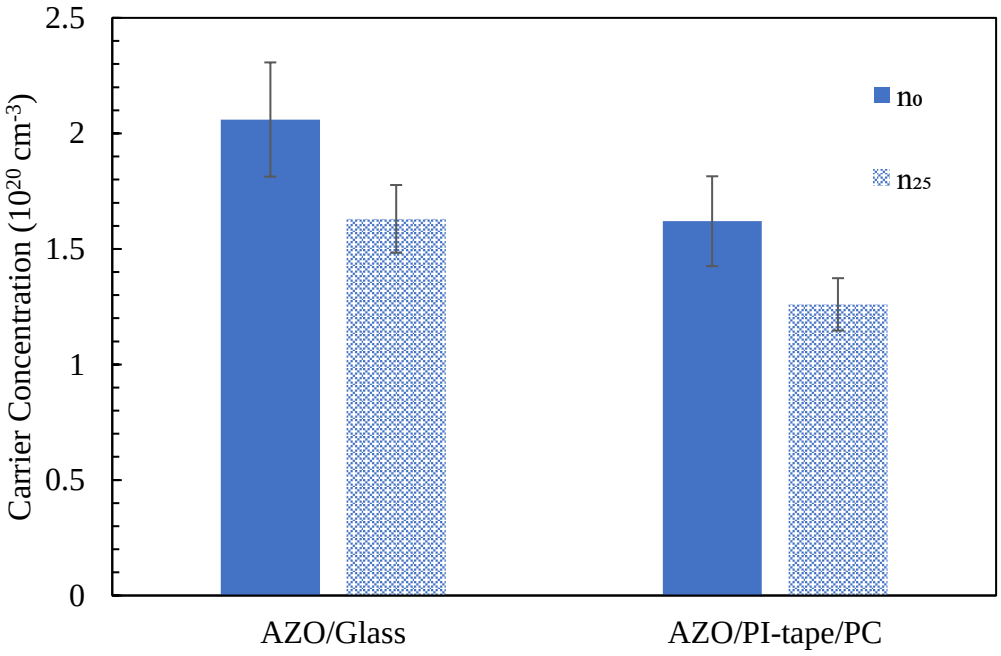

Fig. 6-8. Carrier concentrations of the AZO films deposited on the glass and PI-tape/PC substrates before and after the damp-heat (DH) test.

The different crystallinity of both samples (Fig. 6-5) might have caused this difference in carrier concentration (Fig. 6-8), in which the more increased crystallinity of AZO/glass samples is causing less defects and less dangling bonds at the grain boundaries as relatively compared to AZO/PI-tape/PC samples, contributing to the increase of carrier concentration of AZO thin films as reported by Maejima et al. [25]

Conversely, the AZO/PI-tape/PC samples exhibited slightly higher Hall mobility than the AZO/glass samples (Fig. 6-9), providing a similar sheet resistance of both samples (Fig. 6-7) despite the lower carrier concentration of the AZO/PI-tape/PC samples (Fig 6-8) before the DH test.

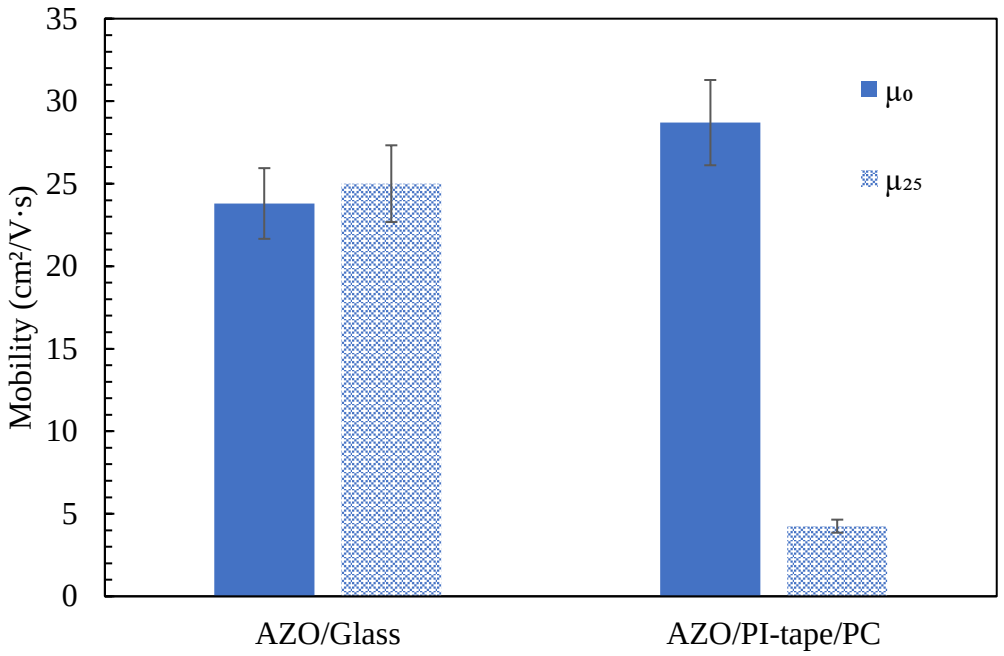

Fig. 6-9. Hall mobility of the AZO films deposited on the PI-tape/PC and glass substrates before and after the damp-heat (DH) test.

This slightly lower Hall mobility of the AZO/glass samples was caused by increased ionized-impurity scattering [26,27], in which the Hall mobility of the doped-ZnO based materials decreased with higher carrier concentrations, as reported by Ellmer [28], especially when the carrier concentration became higher than 10^{20} cm^{-3}. This finding is in line with the semi-empirical model for the relationship between carrier mobility and concentrations proposed by Masetti et al. [29], in which mobility decreases with higher carrier concentrations.

Figure 6-7 shows the durability performances of the AZO films deposited on both substrates and exposed to a DH condition of 85% relative humidity at 85 °C. Before the DH test, the sheet resistance of both films were similar (10 Ω/□), as measured by four-point probes. However, during the 25 days of the DH test, the sheet resistance of the AZO/PI-tape/PC samples was more significantly degraded, reaching 68 Ω/□, which was almost seven times higher than the initial sheet resistance. As a comparison, the AZO/glass samples were slightly degraded to 12 Ω/□ after the DH test, which was not significantly different from the initial sheet resistance.

Despite the significant difference in the conductivity degradations between the AZO/PI-tape/PC and AZO/glass samples, the slight decrease in the carrier concentrations of both samples is likewise very similar (Fig. 6-8), as investigated by the Hall effect measurement. These minorly decreased carrier concentrations could be attributed to the crystal orientation (002) of both samples (Fig. 6-5), which would be in line with findings reported by Machda et al. [21] regarding the effectiveness of such a crystal orientation (002) in protecting the carrier concentration of AZO films exposed to a DH condition. As investigated by XPS, the O1s element was slightly increased for both samples after the DH test (Fig. 6-6), which would confirm the oxidation of both samples during the test.

However, the Hall mobility of the AZO/PI-tape/PC samples decreased significantly, while the mobility of the AZO/glass samples did not decrease (Fig. 6-9), which would imply a significant difference in the conductivity degradation between both samples (Fig. 6-7) despite similarities in carrier concentration evolution during the DH test (Fig. 6-8).

Furthermore, the Hall mobilities of the AZO/glass samples were very similar even after the DH test was undergone (Fig. 6-9), which could contribute to the overall conductivity not being significantly degraded for the AZO/glass samples. In other words, the AZO/glass samples were very stable throughout the DH test.

Figure 6-10 shows a comparison of the surfaces of the AZO/glass with AZO/PI-tape/PC samples before and after the DH test, as investigated by SEM. When compared with the initial condition of the surfaces prior to the DH test, the AZO films on the PI-tape/PC substrates were cracked, while no cracks were visible on the surface of the AZO/glass samples.

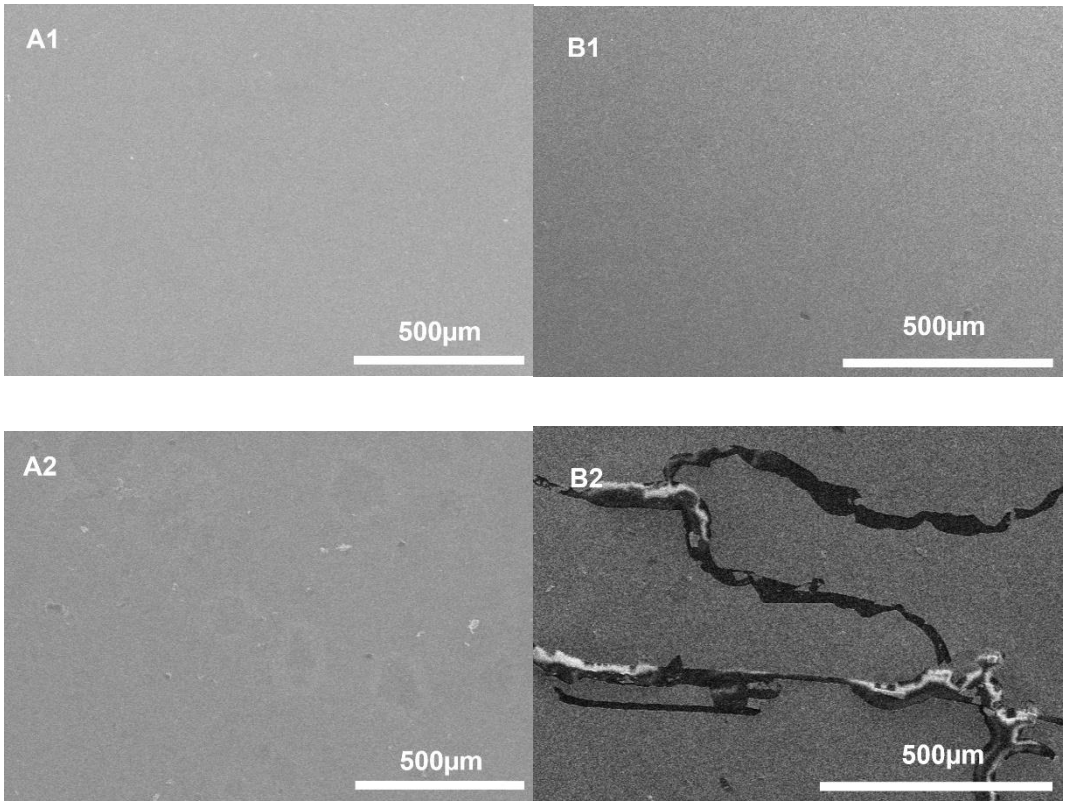

Fig. 6-10. SEM images of the surfaces of the AZO films deposited on the glass substrates before (A1) and after the damp heat (DH) test (A2) when compared with the films deposited on the PI-tape/PC substrates before (B1) and after the DH test (B2)

The propagation of the cracks on the AZO films deposited on the PI-tape/PC substrate could be attributed to the distended PI-tape, which was due to

the deformation of the underlying PC exposed to the high DH test temperature of 85 °C, wherein the range of mold temperature of PCs (82 to 121 °C) [11]. The heat of the DH test (85 °C) was similar to the heat (88 °C) generated by the plasma during the 30-min sputtering deposition to the surface of the PI-tape/PC substrate. When compared to the one-direction heat generated by the sputtering, during which the PC was protected by the PI-tape during the deposition, the heat of the DH chamber of the DH test seemed to heat the AZO/PI-tape/PC samples from multiple directions, attacking the direction of the PC without the protective PI-tape; thus, the PC began to mold and deform. Furthermore, high humidity was applied during the DH test along with a high temperature that would cause the hydrolysis of PC, decreasing its molecular weight and strength and thus contributing to this deformation [30]. Similarly, the hydrolytic degradation of the PI-tape could occur during the DH test when exposed to the DH condition [31]. After the initial cracks in the AZO films, the PI-tape could be exposed to the DH condition, which would contribute to the deformation of the PI-tape/PC substrates, leading to the more severe propagation of AZO thin film cracks during the long duration of the DH test. This deformation of the PC caused the PI-tape to delaminate from the PC and become distended, making its deposited AZO films cracked. This propagation of cracks caused the mobility of the AZO/PI-tape/PC samples to significantly decrease (Fig. 6-9). When compared, no cracks were visible on the AZO/glass samples even after the DH test (Fig. 6-10), since the hard glass substrate could withstand the heat of the DH test, supporting the thin film in being physically stable and contributing to the very stable mobility of the AZO/glass samples (Fig. 6-9).This conductivity degradation difference caused by differences in the mobility evolution of the AZO thin films reveals a different degradation pattern than the results reported by Machda et al. [16,21], in which the evolution of carrier concentrations due to chemical aspects such as oxidation or the diffusion of hydroxyl groups was suggested as key for the varied conductivity degradation of the AZO thin films deposited on the glass substrates.

This different degradation pattern is due to the utilization of the PI-tape/PC substrates along with the glass substrates in this degradation study of AZO films. The chemical aspects seemed to be involved in a similar decrease in the carrier concentrations of the AZO/PI-tape/PC and AZO/glass samples (Fig. 6-8). However, certain physical characteristics, such as the aforementioned propagation of cracks in the film (Fig. 6-10) caused

significant degradation in the conductivity of the AZO/PI-tape/PC samples (Fig. 6-7) through a significant decrease in the Hall mobility (Fig. 6-8) in a comparison with the AZO/glass samples. This finding shows the brittleness of the AZO thin film in its conventional form of a flat single layer of thin films that would easily crack when exposed to the deformation of the substrates, including the deformation caused by the high temperature of the DH harsh environment condition. Unconventional structures seem to be required to support AZO films withstanding such cracks; this includes nanostructured thin films that could be purposed to provide the self-recovery of the thin film cracks, as reported by Itoh et al [32]. Moreover, the films could be mesh-patterned to further stop the propagation of the rigid thin film cracks, as reported by Sakamoto et al [33]. Furthermore, AZO films with smaller thicknesses could be implemented to strengthen the fracture resistance[34], as it is closely related to deformation of substrates exposed to the DH environment.

Overall, this configuration of reactive sputtering with a low oxygen-to-argon gas ratio could produce a conductive AZO thin film at a low temperature without any post-heat-treatment or annealing, maintaining the surface temperature of the substrate at 88 °C throughout the 30 min of deposition. The successful deposition on the surface of both the glass and PI-tape/PC substrates proved the effectiveness of the low-temperature deposition of this sputtering configuration, which could be further utilized in the research field or experimental tests requiring low-temperature processes of AZO thin film deposition. Furthermore, the excellent durability of the AZO/glass samples (Fig. 6-7 -Fig. 6-10) was exhibited during the DH test, which could suggest the advantage of the sputtering condition with a low oxygen-to-argon gas ratio utilized in this present research.

6.3. Conclusion

Reactive RF magnetron sputtering with a low oxygen-to-argon gas ratio at 85 W of RF power sputtering could successfully deposit transparent AZO thin films with similar and high electrical conductivities on both PI-tape/PC and glass substrates at low temperatures. Alterations in the RF power would significantly affect the optoelectrical property of the films: too high of an RF power would deteriorate the transparency of the films, while too

low of an RF power would produce films with a very low conductivity. During the deposition, the surface temperature of the substrates could reach 88 °C, when sustained for 30 min. The optimally high mobility of the sputtered atoms bombarded on the substrate surface at an optimally large energy crystallized the AZO films, making them transparent and conductive, which resulted in the successful deposition of the AZO films on the glass and PI-tape/PC substrates without post-annealing. When exposed to the DH test at a relative humidity of 85% and 85 °C, the AZO films deposited on the glass were stable, while the films deposited on the PI-tape/PC substrates were significantly degraded due to the propagation of several cracks in the films caused by the deformation of the PI-tape/PC substrates. Along with hydrolytic degradation, this deformation was due to the unprotected side of the PC being exposed to its mold temperature during the DH test, suggesting the importance of considering the DH stability of substrates for transparent electrode studies. Such cracks caused a significant decrease in the Hall mobility of the AZO/PI-tape/PC samples, severely degrading their conductivity, which suggested more physical rather than chemical characteristics involved in the degradation. On the other hand, no cracks were found for the AZO/glass samples, which exhibited a stable Hall mobility and conductivity. Upon considering the similar patterns of both samples exhibiting a slight decrease in their carrier concentrations during the DH test, chemical characteristics, such as the oxidation or diffusions of hydroxyl groups, appeared to be less involved in the differences between the conductivity degradations of the AZO/glass and the AZO/PI-tape/PC samples. By utilizing the low oxygen-to-argon gas ratio of reactive sputtering, a strong (002) orientation along with acceptable transparency and conductivity for AZO transparent electrodes could be obtained even at low temperatures, contributing to the DH stability in terms of the chemical characteristics of the AZO films.

Reference

[1] H. Kang, S. Jung, S. Jeong, G. Kim, K. Lee, flexible electronics, Nat. Commun. 6 (2015) 1–7. doi:10.1038/ncomms7503.

[2] T. Yokota, T. Someya, Electronic skin for healthcare monitoring, in: 2019 26th Int. Work. Act. Flatpanel Displays Devices, IEEE, 2019: pp. 1–2. doi:10.23919/AM-FPD.2019.8830621.

[3] E. Lee, J. Ahn, H. Kwon, S. Ma, K. Kim, S. Yun, J. Moon, All-Solution-Processed Silver Nanowire Window Electrode-Based Flexible Perovskite Solar Cells Enabled with Amorphous Metal Oxide Protection, Adv. Energy Mater. 8 (2018) 1702182. doi:10.1002/aenm.201702182.

[4] A.C. Marques, J. Faria, P. Perdigão, B.M.M. Faustino, R. Ritasalo, K. Costabello, R.C. da Silva, I. Ferreira, Stability under humidity, UV-light and bending of AZO films deposited by ALD on Kapton, Sci. Rep. 9 (2019) 17919. doi:10.1038/s41598-019-54451-0.

[5] X. Hao, J. Ma, D.-H. Zhang, Y. Yang, H. Ma, C.-F. Cheng, X.-D. Liu, Comparison of the properties for ZnO:Al films deposited on polyimide and glass substrates, Mater. Sci. Eng. B. 90 (2002) 50–54. doi:10.1016/S0921-5107(01)00828-5.

[6] Y. Sup Jung, H. Wook Choi, K. Hwan Kim, S. Joon Park, H. Hee Yoon, Properties of AZO Thin Films for Solar Cells Deposited on Polycarbonate Substrates, J. Korean Phys. Soc. 55 (2009) 1945–1949. doi:10.3938/jkps.55.1945.

[7] S. Tabassum, E. Yamasue, H. Okumura, K.N. Ishihara, Electrical stability of Al-doped ZnO transparent electrode prepared by sol-gel method, Appl. Surf. Sci. 377 (2016) 355–360. doi:10.1016/j.apsusc.2016.03.133.

[8] M.Y. Zhang, Q. Nian, G.J. Cheng, Room temperature deposition of alumina-doped zinc oxide on flexible substrates by direct pulsed laser recrystallization, Appl. Phys. Lett. 100 (2012) 151902. doi:10.1063/1.3702460.

[9] RTP, General Processing Conditions RTP 4285 Thermoplastic Polyimide (TPI) Carbon Fiber, (2005). http://web.rtpcompany.com/info/data/4200/RTP4285.htm (accessed January 6, 2020).

[10] P. Prepelita, R. Medianu, F. Garoi, A. Moldovan, Growth of ZnO:Al thin films onto different substrates, AIP Conf. Proc. 1292 (2010) 213–216. doi:10.1063/1.3518300.

[11] RTP, General Processing Conditions RTP 300 Polycarbonate (PC) Unreinforced, (2004). http://web.rtpcompany.com/info/data/0300/RTP300.htm (accessed January 6, 2020).

[12] M.C. Subin, J.S. Lourence, R. Karthikeyan, C. Periasamy, Analysis of materials used for Greenhouse roof covering - Structure using CFD, IOP Conf. Ser. Mater. Sci. Eng. 346 (2018). doi:10.1088/1757-899X/346/1/012068.

[13] K.M. Al-Obaidi, M. Ismail, A.M. Abdul Rahman, Design and performance of a novel innovative roofing system for tropical landed houses, Mod. Lang. Q. 85 (2014) 488–504. doi:10.1016/j.enconman.2014.05.101.

[14] A. Leon, K.N. Ishihara, Assessment of new functional units for agrivoltaic systems, J. Environ. Manage. 226 (2018) 493–498. doi:10.1016/j.jenvman.2018.08.013.

[15] A. Leon, K.N. Ishihara, Resources , Conservation & Recycling In fl uence of allocation methods on the LC-CO 2 emission of an agrivoltaic system, Resour. Conserv. Recycl. 138 (2018) 110–117. doi:10.1016/j.resconrec.2018.06.017.

[16] F. Machda, T. Ogawa, H. Okumura, K.N. Ishihara, Evolution and Recovery of Electrical Property of Reactive Sputtered Al-Doped ZnO Transparent Electrode Exposed to Harsh Environment, Phys. Status Solidi. 1900519 (2019) 1900519. doi:10.1002/pssa.201900519.

[17] T. Tohsophon, J. Hüpkes, S. Calnan, W. Reetz, B. Rech, W. Beyer, N. Sirikulrat, Damp heat stability and annealing behavior of aluminum doped zinc oxide films prepared by magnetron sputtering, Thin Solid Films. 511–512 (2006) 673–677. doi:10.1016/j.tsf.2005.12.130.

[18] D.T. Peterside, J.E. Palaia, A.C. Schuerger, M.J. Correll, R.A. Bucklin, Testing of Greenhouse Cladding Materials for Space

Environments, Part 2: Laminates, Appl. Eng. Agric. 34 (2018) 575–580. doi:10.13031/aea.12465.

[19] F. Machda, T. Ogawa, H. Okumura, K.N. Ishihara, Damp-heat durability comparison of Al-doped ZnO transparent electrodes deposited at low temperatures on glass and PI-tape/PC substrates, Ceram. Int. 46 (2020) 16178–16184. doi:10.1016/j.ceramint.2020.03.173.

[20] S. Tabassum, E. Yamasue, H. Okumura, K.N. Ishihara, Sol–gel and rf sputtered AZO thin films: Analysis of oxidation kinetics in harsh environment, J. Mater. Sci. Mater. Electron. 25 (2014) 4883–4888. doi:10.1007/s10854-014-2248-9.

[21] F. Machda, T. Ogawa, H. Okumura, K.N. Ishihara, Damp Heat Durability of Al-Doped ZnO Transparent Electrodes with Different Crystal Growth Orientations, ECS J. Solid State Sci. Technol. 8 (2019) Q240–Q244. doi:10.1149/2.0261912jss.

[22] L.R. Damiani, R.D. Mansano, Zinc oxide thin films deposited by magnetron sputtering with various oxygen/argon concentrations, J. Phys. Conf. Ser. 370 (2012). doi:10.1088/1742-6596/370/1/012019.

[23] P. Novák, T. Kozák, P. Šutta, M. Kolega, O. Bláhová, Influence of Oxygen on the Resistivity of Co-Sputtered Transparent AZO Films, Phys. Status Solidi Appl. Mater. Sci. 215 (2018) 1–5. doi:10.1002/pssa.201700951.

[24] J. Lee, D. Lee, D. Lim, K. Yang, Structural, electrical and optical properties of ZnO:Al films deposited on flexible organic substrates for solar cell applications, Thin Solid Films. 515 (2007) 6094–6098. doi:10.1016/j.tsf.2006.12.099.

[25] K. Maejima, H. Shibata, S. Niki, H. Tampo, K. Matsubara, Correlation between Electrical Properties and Crystal c -Axis Orientation of Zinc Oxide Transparent Conducting Films, Jpn. J. Appl. Phys. 51 (2013) 10NC16. doi:10.7567/jjap.51.10nc16.

[26] H. Liu, V. Avrutin, N. Izyumskaya, Ü. Özgür, H. Morkoç, Transparent Conducting Oxides for Electrode Applocations in Light

Emitting and Absorbing Devices, Superlattices Microstruct. 48 (2010) 458–484. doi:10.1016/j.spmi.2010.08.011.

[27] H. Lee, Electron scattering mechanisms in indium–tin-oxide thin films prepared at the various process conditions, Appl. Surf. Sci. 252 (2006) 3428–3435. doi:10.1016/j.apsusc.2005.03.203.

[28] K. Ellmer, Past achievements and future challenges in the development of optically transparent electrodes, Nat. Photonics. 6 (2012) 808–816. doi:10.1038/nphoton.2012.282.

[29] G. Masetti, M. Severi, S. Solmi, Modeling of Carrier Mobility Against Carrier Concentration in Arsenic-, Phosphorus-, and Boron-Doped Silicon, IEEE Trans. Electron Devices. 30 (1983) 764–769. doi:10.1109/T-ED.1983.21207.

[30] H.E. Bair, D.R. Falcone, M.Y. Hellman, G.E. Johnson, P.G. Kelleher, Hydrolysis of polycarbonate to yield BPA, J. Appl. Polym. Sci. 26 (1981) 1777–1786. doi:10.1002/app.1981.070260603.

[31] D.R. Askins, Hydrolytic degradation of kapton film, J. Plast. Film Sheeting. 1 (1985) 50–59. doi:10.1177/875608798500100109.

[32] S. Itoh, S. Kodama, M. Kobayashi, S. Hara, H. Wada, K. Kuroda, A. Shimojima, Spontaneous Crack Healing in Nanostructured Silica-Based Thin Films, ACS Nano. 11 (2017) 10289–10294. doi:10.1021/acsnano.7b04981.

[33] K. Sakamoto, H. Kuwae, N. Kobayashi, A. Nobori, S. Shoji, J. Mizuno, Highly flexible transparent electrodes based on mesh-patterned rigid indium tin oxide, Sci. Rep. 8 (2018) 3–4. doi:10.1038/s41598-018-20978-x.

[34] H.J. Choi, D. Bin Kim, M.H. Kim, G.H. Lee, Y.S. Cho, Quantitative analysis of improved bending fracture behavior of large-scale graphene monolayer-intervened flexible oxide thin films, J. Mater. Chem. C. 6 (2018) 6125–6131. doi:10.1039/c8tc00084k.

7. Discussion: Models for Durable AZO Transparent Electrodes

In this chapter, several models to extend the durability of AZO transparent electrodes (TEs) are discussed and proposed, which would ultimately extend the usability of AZO TEs for various applications. In the previous chapters of this thesis, the crystal orientation (002) or the columnar structure has been clarified to be very important for the durability and recoverability, which can be strengthened through higher ratio of argon gas to oxygen gas in the reactive atmosphere of sputtering (Chapter 4-6).

However, several considerations were not covered within the limitation of this thesis such as thickness optimization[1], hydrogen-dopant[2], top-alumina nano layer with 2-3 nm of thickness[3], self recoverability[4,5], and mesh-patterned thin films[6].

Based on the findings in this thesis combined with the findings from the recent literature, several models of AZO transparent electrodes are discussed according to specific applications such as touch-screens, light-emitting displays, photovoltaics, and flexible substrates-or-devices.

7.1. Touch-screen

As shown in figure 1-3 a, touch screen devices require the thickness at 50 nm or less. Therefore, the thickness of AZO should be 50 nm at most. Top oxide layer [3] and self-healing of metal droplet [5] can be coated respectively on top of the AZO layer.

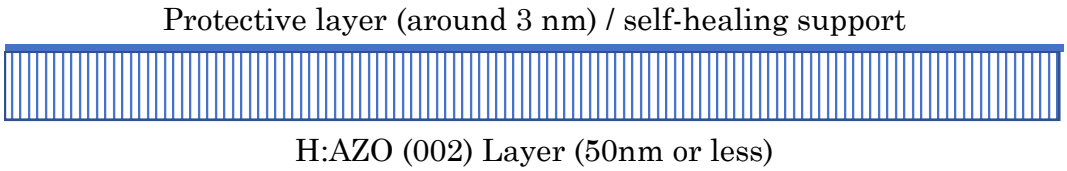

Fig. 7-1. AZO model for Touch-screen applications

The metal droplet layer is to support the AZO films to be able to do self-healing against cracks or defects of the AZO films. Hydrogen dopant can be added to enhance the conductivity and the orientation (002) should be strengthened to improve the quality of AZO layer. Figure 7-1 described the schematic model of this AZO for touch screen device.

7.2. Light-emitting Device

Light emitting device (LED) including lighting and displays. As shown in figure 1-3 a, the LED require the thickness of AZO at 50 nm – 150 nm. Therefore, the thickness of AZO should be 150 nm at most.

Top oxide layer [3] and self-healing of metal droplet [5] then can be coated respectively on top of the AZO layer. Hydrogen dopant can be added and orientation (002) should be strengthened to improve the quality of AZO layer. Figure 7-2 described the schematic model of this AZO for LED device.

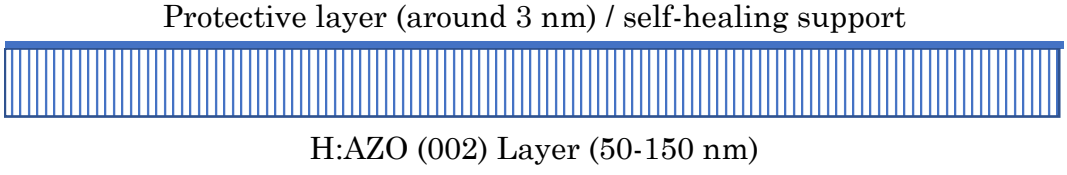

Fig. 7-2. AZO Model for light-emitting applications

7.3. Photovoltaics

Photovoltaic (PV) devices include thin film solar cells in general. As shown in figure 1-3 a, PV device require the thickness at 600 nm or more. Therefore, the thickness of AZO should be around 800 nm.

Top oxide layer [3] and self-healing of metal droplet [5] then can be coated respectively on top of the AZO layer. Hydrogen dopant can be added and orientation (002) should be strengthened to improve the quality of AZO layer. Figure 7-3 described the schematic model of this AZO for PV device.

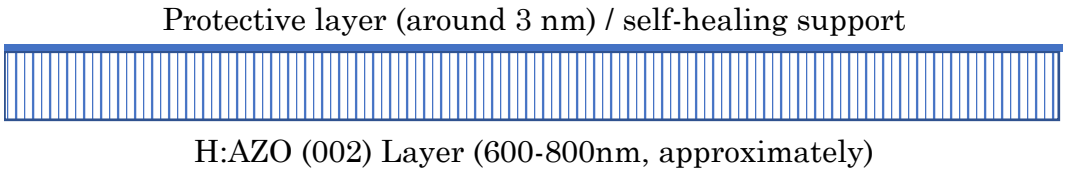

Fig. 7-3. AZO Model for PV applications

7.4. Flexible Substrates

As shown in figure 1-3 b, thickness of the TEs is very related to the flexibility features. The thinner the AZO films is produced, the film will be more flexible. Therefore, the thinner thickness of AZO would be better, such as 100 nm or less, which is possible to be produced by sputtering [7] and other typical thin film fabrication methods.

The thermal budget of the thin film preparation must meet the requirement of the substrates. Top oxide layer [3] and self-healing of metal droplet[5] can be coated respectively on top of the AZO layer. The metal droplets could support the films to do self-healing against cracks by the deformation of the substrates through the mechanical bending or damp-heat degradation.

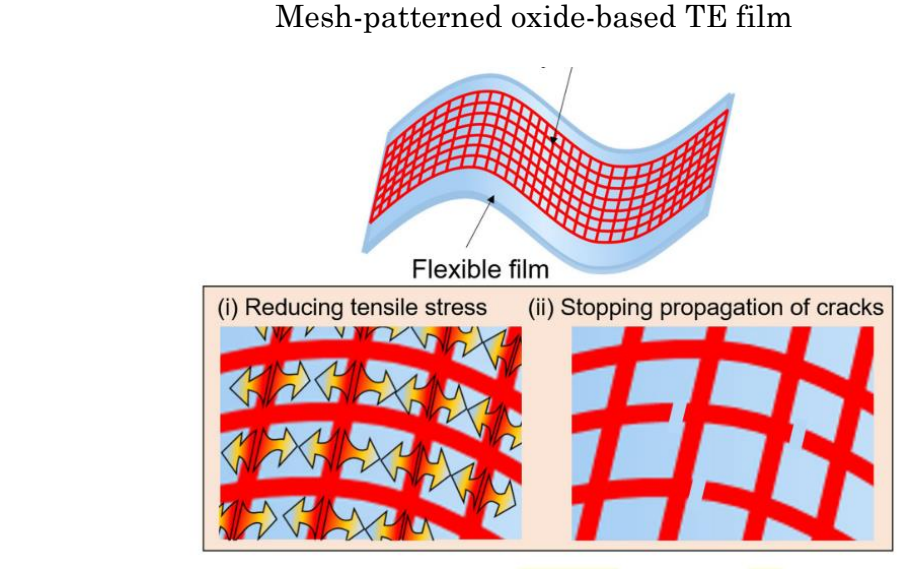

A. Mesh-patterned oxide-based transparent electrode films [6]

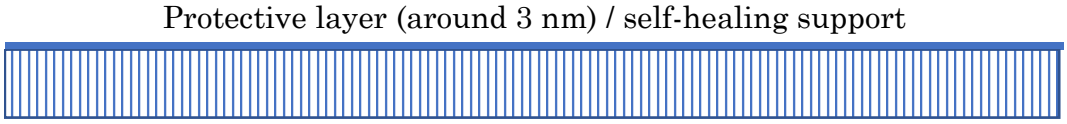

B. Standard-proposed H:AZO layer

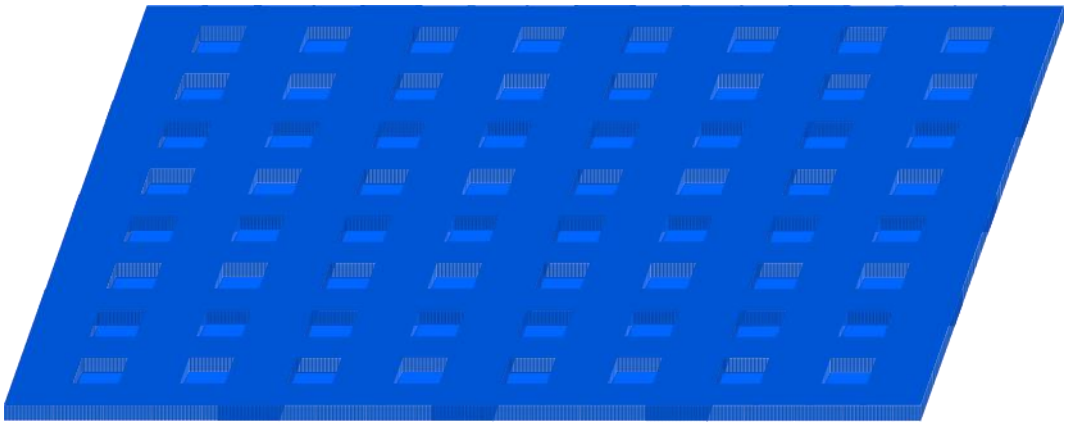

C. Proposed mesh-patterned H:AZO (002) layer with a protective layer

Fig. 7-4. AZO Model for flexible substrate applications

In order to increase the flexibility (stopping crack propagations), mesh-patterned AZO films can be implemented by photolithography and wet etching [6]. Hydrogen dopant can be added to enhance the conductivity of the films and orientation (002) should be strengthened to improve the quality of AZO layer.

The more flexible thin films seems to be more capable to withstand harsh environment by being not cracked due to the deformation of the substrate (chapter 6). Figure 7-4 described the schematic model of this AZO for the flexible substrates or devices.

Reference

[1] P. Novák, Possibilities of Increasing the Usability of Sputtered AZO Films as a Transparent Electrode, Phys. Status Solidi. 216 (2019) 1800814. doi:10.1002/pssa.201800814.

[2] C.G. Van de Walle, J. Neugebauer, Universal alignment of hydrogen levels in semiconductors, insulators and solutions, Nature. 423 (2003) 626–628. doi:10.1038/nature01665.

[3] M.S. Burberry, L.W. Tutt, METHOD OF PASSIVATING ULTRA-THIN AZO WITH NANO-LAYER ALUMNA, US009249504B2, 2016.

[4] S. Itoh, S. Kodama, M. Kobayashi, S. Hara, H. Wada, K. Kuroda, A. Shimojima, Spontaneous Crack Healing in Nanostructured Silica-Based Thin Films, ACS Nano. 11 (2017) 10289–10294. doi:10.1021/acsnano.7b04981.

[5] R. Niu, M. Jin, J. Cao, Z. Yan, J. Gao, H. Wu, G. Zhou, L. Shui, Self-healing flexible conductive film by repairing defects via flowable liquid metal droplets, Micromachines. 10 (2019). doi:10.3390/mi10020113.

[6] K. Sakamoto, H. Kuwae, N. Kobayashi, A. Nobori, S. Shoji, J. Mizuno, Highly flexible transparent electrodes based on mesh-patterned rigid indium tin oxide, Sci. Rep. 8 (2018) 3–4. doi:10.1038/s41598-018-20978-x.

[7] J. Nomoto, K. Inaba, S. Kobayashi, T. Watanabe, H. Makino, T. Yamamoto, Characteristics of carrier transport and crystallographic orientation distribution of transparent conductive Al-Doped ZnO polycrystalline films deposited by radio-frequency, direct-current, and radio-frequency-superimposed direct-current magnetron sputtering, Materials (Basel). 10 (2017) 1–18. doi:10.3390/ma10080916.

8. Conclusion

Transparent electrodes that are made of non-toxic and abundant materials are critical to ensure the safety and the sustainability of manufacturing any optoelectrical devices. With the confirmed toxicology of ITO TEs and the scarcity of In, ITO alternatives are more urgent than before. AZO TEs are featuring the non-toxic and highly abundant material, which becomes the best candidate to replace the ITO.

This thesis has discussed the preparation of highly conductive and transparent AZO thin films with the confirmation of the durability improvement, the excellent recoverability, and the practicability of low-temperature deposition. With these three confirmations, AZO TEs are becoming even promising to offer TE materials that are durable, inexpensive, and processable with low-temperature. With our configuration, AZO TEs are very practicable for solar cell applications, where the thickness of 600 nm or more is still acceptable. These are the primary outcomes of this thesis, detailed in section 8.1.

Although this thesis has contributed to the novel configuration of durable-recoverable AZO TEs, there remain significant efforts before AZO becomes a true ITO alternative.

One point that is not covered in this thesis is to produce acceptable AZO TEs with a thickness of 50-150 nm. This thickness is the requirement for touch screen and LED/OLED devices, which is still solved by ITO materials. In other words, there is still a space to improve AZO for its practicability. The future outlook to improve AZO by considering this issue is detailed in section 8.2.

8.1. Summary

The primary outcomes of this thesis include:

1) AZO thin films prepared through a very low ratio of O_2-to-Ar gas in the reactive atmosphere of RF magnetron sputtering is exhibiting high conductivity and excellent damp-heat durability, even without annealing or intentional heating. This finding opens the possibility for AZO films to be applied in the flexible or polymer-based substrates.

2) The reactive sputtering with a very low ratio of O_2-to-Ar gas will produce very strong crystal orientation (002), which contribute the high conductivity and the excellent damp-heat durability of low-temperature prepared AZO films

3) The transmittance of AZO films prepared through sputtering with a low ratio of O_2-to-Ar gas is very sensitive to the applied RF power. Adjustment of the RF power is crucial to produce high conductivity yet high transparent AZO films

4) The type of substrate contributes significantly to the damp-heat durability of AZO films. Different substrates would exhibit different routes of degradation of the AZO films:

    a. The durability of AZO films deposited on hard glass substrate involve chemical aspect such as oxidation of the films, with the decrease of carrier concentration as the main reason for the electrical degradation of the films

    b. The durability of AZO films deposited on the polymer-based substrate involves both chemical and physical aspects. However, the physical aspect is more involved.

    c. The damp-heat condition can trigger hydrolytic degradation of the polymer-based substrates, causing a deformation of the substrates. With this deformation, the AZO films would crack, decreasing the Hall mobility significantly.

5) The role of crystal orientations to the durability of the AZO film is confirmed in this thesis, where the crystal orientation (002) contribute to making the most durable AZO films in comparison with other crystal orientation, by preventing the oxidation maintaining the stable carrier concentrations.

6) Variation of crystal orientations will affect the durability of the AZO films, where the films with more varied ones would become chemically unstable to the exposure of high humidity and temperature due to many voids in the films

7) Although usually AZO exhibit the main crystal orientation (002), the existence of other minor orientations will contribute to the less stable films. Therefore, it is very important to produce AZO films with only (002) orientation or its order, such as (004)

8) The excellent recoverability of AZO films deposited on the glass is confirmed in this thesis, through high-temperature hydrogen annealing.

9) Spontaneously formed ultra-thin oxide compound on top of the surface AZO films due to the high-temperature post heat treatment is confirmed to contribute to the durability of the films

8.2. Recommendation

The recommendations for the future research on AZO materials for advancing the usability of AZO thin films include as follows:

1) The effect of the sputtering gasses to the microstructure of AZO films are very attractive to discover more, such as the role of varied oxygen gas flow amidst fixed argon gas flow in the reactive sputtering, which was not covered in this thesis. The finding would be useful to define the boundary of the gas configurations for specific crystal orientations of AZO films prepared by sputtering.

2) Incorporating hydrogen gas in the sputtering for AZO thin film deposition while maintaining the low ratio of oxygen gas to the mixture of the atmosphere inside the sputtering chamber. This configuration would make much more conductive AZO films with incorporating hydrogen doping and very strong crystal orientation (002).

3) Characterization apparatus or methods that could precisely detect the hydrogen content of the films should also be utilized, such as neutron reflectometry and deuterium-dopant characterizations.

4) For the characterization of the cross-section of the films, SEM observation on the resin-assisted-then-polished cross-section can be useful, such as to clarify the grain-boundary reconstruction due to the re-annealing or the difference of the grain boundary structures between AZO films having different crystal orientations.

5) The AZO film with less thickness, but the acceptable optoelectrical property should be pursued through this sputtering with hydrogen. Adjustment of the RF power and the duration is the key

6) The flexibility of AZO films should be improved, either by less thickness of the film or layering with nanowire or metal grid. However, single layer with less thickness should be the priority, considering the widely-used single-layer thin film structure of TEs

7) The less thickness of AZO films will be likely to produce more durable AZO films on the polymer-based substrate, due to owning more flexibility facing the deformed substrate.

8) Hydrogen-doped AZO TEs owning strong crystal orientation (002) and the thickness 50-150 nm with ultrathin top-protective alumina layer will be very attractive to investigate for its preparation steps and characterization on various substrates.

List of Publications

This thesis entitled “Durability and Recoverability of Al-doped ZnO Transparent Electrodes Exposed to Harsh Environment” is based on the following publications:

1) Peer-reviewed Journal Papers

    1. Chapter 6

       F. Machda, T. Ogawa, H. Okumura, K.N. Ishihara, Damp-heat durability comparison of Al-doped ZnO transparent electrodes deposited at low temperatures on glass and PI-tape / PC substrates, Ceram. Int. (2020) 0–1. doi:10.1016/j.ceramint.2020.03.173.

    2. Chapter 5

       F. Machda, T. Ogawa, H. Okumura, K.N. Ishihara, Damp Heat Durability of Al-Doped ZnO Transparent Electrodes with Different Crystal Growth Orientations, ECS J. Solid State Sci. Technol. 8 (2019) Q240–Q244. doi:10.1149/2.0261912jss.

    3. Chapter 4

       F. Machda, T. Ogawa, H. Okumura, K.N. Ishihara, Evolution and Recovery of Electrical Property of Reactive Sputtered Al-Doped ZnO Transparent Electrode Exposed to Harsh Environment, Phys. Status Solidi. 1900519 (2019) 1900519. doi:10.1002/pssa.201900519.

2) International Conference Proceedings (Oral Presentation)

    1. Chapter 5

       F. Machda, T. Ogawa, H. Okumura, K.N. Ishihara, Effects of Sputtering Gas on Crystal Growth Orientations and Durability of Al-doped ZnO Transparent Electrodes in Harsh Environment,

in: 2019 26th Int. Work. Act. Flatpanel Displays Devices, IEEE, Kyoto, Japan, 2019: pp. 1-4 (3–3). doi:10.23919/AM-FPD.2019.8830628.

2. Chapter 4

F. Machda, T. Ogawa, H. Okumura, K.N. Ishihara, Development of Carrier Concentration and Its Effects on the Electrical Stability of Al-doped ZnO Transparent Electrode in Harsh Environment, in: 2019 Compd. Semicond. Week, IEEE, Nara, Japan: pp. 1–1. doi:10.1109/ICIPRM.2019.8819365.

3) International Conference (Poster Presentation)

1. Chapter 6

Producing ZnO-based Transparent Electrodes for Flexible Substrates (2018), Kyoto - Japan

- Author(s): Fahmi Machda, Takaya Ogawa, Hideyuki Okumura, Keiichi Ishihara
- Organizer: Eco-Energy and Material Science -Engineering Symposium (EMSES2018)

Acknowledgment

This work is a part of the completion of the doctoral program of International Energy Science Course (IESC) at the Energy Social Engineering Laboratory at the Department of Socio-environmental Energy Science of Graduate School of Energy Science, Kyoto University from October 2017 to September 2020. I am forever grateful to many people around me for their sincere assistance, forgiveness, and encouragement during this beautiful moment in Japan.

I would like to express my sincere gratitude to my supervisor, Prof. Keiichi Ishihara, for his advice, guidance, patience, direction, forgiveness, understanding, and a tremendous help to complete this work appropriately. His constant encouragement and wisdom in promoting academic freedom in this laboratory made my research more enjoyable. I would also like to thank Prof. Hideyuki Okumura for his interest and many fruitful discussions. I am very grateful to Prof. Takaya Ogawa for his continuous encouragement and the clear direction for the completion of my research works.

I am also very grateful to Prof. Eiji Yamasue for his detailed and constructive comments and supports for this work, especially during my first time in Japan. I also would like to thank Mr. Shoji Fujimoto. He helped my efforts in the early stage of preparing the technical equipment. I would like to express my sincere gratitude to Mr. Yohei Takemoto. He has helped me to obtain several materials and maintain laboratory equipment that was essential in this work. I also would like to thank Dr. Tsutomu Shinagawa of the Osaka Research Institute of science and technology (ORIST) for the support of thickness and Hall effect measurement. Also, I greatly appreciate Prof. Takeshi Yabutsuka for helping me to perform the FE-SEM and EDX measurements.

I am deeply sincerely grateful to all of my lab mates for sharing and doing the inspiring works as one great team. I have received a lot of support for settling in Japan, lab-machines assistance, and in-depth discussions. I would like to express my gratefulness to the Honjo International Scholarship Foundation (HISF) for the scholarship of my study at Kyoto University.

Appendix A: Recoverability Rate Comparisons

Table 1. Recovery Rate by Vacuum Annealing[1]

Sample	**Resistivity (ρ) 10^{-3} Ω·cm**			**Rate %**
	ρ_0 250 °C	ρ_{DH}	$\rho_{Reannealed}$ 250 °C	$\frac{\rho_0 \times 100}{\rho_{Reannealed}}$
AZO-870 nm	0.26	1.17	0.42	62
AZO-750 nm (etched)	0.34	1.62	0.60	56

Value extracted by webplotdigitizer

Table 2. Recovery Rate by N_2 Annealing[2]

Sample	**Resistivity (ρ) 10^{-4} Ω·cm**			**Rate %**
	ρ_0	$P_{6\text{-month ambient}}$	$\rho_{Reannealed}$ 180 °C	$\frac{\rho_0 \times 100}{\rho_{Reannealed}}$
AZO	4.2 ± 0.4	22.8 ± 2.3	7.2 ± 0.7	58

Table 3. Recovery Rate by H_2 Annealing[3]

Sample	**Resistivity (ρ) 10^{-3} Ω·cm**			**Rate %**
	ρ_0	ρ_{30}	$\rho_{Reannealed}$	$\frac{\rho_0 \times 100}{\rho_{Reannealed}}$
AZO-400 °C	1.3	98.9	1	126.4
AZO-450 °C	1	7.8	0.9	115.7
AZO-500 °C	0.6	2.1	0.6	111.3
AZO-550 °C	0.4	1.3	0.5	81.5

Reference

[1] T. Tohsophon, J. Hüpkes, S. Calnan, W. Reetz, B. Rech, W. Beyer, N. Sirikulrat, Damp heat stability and annealing behavior of aluminum doped zinc oxide films prepared by magnetron sputtering, Thin Solid Films. 511–512 (2006) 673–677. doi:10.1016/j.tsf.2005.12.130.

[2] M. Mickan, M. Stoffel, H. Rinnert, U. Helmersson, D. Horwat, Restoring the Properties of Transparent Al-Doped ZnO Thin Film Electrodes Exposed to Ambient Air, J. Phys. Chem. C. 121 (2017) 14426–14433. doi:10.1021/acs.jpcc.7b03020.

[3] F. Machda, T. Ogawa, H. Okumura, K.N. Ishihara, Evolution and Recovery of Electrical Property of Reactive Sputtered Al-Doped ZnO Transparent Electrode Exposed to Harsh Environment, Phys. Status Solidi Appl. Mater. Sci. 1900519 (2019) 1–6. doi:10.1002/pssa.201900519.

Appendix B: SEM Images of AZO films having Crystal Orientations (110) and (002) with and without a Damp Heat Test

In this appendix B, the scanning electron microscope (SEM) images of AZO films with crystal orientation (110) (fig. A) and (002) (fig. B) are shown as further explanations for chapter 5. The ratio "X/Y" corresponds to the ratio of argon (X) and oxygen (Y) gas flow during the sputtering deposition, as explained in chapter 5 in this doctoral thesis. The label "DH" corresponds to the sample after 25 days of the damp heat (DH) test.

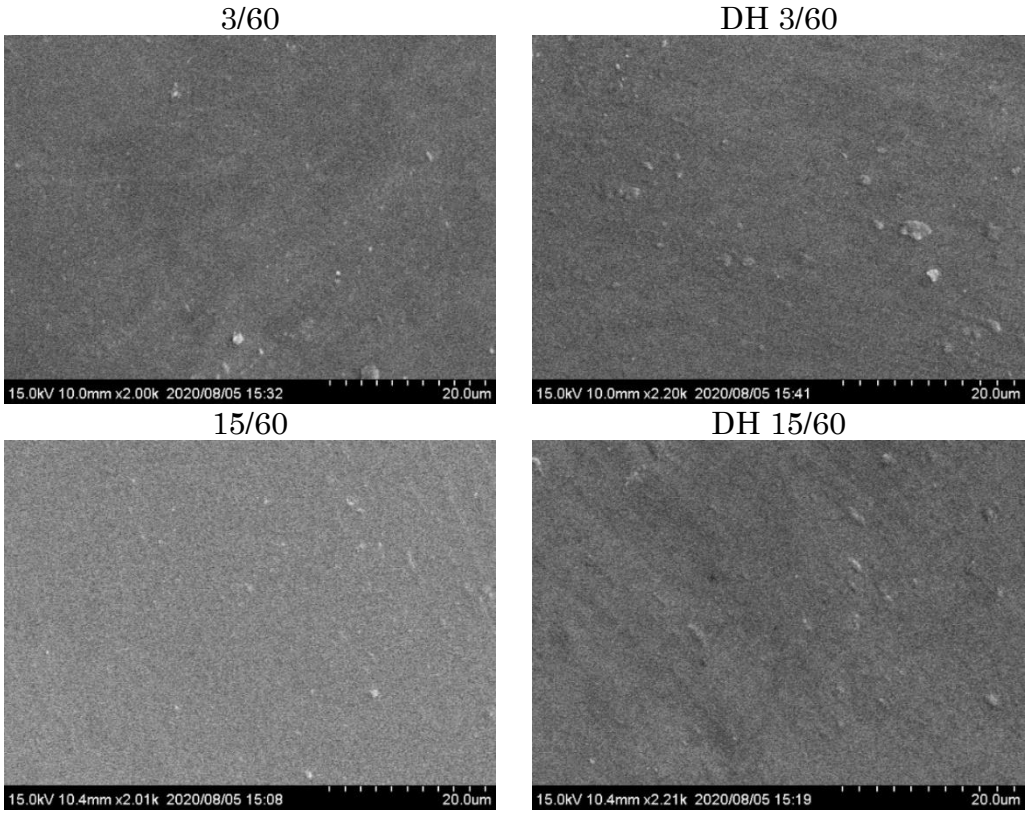

Fig A. SEM images of the surface of AZO films having a major crystal orientation (110) without (left) and with the DH test (right)

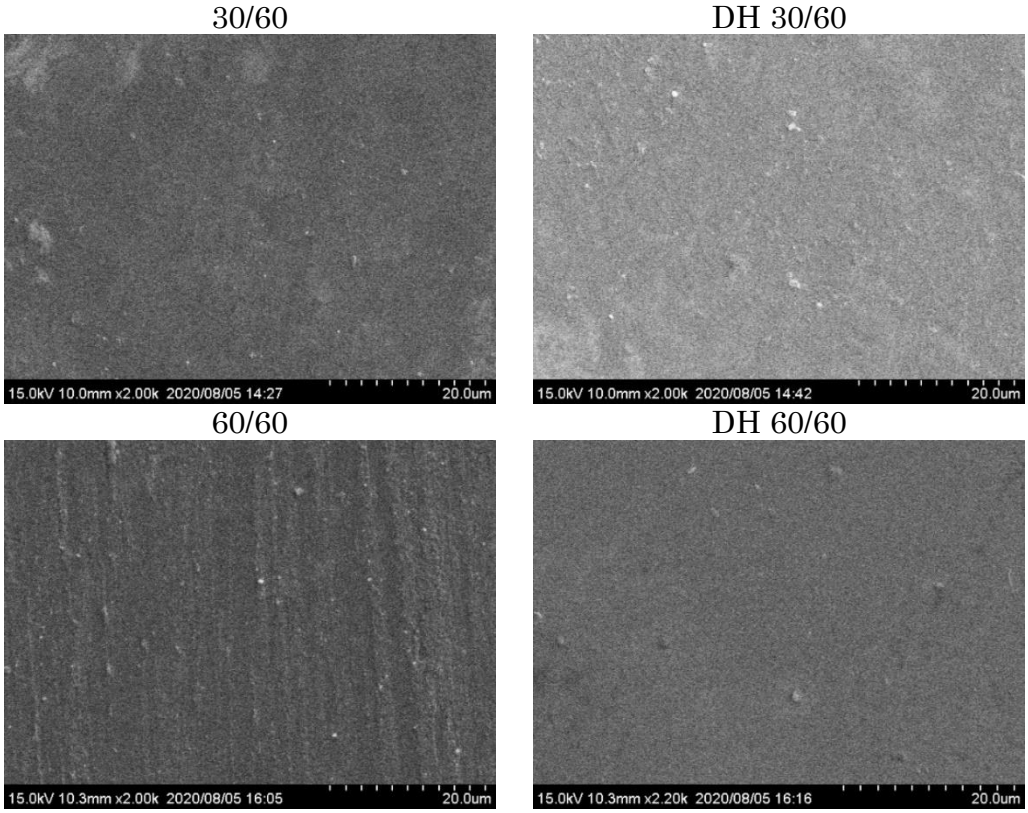

Fig B. SEM images of the surface of AZO films having a major crystal orientation (002) without (left) and with the DH test (right)

These results are in line with the chapter 4 and chapter 6, where there were no cracks or voids produced by the DH test for AZO samples deposited on the glass substrates. This finding suggests that chemical aspects were more involved rather than physical damages such as cracks in the degradation of those AZO films as exposed to the harsh environment represented as the DH test.